AN ABSTRACT OF THE DISSERTATION OF

Nikki B. Marshall for the degree of Doctor of Philosophy in Microbiology presented on December 1, 2009.

Title: Investigations of Regulatory T cell Induction by 2, 3, 7, 8-Tetrachlorodibenzo-*p*-Dioxin During a Graft-versus-Host Response

Abstract approved:

_____

Nancy I. Kerkvliet

The immune toxicity of 2,3,7,8-Tetrachlorodibenzo-*p*-dioxin (TCDD) has been studied for over 35 years, but only recently has the profound immune suppression associated with TCDD exposure been linked to induction of regulatory T cells (Tregs). The effects of TCDD are mediated through binding the aryl hydrocarbon receptor (AhR), a ligand-activated transcription factor. Subsequent AhR-mediated effects of TCDD in T cells that induce Tregs are not yet known. To address this, studies to further characterize $CD25^{+}CD4^{+}$ T cells induced in TCDD-treated mice on day 2 of an acute graft-versus-host (GVH) response were performed by comparing them to naturally-derived Tregs. Results show that TCDD-induced

Tregs are similar to natural Tregs with a lack of IL-2 production, in vitro suppressive function, and reversal of suppressive function through ligation of GITR. However, TCDD-induced Tregs are unique in that they suppress naïve T cells while proliferating, do not express Foxp3, and secrete IL-10. A highly upregulated gene transcript in TCDD-induced Tregs was IL-12Rb2. IL-12Rb2 protein was found to be increased on T cells exposed to TCDD in the presence of IL-12. This correlated with increased binding of AhR upstream of the IL-12Rb2 gene. However, transfer of IL-12Rb2 KO T cells into TCDD-treated mice did not affect induction of the Treg phenotype. A second gene found to be upregulated in the TCDD-induced Tregs was IL-10. To inhibit IL-10 expression, a phosphorodiamidate morpholino oligomer conjugated to a cell-penetrating peptide (P-PMO) was utilized. Of several cell-penetrating peptides screened for delivery into murine leukocytes, the arginine-rich $(RXR)_4$ peptide was most effective, particularly into activated T cells. Dosing of TCDD-treated host mice with IL-10 P-PMO-$(RXR)_4$ did not affect induction of the day 2 Treg phenotype. However on day 6, an increased frequency of donor $CD69^+CD4^+$ and $CD69^+CD122^+CD8^+$ T cells was identified in TCDD-treated mice, phenotypes associated with regulatory function. The increased frequency of these populations was suppressed by IL-10 P-PMO treatment. Taken together, the results suggest TCDD induces adaptive $CD4^+$ and $CD8^+$ regulatory T cells during a GVH response that is partially influenced by IL-10. These studies support Treg induction as a mechanism for suppression of T cell-mediated responses by TCDD.

Investigations of Regulatory T Cell Induction by 2, 3, 7, 8-Tetrachlorodibenzo-*p*-Dioxin During a Graft-versus-Host Response

by

Nikki B. Marshall

A DISSERTATION

submitted to

Oregon State University

in partial fulfillment of

the requirements for the

degree of

Doctor of Philosophy

Presented December 1, 2009

Commencement June 2010

Doctor of Philosophy dissertation of Nikki B. Marshall presented on December 1, 2009.

APPROVED:

_____

Major Professor, representing Microbiology

_____

Chair of the Department of Microbiology

_____

Dean of the Graduate School

I understand that my dissertation will become part of the permanent collection of Oregon State University libraries. My signature below authorizes release of my dissertation to any reader upon request.

_____

Nikki B. Marshall, Author

ACKNOWLEDGEMENTS

A dissertation not only reflects the hard work of an individual, but of the many persons who have assisted along the way. I would like to acknowledge these persons who have helped make this all possible:

First off, thank you to Dr. Nancy Kerkvliet for your guidance and support. When we agreed at lab meeting back in 2004 that I would work on regulatory T cells, could either of us have even imagined where it would take us?

Dr. Dan Mourich, thank you for your mentorship and support throughout this entire process. I can say with certainty that I wouldn't have made it without your help.

Thank you to those members of the Kerkvliet laboratory at Oregon State University and the biology laboratory at AVI BioPharma Inc. who assisted and supported me along the way. Even the smallest bit of technical help or bended ear is greatly appreciated.

Thank you to my family and friends for your love and support.

And to Matt, thank you for hanging in there. You have been a critical component to my success!

CONTRIBUTION OF AUTHORS

Co-Authors (in alphabetical order)	Major Contributions
Dr. Patrick L. Iversen	Critical review of manuscript, technical support
Dr. Mark Leid	Critical analysis of experimental design and data, technical support, guidance
Carla A. London	Technical support, critical review of manuscript
Dr. Hong M. Moulton	Critical review of experimental design, data and manuscript
Dr. Dan V. Mourich	Critical review of experimental design, data and manuscripts, technical support, guidance
Shannon K. Oda	Technical support, critical review of manuscript
Diana C. Rohlman	Technical support, critical review of experimental design
Linda B. Steppan	Technical support and design, critical review of experimental design and manuscript
Dr. William R. Vorachek	Technical support, data analysis and discussion

TABLE OF CONTENTS

TABLE OF CONTENTS (Continued)

LIST OF FIGURES

LIST OF FIGURES (Continued)

LIST OF TABLES

LIST OF APPENDICES

LIST OF APPENDIX FIGURES

Investigations of Regulatory T Cell Induction by 2, 3, 7, 8-Tetrachlorodibenzo-*p*-Dioxin During a Graft-versus-Host Response

Chapter 1

Introduction

Authors: Nikki B. Marshall

Nancy I. Kerkvliet

Portions of the introduction are published in: Dioxin and Immune Regulation: Emerging Role of Aryl Hydrocarbon Receptor in the Generation of Regulatory T cells

The Year in Immunology 2, Annals of the New York Academy of Sciences

Blackwell Publishing

January 2010; vol. 1184: *In press*

2, 3, 7, 8-Tetrachlorodibenzo-*p*-dioxin and the Aryl Hydrocarbon Receptor

TCDD overview

The chemical 2, 3, 7, 8-Tetrachlorodibenzo-*p*-dioxin (TCDD) commonly referred to as dioxin, is a member of the class of halogenated aromatic hydrocarbons that are persistent and ubiquitous environmental contaminants (Figure 1.1). TCDD is produced as an unintentional by-product of various industrial, combustion, and natural processes, and can be found in air, water, soil and sediment world-wide. The persistence of TCDD in the environment is owed to its chemical stability, low vapor pressure and low water solubility. Currently, TCDD is released into the environment primarily through combustion sources, such as municipal, medical, and hazardous waste incineration, particularly of chlorinated waste products. TCDD is also formed during the chlorine bleaching process of paper pulp, and released into the environment through waste water. Historically, TCDD is probably best known as a manufacturing by-product of herbicide 2,4,5-trichlorophenoxyacetic acid (2,4,5-T), used during the Vietnam War as a component of the Agent Orange defoliant. Most recently, TCDD was used in a highly publicized assassination attempt of Ukrainian presidential candidate Viktor Yushchenko. And yet, despite the toxicity associated with TCDD, its role as a biological response modifier is studied at sub-acute toxic doses to enhance our understanding of biological systems.

Exposure

Humans are exposed to small amounts of dioxin daily, the majority through

consumption of food (Huwe, 2002). Given that TCDD is highly lipid soluble (K_{OW} 7.0), it bioaccumulates in adipose tissue found in meat, dairy, fish and shellfish. The World Health Organization (WHO) has established a tolerable daily intake of 1-4 picograms of TCDD per kilogram of body weight per day. The average body burden of TCDD in people living in North America and Europe is 2 ppt, primarily stored in adipose tissue and blood lipids (Aylward and Hays, 2002). The half-life of TCDD in the human body ranges from 7-10 years and is affected by dose, age, exposure duration, health status, and diet (Medicine, 2007). This is considerably longer than the half-life in rodents of 2-4 weeks (Miniero et al., 2001). TCDD can be excreted through direct intestinal elimination, or can be absorbed and biotransformed in the liver and excreted through bile into feces (Medicine, 2007). Some TCDD metabolites have also been identified including hydroxylated and methylated derivatives excreted as glucuronide and sulfate conjugates (Registry, 2006). Fortunately, levels of dioxins in the U.S. and Europe continue to decrease in both the population and the environment, reflecting regulatory decisions that have reduced the production and use of dioxin-contaminated substances.

Toxic health effects

The effects observed in animals following exposure to TCDD have intrigued toxicologists for over 50 years (Schecter and Gasiewicz, 2003). Lethal doses of TCDD cause a slow death due to a wasting syndrome that is characterized by thymic atrophy, lipolysis and altered intermediary metabolism. In addition, TCDD produces

a broad spectrum of effects at very low concentrations, leading to TCDD's moniker as an "environmental hormone." The most sensitive effects of TCDD observed in multiple species are developmental, including effects on the developing immune, nervous, and reproductive systems (Birnbaum and Tuomisto, 2000). At non-lethal doses, reproductive effects, immune suppression, hepatocarcinogenesis, and tumor promotion are also observed (Huff et al., 1994; Kerkvliet, 2002; Medicine, 2007). TCDD was upgraded to a Group 1 carcinogen by the International Agency for Research on Cancer in 1997 after it was concluded that sufficient data suggests TCDD increases cancer risk.

There have been opportunities to study the human health effects of TCDD during accidental exposures although no direct human deaths have ever been reported. Thus the LD_{50} for TCDD in humans is not known, however the highest dose ever recorded was for a 30-year old woman at 144,000 pg TCDD/g blood lipid (Geusau et al., 2001). The Agency for Toxic Substances and Disease Registry (ATSDR) of the Centers for Disease Control lists the known toxic effects of dioxin exposure on human health to include transient hepatotoxicity and neuropathy, as well as the skin disorder chloracne (Registry, 2006). Chloracne is a severe form of persistent, scarring skin eruptions characterized by progressive transition of sebaceous gland cells to keratinizing cells with follicular hyperkeratosis (Moses and Prioleau, 1985).

The spectrum of toxicities associated with TCDD exposure are now known to be mediated through the ligation and activation of the aryl hydrocarbon receptor (AhR), first identified by Poland et al. in 1976 (Poland et al., 1976). The

transformation of the polycyclic aromatic hydrocarbon benzo[a]pyrene to 3-hydroxybenzo[a]pyrene was only detected in liver extracts from "responsive mice" (Poland et al., 1974). The crossing and back-crossing of inbred mouse strains eventually led to the identification of the aryl hydrocarbon locus suspected to control expression of the enzyme responsible for this biotransformation (Gielen et al., 1972), later named Cytochrome P450 1A1 (CYP1A1). Activation of AhR induces a variety of drug-metabolizing enzymes in addition to CYP1A1, termed the AhR battery (Nebert et al., 2000). Unlike most other AhR ligands that induce their own metabolism, TCDD is resistant to this enzyme battery, and its persistent occupancy of AhR is postulated to contribute to its potent toxicity.

Aryl hydrocarbon receptor

AhR belongs to the basic helix-loop-helix-PER-ARNT-SIM family of proteins, and functions as a ligand-activated transcription factor (Burbach et al., 1992) consisting of three functional domains (Figure 1.2) (Fukunaga et al., 1995). The DNA-binding domain is made up of the basic helix-loop-helix motif found in a variety of transcription factors (Jones, 2004). The PAS-A and PAS-B domains, homologous to *Drosophila* proteins Per and Sim, make up the ligand-binding domain (Coumailleau et al., 1995; Goryo et al., 2007). A third glutamine-rich region contains the transactivation domain involved in co-activator recruitment (Kumar et al., 2001). Located in the cytoplasm of most cells, non-ligand bound AhR forms a receptor complex with several proteins including a 90 kDa heat shock protein dimer (hsp90), hepatitis B virus X-associated protein 2 (XAP2), also known as AhR-

interacting protein (AIP), and phosphoprotein p23 (as reviewed by Beischlag et al., 2008). Once bound by ligand, the ligand-receptor complex undergoes a conformational change and translocates to the nucleus where hsp90 is exchanged for the AhR Nuclear Translocator protein (ARNT) to form a heterodimer (Figure 1.3). This heterodimer binds cis elements of DNA with the core sequence 5'-GCGTG-3' (Shen and Whitlock, 1992) known as xenobiotic- or dioxin-responsive elements (DREs) which can be found in gene promoter and/or enhancer regions. The AhR/ARNT transcriptional complex recruits other proteins (e.g. SRC-1, CBP, NCoA2) that modulate transcriptional activity and chromatin structure (Beischlag et al., 2008). The result is enhanced or repressed expression of AhR/ARNT-responsive genes.

AhR is polymorphic both in mice and humans, thus the specific AhR haplotype expressed by an individual determines their responsiveness to TCDD. Inbred mouse strains such as C57Bl/6 and BALB/c express a high affinity AhR allele (AhR^b). Other mouse strains including DBA/2 and SJL express a low affinity allele (AhR^d), which, because of point mutations in the ligand-binding domain and stop codon, is approximately 30-fold less responsive to TCDD. Mice expressing a lower affinity AhR require a higher dose of TCDD to achieve equivalent AhR-mediated effects. There is an estimated 10-fold increased affinity of TCDD for AhR^b compared to human AhR (Ramadoss and Perdew, 2004). AhR sequence comparisons between mouse and human show <60% homology at the carboxyl terminus, 100% conservation for the basic region, 98% homology for the helix-loop-helix domain, and 87% homology for the PAS domain (Beischlag et al., 2008).

The most commonly used biomarker for AhR activation is induction of Cyp1a1, and more recently, AhR repressor (AHRR) (Hahn et al., 2009). The absence of TCDD toxicity in mice carrying a mutation in the DNA-binding domain of the AhR (Bunger et al., 2008) suggests that inappropriate transcriptional enhancement or repression of AhR-responsive genes mediates the majority of known toxic effects of TCDD. However, some studies indicate that AhR-mediated changes in gene expression are not limited to AhR/ARNT-dependent transcriptional activity. AhR has also been shown to interact directly with proteins in other signaling pathways including NF-κB (Kim et al., 2000; Tian et al., 1999), retinoblastoma protein (Puga et al., 2000), E2F1 (Marlowe et al., 2008) and estrogen receptor (Klinge et al., 2000; Ohtake et al., 2003). AhR has also been reported to act as part of a ligand-dependent E3 ubiquitin ligase complex that regulates protein degradation (Ohtake et al., 2007). Clearly, we are only beginning to understand the diversity in AhR activity and function which coalesce to form complex mechanisms by which AhR alters gene expression.

AhR-Mediated Effects of TCDD on Leukocytes

The immune toxicity of TCDD has been studied for more than 35 years, as this small molecule is one of the most potently immunosuppressive chemicals known. AhR is not required for the development of a functional immune system but its absence precludes the immunosuppressive effects of TCDD (Sulentic et al., 1998;

Vorderstrasse et al., 2001). Some of the reported effects of TCDD include thymic involution, decreased host resistance to pathogens and tumors, suppressed fetal lymphocyte development and maturation, and suppressed adaptive immune responses including antibody production, cytotoxic T lymphocyte activity and delayed hypersensitivity responses (Kerkvliet, 1994; Kerkvliet, 2002; Lawrence and Kerkvliet, 2007). Thymic involution, a hallmark immunotoxic effect of TCDD in all species examined (Kerkvliet, 1994), is dependent upon AhR expression in hematopoietic cells (Fernandez-Salguero et al., 1996; Staples et al., 1998). AhR is expressed by all major cell types of the immune system including B cells, T cells, dendritic cells, macrophages, granulocytes, and natural killer cells (Lawrence and Kerkvliet, 2007). Moreover, macrophages (Hayashio et al., 1995), B cells (Marcus et al., 1998) and T cells (Negishi et al., 2005) have all been shown to increase their expression of AhR upon activation. Many genes involved in immune regulation contain multiple DREs in their promoter region (Sun et al., 2004), but these regions of DNA are not necessarily accessible for AhR/ARNT binding. Since TCDD primarily affects immune cells responding to stimulation, the window of promoter and enhancer availability created by other signaling events may dictate when TCDD must be present to produce an AhR-mediated effect. Ultimately, the specific effects of AhR activation by TCDD on an immune response are context-dependent, determined by what cell types are involved, the activation status of the cells, the timing, and the type of antigenic stimulation.

T cells

Adaptive immunity consists of activation, effector differentiation, and clonal expansion of antigen-specific populations of lymphocytes including CD4+ T cells, CD8+ T cells and B cells. As the cells encounter their specific antigen and are exposed to costimulatory signals and cytokines, they differentiate into effector cells capable of carrying out functions best suited to clear the antigenic stimulus. In fact, few TCDD-induced changes are detected in the immune system unless cells are stimulated with antigen (Kerkvliet, 2002). T cells were thought to be indirect targets of TCDD until in vivo studies showed that suppression of T cell functions in an acute graft versus host response (GVHR) required the presence of AhR in the donor T cells themselves (Kerkvliet et al., 2002).

The mechanisms for suppression of effector T cell differentiation by TCDD are still not well understood. Upon antigenic challenge, both CD4+ and CD8+ T cells proliferate normally in TCDD-treated mice, however a significant decline in their numbers have been observed as early as day 5 of an immune response that appears to reflect a cessation of proliferation rather than apoptosis (Camacho et al., 2002; Funatake et al., 2004; Shepherd et al., 2000). Furthermore, activation of CD8+ cytotoxic T lymphocyte (CTL) precursors is suppressed as early as day 5 in a CD4+ T cell-dependent tumor allograft response (Oughton and Kerkvliet, 1999) that is not explained by insufficient interleukin-2 (IL-2) or deletion of CD8+ T cells (Kerkvliet et al., 1996; Prell et al., 2000). Suppressed CTL development was also observed in a CD4+ T cell-independent CD8+ T cell response to influenza (Mitchell and Lawrence, 2003a; Warren et al., 2000) that was also not explained by increased

apoptosis (Mitchell and Lawrence, 2003a). Thus TCDD appears to cause a premature cessation of T cell proliferation and inhibition of CTL activation which does not appear to be linked to increased T cell death.

Extensive chromatin remodeling that occurs during T cell activation may explain why activated T cells are particularly sensitive to the effects of TCDD as compared to resting T cells (Funatake et al., 2004; Lundberg et al., 1992; Prell et al., 1995; Pryputniewicz et al., 1998; Shepherd et al., 2000). As T cells differentiate into effectors over the course of several days, it is likely that direct AhR-DRE mediated effects occur throughout this time instead of just in the first few hours of TCR ligation. A recent review highlights some of the genes altered in CD4+ T cells by TCDD both in vivo and in vitro including lineage-specific transcription factors, cytokines, cytokine receptors, and signaling kinase families, many of which contain multiple DREs in their promoters (Kerkvliet, 2009). This complex network of genetic and epigenetic interactions that occurs during T cell effector differentiation ultimately determines T cell fate, and is sensitive to the effects of AhR activation by TCDD.

B cells

B cells were identified early as direct cellular targets of TCDD as effects could be easily observed in cell culture (Dooley and Holsapple, 1988; Karras and Holsapple, 1994a; Karras and Holsapple, 1994b; Luster et al., 1988; Tucker et al., 1986). TCDD suppresses primary antibody responses and antibody class switching (Kerkvliet, 1994), which is partially explained by suppressed cytokine production

(Fujimaki et al., 2002; Inouye et al., 2005; Ito et al., 2002). Other factors contribute to altered antibody-mediates responses with TCDD exposure, as suppressed production of IgG2a in response to influenza was not associated with suppressed cytokine levels (Mitchell and Lawrence, 2003b). T cells, as primary cellular targets of TCDD, have also been shown to mediate the inhibition of antibody responses (Allan and Sherr, 2005; Ito et al., 2002).

TCDD also alters the expression of many B cell genes including Cd19, Socs2, Pax5, p27kip1, Ap-1 and Blimp-1 (Lawrence and Kerkvliet, 2007; Schneider et al., 2009). The differentiation of pro-B cells into mature B cells in bone marrow is also suppressed (Thurmond and Gasiewicz, 2000; Thurmond et al., 2000), which is partially explained by the AhR-mediated effects in bone marrow stromal cells (Wyman et al., 2002). Collectively, the data suggest that there a diversity of cellular stages and processes in which B cells are disrupted by TCDD which leads to suppressed B cell responses.

Dendritic cells

The innate immune system consists of cells and mechanisms that protect a host from infection by a broad spectrum of pathogens. Cells including macrophages, natural killer cells, neutrophils and dendritic cells are part of this first line of host defense that can be affected by TCDD exposure (Head and Lawrence, 2009; Kerkvliet, 1994; Lawrence and Kerkvliet, 2007). Dendritic cells (DCs) are an important link between the innate and adaptive immune systems. DCs migrate to lymph nodes and present antigen to T cells on MHC class II molecules while

providing additional costimulation to promote full CD4+ helper T cell activation. Splenic DCs isolated from mice exposed to TCDD expressed increased levels of MHC Class II, adhesion molecules ICAM-1 (CD54) and CD24, and costimulatory molecule CD40 (Vorderstrasse and Kerkvliet, 2001). The DCs also produced increased levels of IL-12 and enhanced T cell proliferative responses in a mixed lymphocyte reaction. Antigen-processing appeared unaffected as phagocytosis of latex beads and antigen presentation were not altered by TCDD (Vorderstrasse et al., 2003). Bone marrow-derived DCs exposed to TCDD were also shown to express increased MHC II, CD86, CD40 and CD54 with increased T cell stimulating ability (Lee et al., 2007; Ruby et al., 2005). Taken together, these results suggest that TCDD enhances the activation and stimulatory capacity of DCs. However, the number of DCs in the spleen of TCDD-treated mice was significantly reduced one week after treatment (Vorderstrasse et al., 2003), and bone marrow-derived DCs treated with TCDD were shown to undergo increased Fas-mediated apoptosis (Ruby et al., 2005). This premature loss of DCs would likely reduce the strength and duration of a T cell-mediated response.

Effects of TCDD on Host Resistance

TCDD exposure can cause increased mortality after challenge with an infectious pathogen (Kerkvliet, 1994), however the susceptibility ultimately depends on the type of pathogen, and in some cases the animal model that is used. For example, TCDD increased the mortality of rodents challenged with *Salmonella*

(Hinsdill et al., 1980; Thigpen et al., 1975; Vos et al., 1978), *Herpes simplex type 2* (Clark et al., 1983), and *Influenza A virus* (House et al., 1990). However, TCDD exposure enhanced host resistance to *Leishmania major* (Bowers et al., 2006), *Listeria monocytogenes* (Shi et al., 2007) and *Streptococcus pneumoniae* (Vorderstrasse and Lawrence, 2006). For the parasite *Trichinella spiralis*, decreased resistance was observed in B6C3F1 mice treated with TCDD, but enhanced resistance was seen in TCDD-treated F344 rats (Luebke et al., 1995; Luebke et al., 1994). Thus TCDD does not suppress host resistance to all pathogenic infections, rather the effects are pathogen- and species-specific.

The suppression of host resistance to influenza virus in TCDD-treated mice has been extensively studied and is recently reviewed (Head and Lawrence, 2009.) Mice exposed to TCDD during challenge with influenza virus experience a decreased survival at a very low dose of 0.1 µg/kg TCDD (House et al., 1990). This increased mortality was not due to an inability to clear the virus (Burleson et al., 1996; Lawrence et al., 2000), rather AhR-mediated excessive neutrophil recruitment to the lung that contributed to the increased mortality (Teske et al., 2005). Although TCDD treatment enhanced neutrophil activity, it suppressed clonal expansion and differentiation of virus-specific CD8+ CTL which was not dependent on AhR in the CD8+ T cells. The recall of virus-specific memory CD8+ T cells however was preserved (Lawrence et al., 2006). Also suppressed was the production of anti-viral antibodies, excluding IgA levels which were increased due to enhanced phagocyte-derived interferon gamma (IFN-g) (House et al., 1990; Lawrence and Vorderstrasse, 2004; Neff-LaFord et al., 2007; Warren et al., 2000). Thus, the effects of TCDD on

host resistance to infectious disease are specific and complex.

Effects of AhR Activation on CD4+ T cell Effector Differentiation and Disease

The immunosuppressive effects of TCDD are undesirable in terms of host resistance where increased susceptibility to bacterial and viral infections as well as increased tumor growth has been observed in some animal models. During inappropriate immune responses, however, the effects of AhR activation by TCDD are beneficial for preventing the development of disease. TCDD has been shown to suppress allograft responses (Kerkvliet et al., 1996; Kerkvliet et al., 2002), allergic responses (Fujimaki et al., 2002; Luebke et al., 2001), and autoimmune responses in models of multiple sclerosis (experimental autoimmune encephalomyelitis (EAE)) (Quintana et al., 2008) and type I diabetes (Kerkvliet et al., 2009). These disease conditions are mediated by different subtypes of effector CD4+ T cells suggesting that TCDD suppresses effector T cell-mediated responses in vivo. However, the development of regulatory T cells (Tregs) with suppressive function appears to be enhanced or preserved in the presence of TCDD (Funatake et al., 2005; Kerkvliet et al., 2009; Quintana et al., 2008). Given the therapeutic potential for Tregs to suppress undesirable immune responses, there is considerable interest in furthering our understanding of how TCDD acts through AhR to suppress CD4+ T cell differentiation but enhance the development of Tregs.

Suppression of Th2-mediated responses

Type 2 CD4+ T cells (Th2) predominate in antibody-mediated immune responses including responses to extracellular bacteria and viruses, parasitic infections, as well as allergens that cause immediate hypersensitivity. Th2 cells express the transcription factor GATA-3 which mediates epigenetic changes at the IL-10 and IL-4 loci to promote the Th2 phenotype (Ranganath et al., 1998; Shoemaker et al., 2006). TCDD has been shown to suppress Th2-mediated immune responses including allergic response to dust mite antigen (Luebke et al., 2001), development of atopic dermatitis (Fujimaki et al., 2002), and antibody responses to ovalbumin in alum adjuvant (Inouye et al., 2005; Nohara et al., 2002). Suppressed production of Th2 cytokines including IL-4 and IL-5 has been shown in TCDD-treated mice (Fujimaki et al., 2002; Nohara et al., 2002), at doses as low as 0.3 μg/kg (Inouye et al., 2005). IgE production was suppressed in TCDD-treated NC/Nga mice prone to develop atopic dermatitis (Fujimaki et al., 2002), and in TCDD-treated rats sensitized to dust mite allergen (Luebke et al., 2001). Interestingly, the anti-allergic drugs M50354 and its derivative M50367 have been shown to act as AhR agonists that suppress Th2 development (Morales et al., 2008; Negishi et al., 2005). Although Treg-mediated suppression of Th2 responses has been described (Nouri-Aria and Durham, 2008), no link has yet been established between suppressed Th2 responses and induction of Tregs in TCDD-treated mice.

Suppression of Th1-mediated allograft responses

Type 1 CD4+ T cell (Th1) cells are involved with cell-mediated immunity and promote the development of CD8+ cytotoxic T lymphocytes (CTL). Th1 cells

express the transcription factor T-bet which mediates epigenetic changes to promote Th1 phenotype including IFN-g and upregulation of IL-12 receptor beta 2 (IL-12Rb2) (Mullen et al., 2001; Wei et al., 2009). Much work has been done in the Kerkvliet laboratory studying the effects of TCDD on allograft immunity. The Th1-mediated CTL- and alloantibody-mediated responses to P815 mastocytoma (H-2^d haplotype) are suppressed in B6 mice (H-2^b) treated with TCDD (Kerkvliet et al., 1996). To observe the suppression of CTL, TCDD must be given within the first 3 days of the allograft being introduced, and the animals must express AhR (Vorderstrasse and Kerkvliet, 2001). The primary target for the early-stage suppression by TCDD appears to be the development of Th1 cells that are required during the first three days of the allograft response to activate the CTL precursors (Kerkvliet et al., 1996). These findings suggest that once CTL precursors have gone through normal activation, TCDD does not inhibit their clonal expansion or cytolytic activity.

A second allograft model we have utilized in our lab is an acute graft-vs-host response (GVHR) model in which donor T cells from B6 mice (H-2^b) are injected intravenously into B6D2F1 (F1) mice of mixed haplotype (H-$2^{b/d}$). Alloreactive donor T cells respond to H-2^d alloantigens expressed by host tissues inducing an anti-H-2^d Th1-dependent CD8+ CTL response. When host mice were treated with TCDD within 24 hours before the adoptive transfer of donor T cells, the allospecific CTL response was suppressed (Kerkvliet et al., 2002). If however, the donor T cells were $AhR^{-/-}$, the CTL response was unaffected by TCDD, demonstrating that AhR in the donor T cells is the direct target for suppression of the CTL response.

Furthermore, when donor CD4+ T cells from B6 $AhR^{-/-}$ mice were adoptively transferred with CD8+ T cells from B6 WT mice, the CTL response was only partially suppressed, indicating that TCDD acts directly on alloreactive CD4+ T cells to impair their ability to support CTL development.

Generation or preservation of $Foxp3^+$ Tregs

Naturally-occurring Tregs are a sub-population of suppressive $CD25^{high}$ CD4+ T cells whose phenotype and function are governed by the forkhead family transcription factor Foxp3 (Fontenot et al., 2003; Hori et al., 2003). $Foxp3^+$ Tregs constitute 5-10% of peripheral CD4+ T cells, and play an important role in self-tolerance. Tregs suppress cell- and antibody-mediated immune responses and protect a host against autoimmunity. Although natural $Foxp3^+$ Tregs appear to be derived in the thymus, Foxp3 expression can be induced in peripheral T cells by stimulation in the presence of TGF-beta (Chen et al., 2003) and IL-2 (Zheng et al., 2008). AhR is expressed by $Foxp3^+$ Tregs (Frericks et al., 2007; Hill et al., 2007), and DRE sequences in the Foxp3 promoter are capable of binding AhR (Quintana et al., 2008), suggesting AhR can directly influence Foxp3 expression. TCDD alone at 100 nM was reported to induce a small increase in the frequency of $Foxp3^+$ T cells in vitro (Quintana et al., 2008), while another laboratory found that co-treatment with TGF-beta was needed to increase $Foxp3^+$ T cell frequency at 160 nM (Kimura et al., 2008). $Foxp3^+$ T cell frequency was also found to be increased in AhR^b B6 mice compared to congenic AhR^d B6 mice (Quintana et al., 2008). However, the frequency of $Foxp3^+$ Tregs in B6 mice was not different than in B6 $AhR^{-/-}$ mice

(Veldhoen et al., 2008), suggesting AhR does not play a necessary role in maintenance of natural Foxp3+ Treg populations.

An increase in $Foxp3^+$ Treg frequency has been observed in mouse models of disease with TCDD treatment. Quintana et al. reported that administering 1 µg of TCDD (~50 µg/kg) increased $Foxp3^+$ Treg frequency and inhibited development of EAE in B6 mice (Quintana et al., 2008). However no increase was seen at the 0.1 µg dose which is an immunosuppressive dose for AhR^b B6 mice. An increase in $Foxp3^+$ Treg frequency was also found in the pancreatic lymph node of non-obese diabetic (NOD) mice treated with TCDD which correlated with suppression of type 1 diabetes (Kerkvliet et al., 2009). The body burden of TCDD in NOD mice (AhR^d) was maintained at approximately 15 µg/kg (0.4 µg per mouse) over the course of 30 weeks as blood glucose was monitored. Mice that were taken off of TCDD treatment began developing diabetes as the body burden of TCDD dropped below an estimated 4 µg/kg concentration. These data suggest that TCDD must be present at sufficient concentrations to sustain an increase in $Foxp3^+$ Treg frequency, likely due to the continued emergence of differentiating effector T cells in the periphery. It is not yet clear whether these results reflect a preservation or induction of $Foxp3^+$ Tregs. Since TCDD has little effect on fully-differentiated effector T cell activity, natural $Foxp3^+$ Tregs may be relatively resistant to the AhR-mediated effects of TCDD compared to other T cell subsets. This could explain their increased frequency in vivo in TCDD-treated mice during autoimmune responses. Thus the relationship between Foxp3 expression and mechanisms of TCDD-induced immune suppression requires further study.

Some studies have linked the generation of tolerogenic DCs with increased Foxp3$^+$ Treg frequency in TCDD-treated mice. Vogel et al. showed that activation of AhR by TCDD induced indoleamine 2,3-dioxygenase 1 (IDO1) and IDO-like protein IDO2 in the lung and spleen of C57Bl/6 (B6) mice which correlated with a 2.5-fold increase in expression of Foxp3 transcript in the spleen (Vogel et al., 2008). The increase in Foxp3 expression was prevented when IDO activity was inhibited. The induction of IDO expression is associated with suppression of T cell responses (Puccetti and Grohmann, 2007) and generation of tolerogenic DCs that induce Tregs (Belladonna et al., 2007; Curti et al., 2007; Mellor et al., 2004). Both the *IDO1* and *IDO2* genes contain putative DREs (Sun et al., 2004; Vogel et al., 2008), thus the induction of IDO expression by DCs may be DRE-mediated. Also, IDO expression requires signaling of the NF-κB pathway, (Puccetti and Grohmann, 2007; Tas et al., 2007) which is also affected in DCs by TCDD (Lee et al., 2007; Ruby et al., 2002), likely through direct interactions with AhR (Kim et al., 2000; Tian et al., 1999; Vogel and Matsumura, 2009).

The low molecular weight compound VAG539 has been shown to activate AhR and suppress allergic lung inflammation (Lawrence et al., 2008) and promote allograft acceptance (Hauben et al., 2008). This acceptance was correlated with an increase in Foxp3$^+$ Treg frequency, and could only be transferred by either the CD25$^+$CD4+ Tregs or, surprisingly, the CD11c$^+$ DCs from VAG539-treated mice. Thus AhR ligands may be capable of inducing tolerogenic DCs that play a role in the expansion or preservation of Foxp3$^+$ Tregs. Furthermore, tolerogenic IDO$^+$ DCs can also be induced by the engagement of costimulatory molecules CTLA-4 or

GITR expressed on the surface of Tregs (Fallarino et al., 2003; Grohmann et al., 2007; Munn et al., 2004). The induction or preservation of Tregs by TCDD could play a role in the upregulation of IDO and the further perpetuation of Treg induction.

The cytokine transforming growth factor beta (TGF-beta) is associated with the induction and effector function of Tregs. The interactions of AhR and TGF-beta signaling pathways have been extensively studied (Gomez-Duran et al., 2009; Haarmann-Stemmann et al., 2009), however not as thoroughly in T cells. Draining lymph node cells from TCDD-treated mice secreted increased levels of TGF-beta 1 in the EAE mouse model and transfer of these cells into new hosts suppressed EAE dependent upon signaling through the TGF-beta receptor (Quintana et al., 2008). Interestingly, a second isoform, TGF-beta 3, also binds TGF-beta receptor II and was shown to be upregulated in thymocytes exposed to TCDD (Lai et al., 1997). Both TGF-beta 1 and TGF-beta 3 have multiple DREs in their promoters (Sun et al., 2004), which suggests AhR may act directly to upregulate their expression. Taken together, it appears that TCDD induces or preserves TGF-beta expression in T cells which may be important for mediating suppression of disease, particularly through the induction or preservation of Tregs.

Generation of adaptive Tregs

Adaptive Tregs are naïve T cells that are induced to develop suppressive capacity that may or may not express the transcription factor Foxp3. Many different types of adaptive Tregs have been described including inducible $CD25^{+}CD4+$ Tregs

(Apostolou and von Boehmer, 2004; Kretschmer et al., 2005), $CD25^{-}Foxp3^{-}CD4+$ Tregs (Chen et al., 2004; Hansen et al., 2007), TGF-beta-induced CD4+ Tregs (Weiner, 2001; Zheng et al., 2002), IL-10-induced CD4+ Tregs (Tr1) (Battaglia et al., 2006; Roncarolo et al., 2006), $Foxp3^{+}CD8+$ Tregs (Najafian et al., 2003), and $CD69^{+}CD25^{-}CD4+$ Tregs (Han et al., 2009). Our lab was the first to identify an adaptive Treg-like population of $CD25^{+}CD4+$ cells generated in TCDD-treated mice during an acute GVH response (Funatake et al., 2005).

Flow cytometric and functional analysis of CD4+ and CD8+ donor T cells following adoptive transfer into F1 hosts was performed to determine the effects of TCDD on the T cell response to alloantigen (Funatake et al., 2008; Funatake et al., 2005; Marshall et al., 2008). Phenotypic analysis of proliferating, alloreactive donor T cells revealed significant increases in the frequency of $CD25^{+}$ T cells (both CD4+ and CD8+), and in the level of CD25 expressed per cell 48 h after adoptive transfer into TCDD-treated host mice. When pre-existing $CD25^{+}$ cells were depleted from the donor inoculum prior to adoptive transfer, there was no effect on the generation of the $CD25^{high}$ population suggesting de novo induction rather than expansion of a pre-existing $CD25^{+}$ population. The $CD25^{high}$ cells also expressed increased levels of CTLA-4, glucocorticoid-induced TNF receptor (GITR), and down-regulated CD62-L expression compared to cells from vehicle-treated mice (Funatake et al., 2005). These phenotypic changes were not seen in $Ahr^{-/-}$ donor T cells suggesting AhR activation by TCDD may be inducing adaptive Tregs. A functional assessment of the cells using a standard suppression assay showed that donor CD4+ and CD8+ T cells suppressed the proliferation of CD4+ T cell responders stimulated in vitro

with anti-CD3 even more potently than a population of natural $CD25^{+}CD4+$ regulatory T cells (Funatake et al., 2008; Funatake et al., 2005). Thus, alloreactive donor CD4+ and CD8+ T cells exposed to TCDD during acute GVHR appear to be both phenotypically and functionally consistent with Tregs, although further characterization of the cells is still needed.

These GVH studies were the first to link AhR activation by TCDD with the induction of CD4+ and CD8+ Treg-like cells, suggesting AhR may act as an alternative transcription factor to induce Treg phenotype and function. Interestingly, these phenotypic changes in both CD4+ and CD8+ donor T cells exposed to TCDD were primarily dependent upon the AhR expression in the donor CD4+ T cells (Funatake et al., 2008). Thus it is possible CD8+ T cells were converted to Treg-like cells through direct interactions with the CD4+ T cells, or indirectly through interactions with CD4+ T cell-licensed DCs. The AhR status of the host did not influence suppression of the GVH response (Funatake et al., 2009) suggesting that direct AhR-mediated effects on host antigen-presenting cells did not mediate the induction of the cells. Thus direct AhR-mediated effects of TCDD on CD4+ T cells is necessary for the induction of Treg-like cells in the acute GVHR model.

Effects on Th17 development

IL-17-secreting T cells (Th17) are a recently identified lineage of effector T cells. Th17 cells are generally found in the skin and GI tract and are involved with inflammatory immune responses and autoimmune conditions such as inflammatory bowel disease, multiple sclerosis and rheumatoid arthritis (Tesmer et al., 2008).

Th17 cell express the transcription factor retinoid-related orphan receptor γt (ROR-γt) which promotes Th17 phenotype including IL-17 expression (Unutmaz, 2009). Th17 cells can be generated in vitro upon co-treatment with TGF-beta and IL-6 and/or IL-21 (Awasthi and Kuchroo, 2009; Bettelli et al., 2006; Wilson et al., 2007). Although T cells increase their expression of AhR upon activation (Negishi et al., 2005), AhR was shown to be significantly upregulated in Th17-polarized T cell cultures treated with TGF-beta and IL-6 (Kimura et al., 2008; Quintana et al., 2008). Macrophages treated with TGF-beta and IL-6 however, did not upregulate AhR (Kimura et al., 2009), suggesting it is a cell-type specific phenomenon. The implications of this increased AhR expression during Th17 differentiation is not known, as it could allow Th17 effector T cells to be more sensitive to the effects of TCDD and other AhR ligands compared to other T cell effector subsets. However, Kimura et al. showed only a small effect of TCDD on the induction of IL-17 producing cells in vitro (Kimura et al., 2008). Importantly however, TCDD does not induce Th17-like effector activity, but rather appears to suppress Th17 differentiation (Quintana et al., 2008).

Another high affinity ligand of AhR, 6-formylindolo[3,2-b]carbazole (FICZ), is an endogenous photoproduct of tryptophan which unlike TCDD, was shown to exacerbate the onset and severity of EAE (Quintana et al., 2008; Veldhoen et al., 2008). These effects were AhR-dependent, and correlated with an increased frequency of Th17 cells. FICZ has also been shown to enhance Th17 cell generation in cultures treated with TGF-beta/IL-6 (Kimura et al., 2008; Quintana et al., 2008; Veldhoen et al., 2008). Kimura et al. showed that FICZ enhanced TGF-beta/IL-6-

induced Th17 development to approximately the same degree as TCDD (Kimura et al., 2008). These effects were not seen when the cells were $AhR^{-/-}$. FICZ also inhibited TGF-beta-induced Treg development in vitro (Quintana et al., 2008). The differential effects of TCDD and FICZ on Th17 and Treg development is not yet understood, however the rapid metabolism of FICZ by AhR-induced enzymes (Wei et al., 1998) is one plausible explanation for the discrepancies between the two ligands (Kerkvliet, 2009). The finding that TCDD enhanced Th17 generation in vitro, but inhibited Th17 development during EAE is contradictory, however it is likely that TCDD affects other cell types in vivo to influence Th17 generation. For example, IL-6 production is affected by TCDD exposure in different cell types (Hollingshead et al., 2008; Jensen et al., 2003; Kimura et al., 2009), in contrast to the direct addition of IL-6 to the in vitro cultures.

Natural AhR Ligands

A known high-affinity endogenous ligand of AhR has not been identified, thus AhR is still considered an orphan receptor. The ligand-binding site of AhR is promiscuous; structurally diverse synthetic and naturally occurring AhR ligands have been identified. TCDD, as the most potent ligand of AhR, is a good prototype for studying the effects of AhR activation as there is reduced chance for high dose off-target effects by a lower-affinity ligand or confounding effects due to ligand metabolism. Given the profound immunotoxicity of TCDD however, there is interest

in studying the effects of alternative AhR ligands on the immune system to not only identify putative natural endogenous ligands of AhR, but also explore the potential for alternative AhR ligands to alter disease outcome.

In addition to other synthetic halogenated aromatic hydrocarbon ligands of AhR like benzo[a]pyrene and TCDD, there is an abundance of naturally-occurring AhR ligands that we are exposed to both through endogenous biological processes and in our diet. Some of these compounds are converted in the gut to high affinity AhR ligands. Indole-3-carbinol, a metabolite of glucobrassicin found in cruciferous vegetables, is a weak AhR ligand that is converted to its acid condensation product indole[3,2-b]carbazole (ICZ) that binds and activates AhR with high affinity (Bjeldanes et al., 1991). The flavonoids are a large group of dietary AhR ligands that includes flavones, flavanols, flavanones and isoflavones which are a mixture of agonists and antagonists of AhR (Amakura et al., 2008; Zhang et al., 2003). Resveratrol, a known antagonist of AhR in the flavonoid family, was found to inhibit both TGF-beta- and TGF-beta/IL-6-mediated-induction of Treg and Th17 cells in culture, respectively (Quintana et al., 2008).

AhR ligands are also produced during different endogenous biological processes. The essential amino acid Tryptophan (Trp) is metabolized and photooxidized into multiple AhR ligands. One such photoproduct is FICZ, which was found to promote Th17 differentiation (Kimura et al., 2008; Quintana et al., 2008; Veldhoen et al., 2008). Trp photoproducts generated in cell culture media have been shown to affect AhR activity (Oberg et al., 2005). The enzyme IDO catalyzes degradation of Trp into products such as kynurenine which have been

implicated in immune suppression and induction of tolerance (Bauer et al., 2005; Belladonna et al., 2007; Frumento et al., 2002; Terness et al., 2002). Interestingly, kynurenine has been shown to activate AhR (Heath-Pagliuso et al., 1998) and induce a Treg phenotype (Fallarino et al., 2006). The antiallergic drug Tranilast is a derivative of Trp metabolite 3-hydroxyanthranilic acid which binds and activates AhR (Kerkvliet, 2009) and has been shown to suppress EAE in a mechanism linked to Tregs (Platten et al., 2005). Other endogenous ligands include the tetrapyrole heme degradation products biliverdin and bilirubin (Phelan et al., 1998; Sinal and Bend, 1997), modified low-density lipoprotein (McMillan and Bradfield, 2007), arachadonic acid metabolites lipoxin A4 (Schaldach et al., 1999) and [12(R)-HETE] (Chiaro et al., 2008) and prostaglandins including PGG2 (Seidel et al., 2001) have all been shown to activate AhR. Ultimately, studies of the effects of alternative AhR ligands on immune responses could provide further insight into how our diet and endogenous environments rich in AhR ligands influence the immune system.

Emerging Story for AhR Activation and Treg Development

The mechanism(s) underlying enhanced Treg induction and frequency in TCDD-treated mice is not yet understood. Activation of AhR by TCDD has been shown to induce adaptive Treg-like cells during acute GVHR, and is associated with increased numbers of $Foxp3^+$ Tregs in different mouse models. The induction of IDO expression in tolerogenic DCs and upregulation of TGF-beta expression in T cells by TCDD are some of the factors proposed to contribute to Treg induction.

AhR-mediated changes in gene expression patterns during effector T cell differentiation interferes with effector T cell development, and may result in the generation of adaptive Tregs by default. Whether preexisting $Foxp3^+$ Tregs are relatively resistant to the AhR-mediated effects of TCDD, and thus are functionally preserved during an immune response to explain increased frequency is also not yet known. Ultimately, furthering our understanding of how AhR acts to suppress immune responses, and specifically preserves and/or induces Tregs, may open up new approaches for drug development for treatment of conditions such as autoimmunity, allergic reactions and transplant rejection.

Objectives

First Objective

Further characterize the $CD25^+CD4+$ T cells generated in TCDD-treated mice during an acute GVH response by comparing and contrasting the cells phenotypically and functionally with naturally-derived $CD25^+CD4+$ Tregs.

Second Objective

Determine the role of selected genes expressed by the $CD25^+CD4+$ T cells in the induction of the Treg phenotype and/or suppression of CTL development in TCDD-treated mice.

Third Objective

Explore the utilization of phosphorodiamidate morpholino oligomers conjugated to cell-penetrating peptides to deliver into primary leukocytes and alter pre-mRNA splicing as a method to inhibit expression of genes identified in the second objective.

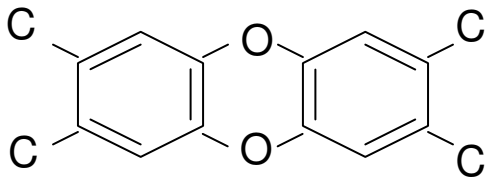

Figure 1.1. The basic chemical structure of 2, 3, 7, 8-Tetrachlorodibenzo-*p*-dioxin.

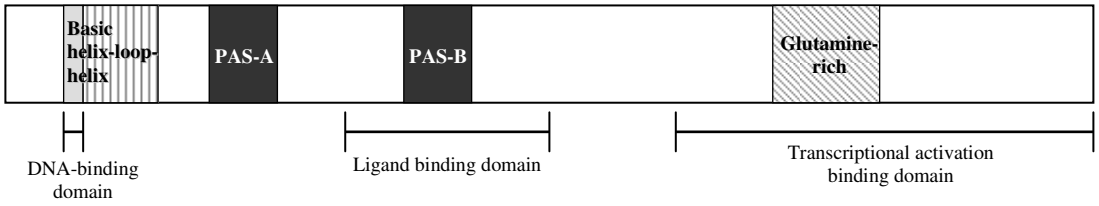

Figure 2.1. Functional domains of the aryl hydrocarbon receptor (AhR).
AhR contains several functional domains including a basic helix-loop-helix domain with a basic-region involved in DNA binding and a helix-loop-helix region that facilitates protein interactions. There are also two PAS domains, PAS-A and PAS-B, that are homologous to protein domains that were originally identified in the *Drosophila* genes period (Per) and single minded (Sim). The ligand-binding site of AhR is contained within the PAS-B domain. A glutamine-rich domain is located in the C-terminal region and is involved in co-activator recruitment and transactivation.

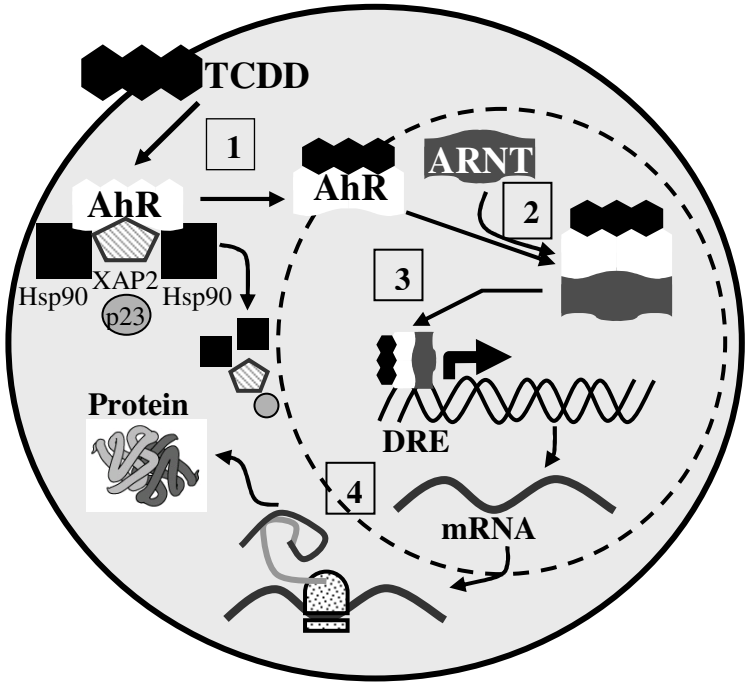

Figure 1.3. Schematic of the AhR signaling pathway.
Non-ligand bound AhR remains in the cytoplasm complexed with a dimer of heat shock protein 90 (Hsp90), prostaglandin E synthase 3 (p23), and immunophilin-like protein hepatitis B virus X-associated protein 2 (XAP2) (1). Upon ligand binding, a conformation change allows release of the chaperone proteins and nuclear trafficking of AhR where it heterodimerizes with the aryl hydrocarbon nuclear translocator (ARNT) (2). This heterodimer binds dioxin response elements of DNA containing the core sequence 5'-GCGTG-3' (3). This causes changes in gene expression that can be measured at the mRNA and protein levels (4).

Chapter 2

Functional Characterization and Gene Expression Analysis of $CD4^+$ $CD25^+$ Regulatory T Cells Generated in Mice Treated with 2, 3, 7, 8-Tetrachlorodibenzo-*p*-Dioxin

Authors: Nikki B. Marshall

William R. Vorachek

Linda B. Steppan

Dan V. Mourich

Nancy I. Kerkvliet

The Journal of Immunology

9650 Rockville Pike, Bethesda, MD. 20814-3998

August 2008; 181:2382-2391

Abstract

Although the effects of 2, 3, 7, 8-tetrachlorodibenzo-*p*-dioxin (TCDD) are mediated through binding and activation of the aryl hydrocarbon receptor (AhR), the subsequent biochemical and molecular changes that confer immune suppression are not well understood. Mice exposed to TCDD during an acute B6-into-B6D2F1 graft-vs.-host response do not develop disease, and recently this has been shown to correlate with the generation of $CD4^+$ T cells that express CD25 and demonstrate in vitro suppressive function. The purpose of this study was to further characterize these $CD4^+$ cells (TCDD-$CD4^+$s) by comparing and contrasting them with both natural regulatory $CD4^+$ T cells (T-regs) and vehicle-treated cells. Cellular anergy, suppressive functions and cytokine production were examined. We found that TCDD-$CD4^+$ cells actively proliferate in response to various stimuli but suppress IL-2 production and proliferation of effector T cells. Like natural T-regs, TCDD-$CD4^+$ cells do not produce IL-2, and their suppressive function is contact-dependent but abrogated by costimulation through GITR. TCDD-$CD4^+$ cells also secrete significant amounts of IL-10 in response to both polyclonal and alloantigen stimuli. Several genes were significantly upregulated in TCDD-$CD4^+$ cells including TGF-β3, Blimp-1, and granzyme B, as well as genes associated with the IL12-Rb2 signaling pathway. TCDD-$CD4^+$ cells demonstrated an increased responsiveness to IL-12 indicated by the phosphorylation levels of STAT4. Only 2% of TCDD-$CD4^+$s express Foxp3 suggesting that the AhR does not rely on Foxp3 for suppressive activity. The generation of $CD4^+$ cells with regulatory function mediated through

activation of the AhR by TCDD may represent a novel pathway for the induction of T-regs.

Introduction

The 2, 3, 7, 8-tetrachlorodibenzo-*p*-dioxin (TCDD) is a wide-spread environmental contaminant that induces profound immune suppression in mice. Although the immunosuppressive effects of TCDD are mediated through binding and activation of the aryl hydrocarbon receptor (AhR) (Ema et al., 1994; Okey et al., 1994), the subsequent biochemical and molecular changes that confer suppression are still not well elucidated. After binding TCDD, the AhR translocates to the nucleus where it dimerizes with the AhR nuclear-translocator (ARNT). This basic-helix-loop-helix PER-ARNT-SIM ligand-activated transcription factor can then bind core consensus sequences of DNA (5'-GTGCG-3') known as dioxin responsive elements (DREs), causing specific changes in gene expression (Schmidt and Bradfield, 1996; Yao and Denison, 1992). DREs have been identified in the promoter regions of several genes important for cell activation, proliferation, and differentiation (Lai et al., 1996; Sun et al., 2004). In 2002, Kerkvliet et al. demonstrated that T cells are direct, AhR-dependent targets of TCDD (Kerkvliet et al., 2002), and yet the implications of AhR activation during the process of effector T cell differentiation are not clear, with anergy, deletion and/or induction of regulatory T cells suggested in recent reports (Camacho et al., 2001; Camacho et al., 2005; Funatake et al., 2004; Funatake et al., 2005; Lawrence et al., 2006; Mitchell

and Lawrence, 2003a).

Regulatory T cells (T-regs) are a subset of T cells with immunosuppressive capabilities. Although the concept of suppressor T cells was described as far back as the early 1970s (Gershon et al., 1972), the naturally occurring $CD4^+$ $CD25^+$ T regulatory cells were not described until the mid-1990s (Sakaguchi et al., 1995). Subsequently, it was identified that natural T-regs express Foxp3, a transcription factor required for their development and regulatory function (Fontenot et al., 2003; Hori et al., 2003). Additional populations of adaptive regulatory T cells with distinct markers and activity have also since been described including inducible-$CD4^+$ $CD25^+$ T-regs (Apostolou and von Boehmer, 2004; Kretschmer et al., 2005), $CD4^+$ $CD25^-$ $Foxp3^-$ T-regs (Chen et al., 2004; Hansen et al., 2007), TGF-β-induced $CD4^+$ T-regs (Weiner, 2001; Zheng et al., 2002), IL-10-induced $CD4^+$ T-regs (Tr1) (Battaglia et al., 2006; Roncarolo et al., 2006), and $CD8^+$ $CD28^-$ $Foxp3^+$ cells (Najafian et al., 2003). The ability of immunosuppressive agents to induce T-regs has also been previously demonstrated. For example, the combination of vitamin D3 and dexamethasone has been shown to induce IL-10 secreting T-regs in culture (Barrat et al., 2002; Vieira et al., 2004). Rapamycin has been shown to cause de novo induction and maintenance of T-regs in culture (Valmori et al., 2006), and generate IL-10-secreting donor T cells in a lymphohematopoietic graft-vs.-host (GVH) model (Durakovic et al., 2007).

Our previous studies have shown that TCDD suppresses the $CD4^+$ T cell-dependent CD8+ cytotoxic T lymphocyte (CTL) response in a B6-into-B6D2F1 (F1) acute GVH response mouse model. In this model, the presence of AhR in both the

grafted $CD4^+$ and $CD8^+$ T cells is necessary for the full suppression of CTL in TCDD-treated mice (Kerkvliet et al., 2002). The alloreactive donor-derived CD4+ T cell population in TCDD-treated mice (TCDD-$CD4^+$ cells) consists primarily of proliferating $CD25^+$ cells that coexpress CTLA-4 and glucocorticoid-induced TNFR (GITR) at 48 h after adoptive transfer (Funatake et al., 2005). Furthermore, TCDD-$CD4^+$ cells share some functional characteristics with regulatory T cells including the ability to potently suppress the proliferation of anti-CD3 Ab-stimulated naïve $CD4^+$ T cells in culture, and a lack of proliferation in response to anti-CD3 Ab stimulation (Funatake et al., 2005).

The studies presented in this article provide an ex vivo characterization of TCDD-$CD4^+$ cells, including direct comparisons with natural T-regs. The purpose was to identify effector mechanisms as well as changes in gene and protein expression that help to explain the function and/or generation of TCDD-$CD4^+$ cells. TCDD-$CD4^+$ cells share several characteristics with natural T-regs but exhibit unique properties, including the ability to retain suppressive function in culture during proliferation. TCDD-$CD4^+$ cells produce significant amounts of IL-10 in response to polyclonal and alloantigen stimuli and express elevated levels of several gene transcripts including *TGF-β3*, *Blimp-1*, *granzyme B*, and *IL-12Rb2*. Little is known about the effects of TCDD on regulatory T cells and whether the induction of T-regs is one of the mechanisms by which TCDD suppresses the immune system. Activated AhR may act as an alternative to Foxp3 during activation-induced differentiation of naïve T cells to produce T-regs in TCDD-treated mice.

Materials and Methods

Mice

B6 and F1 mice were purchased from The Jackson Laboratory; B6.PL-Thy1^{a}/CyJ (Thy1.1^{+}, originally purchased from The Jackson Laboratory) were maintained as a breeding colony on-site. All animals were kept in a pathogen-free animal facility at Oregon State University (Corvallis, OR) and treated according to animal use protocols approved by the Institutional Animal Care and Use Committee at Oregon State University.

TCDD preparation and treatment

TCDD (99% purity; Cambridge Isotope Laboratories) was dissolved in anisole (JT Baker) and diluted in peanut oil. The anisole/peanut oil solution alone served as vehicle control. Host F1 mice were dosed with 15 µg/kg TCDD or with vehicle control by oral gavage within 24 h before the adoptive transfer of splenic Thy1.1^{+} donor T cells.

Preparation and injection of Thy1.1^{+} donor T cells

Splenocyte suspensions were prepared by dissociation of spleens between frosted microscope slides in HBSS containing 2.5% FBS, 50 µg/ml gentamicin and 20 mM HEPES followed by a 10-s water lysis of RBC. T cells (CD4^{+} and CD8^{+}) were isolated from pooled splenocytes using a Pan T cell isolation kit and autoMACS separator (Miltenyi Biotec) to >90% purity. In some experiments the

cells were labeled with 2 μM CFSE (Molecular Probes) before adoptive transfer. Sex-matched F1 host mice were injected i.v. via the tail vein with 2 X 10^7 B6 donor T cells. Host spleens were then harvested 48 h after the transfer.

Purification of Thy1.1$^+$ donor CD4+ T cells during GVH response

Donor Thy1.1$^+$ CD4$^+$ cells were isolated from F1 host splenocytes using a combination of panning and magnetic sorting methods. In this procedure, pooled splenocyte suspensions were isolated on the second day of the GVH response from vehicle- or TCDD-treated host mice and resuspended in HBSS containing 10% FBS, 50 μg/ml gentamicin, and 20 mM HEPES. The cells were added to non tissue culture treated petri plates coated with ant-mouse IgG (Jackson ImmunoResearch Laboratories) and then incubated (4˚C) to allow B cells to adhere. The remaining cell suspensions were transferred to new petri plates coated with anti-mouse IgG and anti-CD8a and incubated (4°C) to allow CD8$^+$ cells and additional B cells to adhere. Next, the remaining suspended cells were stained with PE-labeled anti-mouse Thy1.1 (clone OX-7; BD Pharmingen) and sorted with anti-PE microBeads on an autoMACS separator (Miltenyi Biotec). The purified cells (>80% CD4$^+$ Thy1.1$^+$) are designated as VEH-CD4$^+$ cells or TCDD-CD4$^+$ cells from vehicle- and TCDD-treated hosts, respectively. In some experiments, the dividing VEH-CD4$^+$ cells and TCDD-CD4$^+$ cells were identified by CFSE dilution and were sorted from pooled host spleens using a MoFlo cell sorter to >95% purity.

Splenocyte cultures

Splenocytes were cultured in RPMI 1640 medium containing 10% FBS, 50 µg/ml gentamicin and 50 µM 2-ME (cRPMI). For suppression assay cultures, naive B6 splenocytes were fractionated using a mouse $CD4^+$ $CD25^+$ regulatory T cell isolation kit and an autoMACS separator (Miltenyi Biotec). Isolated fractions included $CD4^+$ $CD25^+$ natural T-regs, $CD4^+$ $CD25^-$ responders that were labeled with CFSE (2 µM; Molecular Probes), and T cell-depleted accessory cells that were either gamma irradiated (3 kilorad) or mitomycin C treated (50 µg/ml) before culture. Naïve $CD4^+$ $CD25^+$ natural T-regs or donor CD4+ cells isolated from TCDD- or vehicle-treated F1 mice 48 h after adoptive transfer of donor T cells were titrated into culture (1:1 to 1:16 suppressor to responder ratio) with 2 X 10^5 responder CD4+ T cells, 1 X 10^5 accessory cells (ACs), and 0.25 µg/ml soluble anti-CD3 Ab (BD Biosciences) in cRPMI. Cells and supernatants were harvested 72 h later and dilution of CFSE in responder cells was measured by flow cytometry.

To some cultures containing purified donor $Thy1.1^+$ $CD4^+$ cells, exogenous rIL-2 (IL-2, eBioscience), IL-12 (eBioscience), or plate-bound anti-CD3 Ab was added as indicated. IL-2, IL-17A (eBioscience), TGF-β1 (Anogen), and TGF- β3 (R&D Systems) were measured in supernatants by ELISA as per manufacturer's instructions. IL-10, IL-4, and IFN-γ were measured with FlowCytomix Simplex kits (Bender MedSystems) according to the manufacturer's instructions on a Beckman Coulter FC-500 flow cytometer. Abs added to neutralize or ligate molecules in the assay included anti-mouse IL-10 (clone JES5-2A5; BD Pharmingen), anti-mouse GITR (clone DTA-1; eBioscience), and purified rat IgG2a (eBioscience) as isotype control. Recombinant soluble mouse TGF-βRII/mouse Fc (R&D Systems) was

added to bind and sequester TGF-β1 and TGF-β3.

To determine requirements for cell contact, a Corning HTS Transwell-96 tissue culture system with a 0.4-μM polycarbonate membrane was used to separate cultures containing TCDD-$CD4^+$ cells (or natural T-regs) (2.5 X 10^4) with ACs (5 X 10^4) (top insert) from CFSE-labeled $CD4^+$ responders (5 X 10^4) and ACs (5 X 10^4) (bottom insert) in cRPMI containing 0.5 μg/ml soluble anti-CD3 Ab.

Dendritic cell isolation and cultures

F1 dendritic cells (DCs) were derived from bone marrow cells flushed from tibias with a 25-gauge needle containing HBSS medium with 2.5% FBS and 50 μg/ml gentamicin. Cells were dissociated through a 100-μM nylon mesh cell strainer and cultured in non-tissue culture-treated 100 X 15-mm petri dishes in cRPMI containing 15 ng/ml GM-CSF (eBioscience). After three days of culture, floating and loosely adherent cells were collected and recultured in fresh cRPMI supplemented with GM-CSF for an additional 7 days of culture. The DCs were then used within an additional 14 days. Removal of adherent DCs was achieved with a 15-min incubation (4°C) with 5 mM EDTA followed by gentle-trituration. Maturation of DCs was achieved by incubation with 500 ng/ml LPS (E. coli 0111:B4, Sigma) for 24 h.

Flow cytometry

Splenocytes were washed and stained on ice in Dulbecco's PBS containing 1% BSA and 0.1% sodium azide. Cells were first incubated with rat IgG (Jackson

ImmunoResearch Laboratories) for Fc-receptor blocking and then stained with optimal concentrations of different combinations of anti-mouse mAbs including biotinylated-Thy1.1 (clone OX-7), allophycocyanin-Cy7-CD4 (clone GK1.5), PE-CD25 (clone PC61), or allophycocyanin-CD25 (clone PC61) from BD Biosciences. Foxp3 (clone FJK-16s) was measured using a PE anti-mouse/rat Foxp3 staining kit (eBioscience). STAT4 was measured using BD Phosflow reagents including mouse PE-STAT4 (clone 38/p-Stat4) as per the manufacturer's instructions. Samples lacking one of the individual stains (called fluorescence minus one) or antibody isotypes were used as staining controls. Viability of unfixed cells was measured with 7-amino-actinomycin D (Calbiochem), or with ethidium monoazide (Sigma-Aldrich) for fixed cells. A minimum of 5,000 donor $CD4^+$ events, or >10,000 nondonor events were collected per sample on a Beckman Coulter FC-500 flow cytometer. Data analysis and software compensation were performed using WinList (Verity Software).

Real-Time RT-PCR

IL-2 mRNA levels were measured in cultured cells using the RNAqueous-4PCR kit (Ambion) followed by cDNA synthesis. PCRs were conducted using the SuperScript III Platinum two-step quantitative RT-PCR Kit (Invitrogen). The following are the sequences of the IL-2-specific and 18S ribosomal subunit-specific (Proudnikov et al., 2003) primers and probes used: IL-2: 5'-CCTGAGCAGGATGGAGAATTACA-3' (forward), 5'-TCCAGAACATGCCGCAGAG-3' (reverse) (Biosource International), and 5'-

FAM-CCCAAGCAGGCCACAGAATTGAAAG-BHQ1-3' (probe) (Integrated DNA Technologies); 18S ribosomal subunit: 5'-CTTTGGTCGCTCGCTCCTC-3' (forward), 5'-CTGACCGGGTTGGTTTTG AT-3' (reverse), and, 5'-FAM-TGCCGACGGGCGCTGACC-BHQ1-3' (probe) (Biosource International). The real-time PCR protocol was one cycle at 50˚C for 2 min, 1 cycle at 95˚C for 2 min, and then 40 cycles at 95˚C for 20 s and 61˚C for 1 min. RT-PCRs were performed using a Bio-Rad iCycler instrument. mRNA levels of other genes were measured by semiquantitative RT-PCR (qPCR) in VEH-$CD4^+$ cells or TCDD-$CD4^+$ cells (n = 3; two pooled mice per *n*; >90% $Thy1.1^+$ purity) using the RNeasy mini kit and SuperArray ReactionReady first strand cDNA synthesis kit (Qiagen). PCRs were performed with RT^2 real-time SYBR Green/ROX master mix (SuperArray Bioscience) including gene-specific primers, and normalized for β-actin expression. Reactions were performed on an Applied Biosystems 7500 sequence detection instrument using the protocol: one cycle at 95˚ for 10 min, then 40 cycles at 95˚ for 15 s and 60˚ for 1 min followed by a denaturation step. Results were analyzed using ABI 7500 system software. The same VEH-$CD4^+$ and TCDD-$CD4^+$ cDNA samples were also used to measure the expression of 84 genes associated with T cell differentiation using a RT^2 Profile mouse Th1-Th2-Th3 PCR Array (SuperArray BioScience). The assay and data analysis were conducted as per the manufacturer's instructions.

Statistical analyses

Results are presented as the mean ± SEM for individual mouse and/or culture

well replicates as indicated. Unpaired *t* tests were performed using GraphPad Prism, GraphPad software where $p < 0.05$ (*), $p < 0.005$ (**), and $p < 0.0005$ (***) indicate statistical significance.

Results

TCDD does not induce Foxp3$^+$ cells during an acute GVH response

Foxp3, a Forkhead/winged-helix transcription factor, is expressed by natural $CD4^+$ $CD25^+$ T-regs, and is necessary for their development and suppressive function (Miyara and Sakaguchi, 2007). Because donor $CD4^+$ cells express a $CD25^{high}$ phenotype during the second day of the B6-into-F1 acute GVH response in TCDD-treated F1 host mice and demonstrate suppressive function in vitro (Funatake et al., 2005), it was important to determine if these cells also express Foxp3. B6 donor T cells were identified in spleens from F1 hosts treated with TCDD (TCDD-$CD4^+$) or vehicle control (VEH-$CD4^+$) by their expressions of the congenic marker Thy1.1, from which Foxp3, and CD25 were measured (Fig. 2.1*A*). As shown in Fig. 2.1*B*, Foxp3 was expressed at a low frequency in both TCDD-$CD4^+$ cells and VEH-$CD4^+$ cells (2-3% of cells), and significantly fewer TCDD-$CD4^+$ cells expressed Foxp3 (2.2% ± 0.15) than VEH-$CD4^+$ cells (2.7% ± 0.1; $p < 0.05$). When the co-expression of CD25 and Foxp3 was examined, only 9% of the $CD25^+$ TCDD-$CD4^+$ cells expressed Foxp3 compared with 21% of the $CD25^+$ VEH-$CD4^+$ cells (Fig. 2.1*C*). Furthermore, the Foxp3$^+$ cells present in the TCDD-$CD4^+$ population were not among those actively proliferating in response to alloantigen according to CFSE

dilution (data not shown), suggesting they represent residual natural T-regs present in the donor inoculum at the time of adoptive transfer. These data suggest that TCDD does not induce de novo generation of Foxp3$^+$ CD4$^+$ cells or expand the existing population. This is further supported by the finding that depleting CD25$^+$ cells from the donor cell inoculum before transfer into hosts does not influence the effects of TCDD on TCDD-CD4$^+$ cells (Funatake et al., 2005). Foxp3 protein expression was also measured in F1 host CD4$^+$ T cells and the percentages that were Foxp3$^+$ were not different between TCDD-treated (13.1% ± 0.4) and vehicle-treated mice (14.0% ± 0.7).

TCDD-CD4$^+$ cells do not produce IL-2 and suppress IL-2 production by responder T cells

Another important feature of natural T-regs is their lack of IL-2 production despite high CD25 expression. To determine whether this feature was shared by TCDD-CD4$^+$ cells, soluble IL-2 protein was measured in the supernatants of anti-CD3 Ab-stimulated naïve CD4$^+$ T cells, TCDD-CD4$^+$ cells, or natural T-regs at 24, 48, and 72 h. The highest levels of IL-2 were found at 48 h, at which time the supernatants from anti-CD3 Ab-stimulated naïve CD4$^+$ T cells contained 766 ± 34.9 pg/ml IL-2, compared with 19.6 ± 7.5 pg/ml and 8.9 ± 0.8 pg/ml IL-2 in TCDD-CD4$^+$ and natural T-reg supernatants, respectively (Fig. 2.2*A*). We suspected that the low levels of IL-2 in TCDD-CD4$^+$ and natural T-reg supernatants came from small numbers of contaminating effector CD4$^+$ T cells still present in the magnetically sort-purified populations. Hence, IL-2 was further examined at the mRNA level

early in culture (14 h) by q RT-PCR for the same purified populations of T cells. *IL-2* was detected in RNA isolated from anti-CD3-stimulated $CD4^+$ T cells but was below detectable levels in RNA isolated from stimulated TCDD-$CD4^+$ cells and natural T-regs, suggesting that, like natural T-regs, TCDD-$CD4^+$ cells do not produce significant amounts of IL-2.

In studies performed to measure suppressive function, TCDD-$CD4^+$ cells were titrated into a suppression assay culture consisting of naïve $CD4^+$ $CD25^-$ responder cells labeled with CFSE, soluble anti-CD3 Ab, and mitomycin-C-treated or gamma-irradiated accessory cells. The dynamics of IL-2 expression in this assay were examined to determine whether the suppressed proliferation of responder T cells in the presence of TCDD-$CD4^+$ cells was due to a lack of IL-2 in culture. As shown in Fig. 2.2*B*, an inverse relationship existed between increasing levels of IL-2 in the supernatants and decreasing numbers of TCDD-$CD4^+$ cells (and natural T-regs) in the culture. To determine whether TCDD-$CD4^+$ cells were sequestering or depleting IL-2 due to the high levels of CD25 being expressed, exogenous IL-2 was added to cultures containing only TCDD-$CD4^+$ cells, natural $CD25^+$ $CD4^+$ T-regs, or no cells (to control for degradation of IL-2 in culture over time), and then IL-2 levels were measured in the supernatants by ELISA 72 h later. We found that cultures containing TCDD-$CD4^+$ cells had at least as much remaining soluble IL-2 (411 ± 19.9 pg/ml) as those containing no cells (362.8 ± 0.36 pg/ml). In comparison, natural T-regs consumed almost half of the IL-2 (218 ± 1.3 pg/ml) over the 72-h period.

To determine whether IL-2 production by naïve $CD4^+$ responders was suppressed in the presence of TCDD-$CD4^+$ cells, IL-2 mRNA transcript levels were

measured at 14 h in suppression assay cultures containing titrated numbers of TCDD-CD4$^+$ cells or natural T-regs. As shown in Fig. 2.2*C*, compared with naïve CD4$^+$ T cells, IL-2 transcript levels were reduced > 90% in the presence of natural T-regs and barely detectable in the presence of TCDD-CD4$^+$ cells. Taken together, these data show TCDD-CD4$^+$ cells produce little IL-2, do not sequester or deplete the culture of IL-2, and suppress early IL-2 production by CD4$^+$ responders at the level of transcription. These findings, in part, account for the reduced proliferation of CD4$^+$ responders cocultured with TCDD-CD4$^+$ cells.

TCDD-CD4$^+$ cells are not anergic to stimuli in culture

Previous studies have shown that TCDD-CD4$^+$ cells are anergic in culture in response to anti-CD3 Ab stimulation without the addition of exogenous IL-2 (Funatake et al., 2005). Unexpectedly however, more recent studies using CFSE dilution to measure proliferation show that TCDD-CD4$^+$ cells continue to proliferate in culture in the presence of various stimuli. Specifically, at the time the donor cells were harvested from the host mice (48 h into the GVH response), the majority had undergone 2-4 divisions, but after 40 h of additional culturing with anti-CD3 Ab or IL-2, the majority of cells had undergone 6-9 divisions (Fig. 2.3*A*). The previous studies of TCDD-CD4$^+$ anergy measured [^{3}H]TdR incorporation after 72 h of anti-CD3-stimulation (Funatake et al., 2005). We have found, however, that the viability of TCDD-CD4$^+$ cells (and VEH-CD4$^+$ cells) stimulated with anti-CD3 can drop to <20% after 72 h, which may explain the original findings. Thus, in the suppression assay which included anti-CD3 Ab as the stimulus, TCDD-CD4$^+$ cells continue to

divide while suppressing the activation and proliferation of naïve $CD4^+$ T cells. The results from these CFSE studies that demonstrate TCDD-$CD4^+$ cells are not anergic in vitro are consistent with our observations that TCDD-$CD4^+$ cells continue to expand if left in vivo through 72 h after adoptive transfer (Funatake et al., 2005).

Suppressive functions of TCDD-$CD4^+$ cells require contact with responder cells but are relieved by costimulation through GITR

Natural T-regs require contact/close proximity with cells they suppress in vitro (Takahashi et al., 1998; Thornton and Shevach, 1998). To determine whether cellular contact was also required for the ex vivo suppressive function(s) of TCDD-$CD4^+$ cells, the TCDD-$CD4^+$ cells were separated from CFSE-labeled responder $CD4^+$ T cells using a Transwell system with a 0.4-μM membrane to prohibit cell contact, but still allow transfer of soluble molecules. We found that when separated by the membrane, the proliferation of the responder T cells was not suppressed by TCDD-$CD4^+$ cells (Fig. 2.3*B*), suggesting that the suppressive mechanism(s) of TCDD-$CD4^+$ cells require contact with the target responder cells in vitro. It has also been demonstrated that costimulatory signals abrogate suppression by natural T-regs, including stimulation through GITR (Shevach and Stephens, 2006; Shimizu et al., 2002). Because TCDD-$CD4^+$ cells also express high levels of GITR (Funatake et al., 2005), we added an agonistic anti-GITR Ab to the suppression assay culture and saw a dose-dependent reduction in the suppression of responder T cell proliferation by TCDD-$CD4^+$ cells (Fig. 2.3*C*). Thus, similar to natural T-regs, the absence of cell contact or the presence of costimulation are both capable of abrogating the

suppressive activity of TCDD-CD4$^+$ cells in culture.

Allostimulation also discriminates TCDD-CD4$^+$ cells from VEH-CD4$^+$ cells

Previous studies used anti-CD3/accessory cell stimulation of TCDD-CD4$^+$ cells to measure their functional activity ex vivo. TCDD-CD4$^+$ cells, however, were generated under conditions of allostimulation in vivo; thus we were interested to see whether continued allostimulation in vitro might discriminate TCDD-CD4$^+$ cytokine production and function from VEH-CD4$^+$ cells. F1 host spleens were harvested 48 h after adoptive transfer of donor T cells, and the splenocytes were cultured as a mixture of donor and host cells (n = 3 mice). Cytokines were measured in the culture supernatants after 18 h. Under these conditions, there was significantly more IL-10 detected in the supernatants from TCDD-treated mice (328.3 ± 34 pg/ml) compared with vehicle-treated mice (179.6 ± 48.3 pg/ml; $p < 0.01$) (Fig. 2.4*A*). In contrast, the supernatants collected from the vehicle-treated splenocytes contained significantly more IL-2 (445.3 ± 84.8 pg/ml) than those from TCDD-treated splenocytes (130.5 ± 15 pg/ml; $p < 0.01$) (Fig. 2.4*B*). The concentration of IL-2 in the supernatants from naïve nonstimulated splenocytes was not significantly different from that in the supernatants from TCDD-treated splenocytes, supporting our earlier observations that TCDD-CD4$^+$ cells produce little IL-2. There was, however, no significant difference in the concentrations of IFN-γ in the supernatants (data not shown).

To compare the suppressive function of VEH-CD4$^+$ cells and TCDD-CD4$^+$ cells under conditions of allostimulation, the cells were titrated into cultures containing LPS-matured F1 bone marrow-derived DCs (allo-DCs) and CFSE-

labeled responder T cells (both $CD4^+$ and $CD8^+$) purified from naïve B6 mice. Results showed significantly more suppression of proliferation of both $CD4^+$ and $CD8^+$ responder T cells in the presence of TCDD-$CD4^+$ cells compared with VEH-$CD4^+$ cells (Fig. 2.4*C*). Taken together these results demonstrate that TCDD-$CD4^+$ cells have suppressive function in culture in response to both anti-CD3 Ab and allo-DC stimuli and that they suppress proliferation of both $CD4^+$ and $CD8^+$ effector T cells.

TCDD-$CD4^+$ cells produce significant amounts of IL-10

Because increased concentrations of IL-10 were detected in the mixed donor and F1 host splenocyte cultures from TCDD-treated mice, it was important to determine whether TCDD-$CD4^+$ cells were producing it. Thus, IL-10, along with other cytokines of interest, were measured in supernatants harvested from sort-purified, actively dividing (according to CFSE dilution) TCDD-$CD4^+$ cells and VEH-$CD4^+$ cells after 72 hrs of anti-CD3 Ab stimulation. As with allostimulation, anti-CD3 Ab-stimulated TCDD-$CD4^+$ cells produced significantly more IL-10 than VEH-$CD4^+$ cells (Fig. 2.5*A*). IL-10 was not detected in cultures containing anti-CD3 Ab-stimulated natural T-regs or naïve $CD4^+$ T cells. When TCDD-$CD4^+$ cells were titrated into a suppression assay with naïve $CD4^+$ responders, the IL-10 concentrations in the supernatants were significantly increased ($p < .005$) compared with cultures containing VEH-$CD4^+$ cells (Fig. 2.5B). Neutralization of IL-10 with Ab had no effect on proliferation of responder T cells in the presence of TCDD-$CD4^+$ cells (data not shown) as has also been reported for natural T-regs in vitro

(Takahashi et al., 1998; Thornton and Shevach, 1998).

TGF-β1, another cytokine implicated in T-reg generation and/or effector function, was not detected in soluble form in TCDD-CD4$^+$ or VEH-CD4$^+$ supernatants; however, expression of cell surface-bound TGF-β1, as has been reported on natural T-regs (Nakamura et al., 2001), was not analyzed. A soluble TGF-β type II receptor was added to culture to sequester TGF-β1/TGF-β3, which had no effect on responder proliferation in the presence of TCDD-CD4$^+$ cells (data not shown) as has been reported for natural T-regs (Takahashi et al., 1998; Thornton and Shevach, 1998). Other soluble cytokines measured, including IFN-γ, IL-4, and IL-17A, were not detected.

Significant changes in gene expression occur in TCDD-CD4$^+$ cells compared with VEH-CD4$^+$ cells

The expressions of genes associated with different T cell differentiation pathways, including cytokines, transcription factors, activation markers and other immune-response-related genes, were examined in purified TCDD-CD4$^+$ cells and VEH-CD4$^+$ cells (n = 3 per treatment) using a commercially available PCR array (SuperArray Bioscience). As shown in Table I, 15 of the 84 genes in the array were significantly up-regulated in TCDD CD4$^+$ cells. The greatest change in expression was seen for *TGF-β3*, which was up-regulated 13-fold compared with VEH-CD4$^+$ cells. Genes associated with T-reg function that were significantly increased in TCDD-CD4$^+$ cells included *Ctla-4*, *IL-2Ra* (CD25), and *IL-10*. Also significantly increased >1.3-fold over VEH-CD4$^+$ cells were *IL-12Rb2*, *Ccr4*, *Stat4*, *Ccr5*, *Socs3*,

Tnfrsf8 (CD30), *Bcl-3*, *Gata-3*, *Icos*, *CD28*, and *Jak2*. In addition, TCDD exposure resulted in the significant down-regulation of some genes compared with vehicle (>1.3-fold) including *Tnfsf4* (OX40-L), *IL-13Ra*, *CD86*, *Bcl-6*, *IL-5*, *Nfkb-1*, and *Ccl5* (Table 2.1).

Using the same RNA samples, relative expression levels of *Cyp1a1* and AhR repressor (*Ahrr*), two genes known to be regulated by TCDD-mediated activation of the AhR, were measured by qPCR. The *Cyp1a1* message was detected in TCDD-$CD4^+$ cells but not in VEH-$CD4^+$ cells, and *Ahrr* message was increased 21-fold in TCDD-$CD4^+$ cells compared with VEH-$CD4^+$s. Expression of two target genes specifically altered by activation of the AhR had been appropriately up-regulated in TCDD-$CD4^+$ cells, allowing us to correlate other gene expression changes with the effects of TCDD-mediated activation of AhR. The relative expression levels of 11 other genes originally identified on a DNA microarray chip, were also measured (Fig. 2.6). Transcripts that were expressed in TCDD-$CD4^+$ cells >3-fold over VEH-$CD4^+$ cells included *Ccr9*, *granzyme B*, and *Blimp-1* (Fig. 2.6). However, the remaining genes including *Ador2b*, *Bach2*, *Entpd1*, *Ncoa1*, *Nfe212*, *Nr3c1*, *Pdcd4* and *Ppp3cb* were not changed compared to VEH-$CD4^+$ cells.

Protein changes in/on TCDD-$CD4^+$ cells consistent with gene expression changes

Several of the genes increased at the transcript level in the PCR array also showed increased expression at the protein level. Increased expression of CTLA-4 and CD25 on donor $CD4^+$ cells from TCDD-treated mice was reported previously using flow cytometry (Funatake et al., 2005), and increased levels of IL-10 had been

identified in the supernatants of cultured TCDD-CD4$^+$ cells (Fig. 2.4*A*, 2.5*A*). Unexpectedly, the *IL-12Rb2* message, along with other components of the IL-12R signaling pathway, *Stat4*, *Jak2*, and *Socs3* were up-regulated in TCDD-CD4$^+$ cells compared with VEH-CD4$^+$ cells. To determine whether the IL-12R pathway was more active in TCDD-CD4$^+$ cells, levels of phosphorylated STAT4 protein were measured in TCDD-CD4$^+$ cells and VEH-CD4$^+$ cells immediately after harvest from F1 host mice 48 h after adoptive transfer of the donor T cells. The percentage of cells expressing phosphorylated STAT4 in the TCDD-CD4$^+$ population was markedly increased compared with VEH-CD4$^+$ cells (Fig. 2.7*A,* time 0), suggesting an enhanced signaling of the IL-12R signaling pathway in TCDD-CD4$^+$ cells.

To examine the responsiveness of TCDD-CD4$^+$ cells and VEH-CD4$^+$ cells to IL-12, the cells were incubated with IL-12 for 1 or 2 h at room temperature and the percentage of cells expressing phosphorylated STAT4 was measured (Fig. 2.7*A*, *inset*). Results showed a time-dependent increase in the percent of TCDD-CD4$^+$ cells expressing phosphorylated STAT4; only after 2 h did the percentage of VEH-CD4$^+$ cells expressing phosphorylated STAT4 attain that of TCDD-CD4$^+$ cells (Fig. 2.7*A*). The mean channel fluorescence values for phosphorylated-STAT4 also increased per cell division, with the greatest levels expressed by TCDD-CD4$^+$ cells incubated with IL-12 (Fig. 2.7*B*). Together, the results suggest that TCDD-CD4$^+$ cells are more responsive to IL-12 than VEH-CD4$^+$ cells, both as a percentage of total cells and on a per cell basis, thus validating the functional significance of increased IL-12Rβ2 and STAT4 expression in TCDD-CD4$^+$ cells.

The gene with the greatest fold-increase in TCDD-CD4+ cells was an

isoform of TGF- β, *TGF-β3*. However, soluble TGF-β3 protein was not detected in TCDD-$CD4^+$ or VEH-$CD4^+$ culture supernatants by ELISA. Whether surface-bound or intracellular levels were present is not yet known. Also identified on the DNA microarray and validated by qPCR was *granzyme B*, increased almost 6-fold in TCDD-$CD4^+$ cells (Fig. 2.6). Soluble granzyme B protein was measured at picogram levels in culture supernatants by ELISA, but levels were not different between TCDD-$CD4^+$ cells and VEH-$CD4^+$ cells stimulated with anti-CD3 Ab or alloantigen (data not shown). Intracellular granzyme B expression as measured by flow cytometry was also not altered by TCDD (data not shown). We were also unable to confirm increased CD30, increased CCR5, or decreased CD86 cell surface protein expression at 48 h by flow cytometry on TCDD-$CD4^+$ cells. Table II summarizes protein expression that has been measured in/on TCDD-$CD4^+$ cells at 48 h and indicates the changes in expression relative to VEH-$CD4^+$ cells. Measurement of protein expression for other genes affected by TCDD exposure and their functional significance are still under investigation.

Discussion

We previously reported that the profound suppression of an acute GVH response in TCDD-treated mice was associated with the generation of donor-derived $CD4^+$ $CD25^+$ T-reg cells that was dependent upon activation of the AhR (Funatake et al., 2005). However, these studies did not address the mechanisms of their suppressive function or identify changes in gene expression associated with AhR

activation that may play a role in the generation or the effector function of these cells (TCDD-$CD4^+$ cells). Here, we have further characterized TCDD-$CD4^+$ cells by comparing and contrasting them ex vivo with natural T-regs as well as identified and validated changes in gene expression that correlate with the activation of AhR by TCDD.

Using natural T-regs as a control in our assays allowed us to identify the characteristics that were shared between them and TCDD-$CD4^+$ cells. Results showed that even though TCDD-$CD4^+$ cells do not express Foxp3, they do share in vitro characteristics with natural T-regs, including the requirement for contact/close proximity with the effector T cells they suppress and abrogation of suppression by costimulation through GITR. It is not yet known whether the GITR costimulatory signal acts on TCDD-$CD4^+$ cells, $CD4^+$ responders, or both to ultimately abrogate suppression. Furthermore, the effects of enhanced costimulation on TCDD-$CD4^+$ cells in vivo and the ability of this stimulation to relieve suppression of the allo-CTL response have not yet been studied. The finding that TCDD-$CD4^+$ cells can suppress the proliferation of both $CD4^+$ and $CD8^+$ allo-responders in culture suggests they could also suppress alloreactive CTL during the GVH response.

Potential suppressive effector molecules used by TCDD-$CD4^+$ cells were also examined. We found a significant increase in the amount of IL-10 produced both at the mRNA transcript and protein levels by TCDD-$CD4^+$ cells. When TCDD-$CD4^+$ cells were titrated into a suppression assay with $CD4^+$ responders, the levels of soluble IL-10 in the supernatants increased, suggesting that either TCDD-$CD4^+$ cells induced the responders to secrete IL-10 or the responders provided TCDD-

CD4+ cells with some factor(s) that enhanced TCDD-$CD4^+$ production of IL-10. Additionally, we found that *TGF-β3* was increased 13-fold in TCDD-$CD4^+$ cells compared to VEH-$CD4^+$ cells. An increase in *TGF-β3* has also been observed in previous studies of mouse thymocytes exposed to TCDD (Lai et al., 1997); however the immunological relevance of this more recently identified TGF-β isoform, primarily studied in processes of cell differentiation and development (Bandyopadhyay et al., 2006; Kaartinen et al., 1997) is not well known. We did not detect TGF-β1 or TGF-β3 protein in supernatants isolated from cultured TCDD-$CD4^+$ cells, however, it is possible they are expressed on the cellular membrane, because surface-bound TGF-β is a mechanism of suppression used by natural T-regs (Nakamura et al., 2001). Recently, Quintana et al. reported that the transfer of $CD4^+$ T cells from TCDD-treated mice offered some protection from the development of experimental autoimmune encephalomyelitis (EAE) that was not observed when transferred into mice expressing a T cell-restricted deficient TGF-β receptor II (Quintana et al., 2008). The authors interpreted this to mean that T-regs induced by the activation of AhR by TCDD controlled EAE by a TGF-β1-dependent mechanism; however, TGF-β3 also binds this receptor. Neutralization of IL-10 or TGF-β in the in vitro suppression assay was unable to abrogate the suppression by TCDD-$CD4^+$ cells; however, the importance of these effector molecules for in vivo suppression of the GVH response in TCDD-treated mice remains to be determined.

Although the collective mechanisms of suppression used by natural T-regs and the identification of the most important of these has not been fully elucidated, the ultimate result is suppressed production of IL-2 by target responder T cells in the

presence of natural T-regs in vitro (Thornton and Shevach, 1998). This same observation for TCDD-CD4$^+$ cells helps explain the suppressed proliferation of effector T cells when they are co-cultured in the suppression assay. Decreased IL-2 in the cultures did not appear to be due to sequestering by TCDD-CD4$^+$ cells, although the CD25 expressed by TCDD-CD4$^+$ cells is functional as measured by increased STAT5 phosphorylation after the addition of exogenous IL-2 (Funatake et al., manuscript in preparation). TCDD-CD4$^+$ cells, like natural T-regs, expressed little to no IL-2 in response to anti-CD3 Ab or alloantigen stimuli. Dioxin response elements distal to the IL-2 gene promoter have been identified that, when bound by liganded AhR, enhance IL-2 gene expression (Jeon and Esser, 2000). Although we observed a lack of IL-2 expression by TCDD-CD4$^+$ cells at 48 h, enhanced IL-2 secretion by TCDD-CD4$^+$ cells appears to occur early in the GVH response (Funatake, manuscript in preparation). Neutralization of IL-2 with Ab during the GVH response did not decrease CD25 expression on TCDD-CD4$^+$ cells (Farrer and Steppan, unpublished observations), suggesting that CD25 expression could be driven independently of IL-2 production at 48 h.

Analysis of changes in gene expression in TCDD-CD4$^+$ cells led to the unexpected finding that genes involved in the IL-12R signaling pathway were up-regulated. *IL-12Rb2* and *Stat4* were upregulated >9-fold and >3-fold over vehicle control, respectively. *Jak2*, the kinase that phosphorylates tyrosine residues on the activated IL-12R and on STAT4 was also up-regulated. At the protein level, the percentage of TCDD-CD4+ cells expressing phosphorylated STAT4 was increased compared with that of the VEH-CD4$^+$ cells, and ex vivo stimulation with IL-12

validated an enhanced IL-12R signaling capacity of TCDD-CD4$^+$ cells with enhanced phosphorylation levels of STAT4 both as a percentage of total cells and on a per cell basis. The implications of enhanced signaling of the IL-12Rb2 pathway on the function or generation of TCDD-CD4$^+$ cells are currently under investigation. Because IL-12-responsive elements can cause chromatin remodeling at the CD25 gene locus and increase CD25 expression (O'Sullivan et al., 2004), IL-12 signaling may be an important pathway for up-regulating CD25 on TCDD-CD4$^+$ cells. The JAK2/STAT4 pathway is also important in the promotion of IFN-γ production; however increased expression of IFN-γ at the transcript or protein level in TCDD-CD4$^+$ cells was not found. This may suggest a breakdown in the signaling pathway distal to JAK/STAT phosphorylation or additional constraints imposed on IFN-γ gene expression by TCDD exposure. For example, *Gata-3* transcript that is upregulated almost 2-fold in TCDD-CD4$^+$ cells, can also induce IL-10 expression (Chang et al., 2007) and inhibit IFN-γ production mediated by STAT4 (Mendoza, 2006).

We were surprised to find *granzyme B* message increased almost 6-fold in TCDD-CD4$^+$ cells compared with VEH-CD4$^+$ cells, and that *granzymes A* and *B* were some of the most highly expressed genes in TCDD-CD4$^+$ cells according to the microarray gene chip. We explored the significance of these findings given that granzymes have been identified as T-reg effector molecules (Gondek et al., 2005; Grossman et al., 2004). Soluble and intracellular granzyme B levels were measured but were not different between TCDD-CD4$^+$ cells and VEH-CD4$^+$ cells stimulated with anti-CD3 Ab or alloantigen. Granzymes, which induce apoptosis, are an

unlikely in vitro suppressive mechanism used by TCDD-CD4$^+$ cells, as there is no additional decrease in the viability of CD4$^+$ responders cocultured with them compared with those cocultured with VEH-CD4$^+$ cells (N. B. Marshall and N. I. Kerkvliet, unpublished observations). The significance of granzyme production by TCDD-CD4$^+$ cells in vivo, however, is still not known.

There were a few additional changes in gene expression that we found particularly interesting with respect to the effects of TCDD on T cells. *Blimp-1*, which is up-regulated ~3-fold at the transcript level in TCDD-CD4$^+$ cells, is a transcriptional repressor that is postulated to play a role in effector T cell differentiation (Kallies et al., 2006). It has been shown that Blimp-1-deficient CD4$^+$ T cells produce excess IL-2 and IFN-γ but reduced IL-10 after TCR stimulation (Martins et al., 2006). Additional findings have suggested a negative feedback loop exists wherein IL-2 inhibits its own production through induction of Blimp-1 (Gong and Malek, 2007). These data support our observations that TCDD-CD4$^+$ cells produce little IL-2 and IFN-γ but significantly more IL-10. However, we have not yet validated increased Blimp-1 expression at the protein level. Also, the >2-fold increase in *CD30* transcript expression in TCDD-CD4$^+$ cells is potentially important, as CD30 increases on T-regs exposed to alloantigen and is critical for protection against acute GVH disease (Zeiser et al., 2007). We were unable to validate increased CD30 protein expression at 48 h, which could suggest that expression increases at a different time point during the response. A significant down-regulation (>2-fold) of *IL-13Ra* and *CD86* gene transcripts was also observed and was consistent with a microarray analysis of genes expressed in PBMCs

collected from humans exposed to TCDD (McHale et al., 2007). Surface CD86 protein expression however, was not different between TCDD-$CD4^+$ cells and VEH-$CD4^+$ cells at 48 h.

We do not yet know the fate of TCDD-$CD4^+$ cells in vivo, as the cells start to disappear from the F1 host spleen at 96 h. The up-regulation of chemokine receptor transcripts associated with T cell homing suggests the cells may be trafficking to other tissues. CCR4, a chemokine receptor associated with homing to allograft tissues and the skin (Campbell et al., 2007; Lee et al., 2005), is expressed by natural T-regs (Hirahara et al., 2006) and is up-regulated almost 5-fold at the transcript level in TCDD-$CD4^+$ cells. The *CCR5* transcript, increased 3-fold in TCDD-$CD4^+$ cells, is a chemokine receptor normally associated with Th1-polarized T cells and yet its expression by T-regs is required for suppression of GVH disease (Wysocki et al., 2005). CCR9, expressed by leukocytes that home to the small intestine, is also up-regulated almost 5-fold at the transcript-level in TCDD-$CD4^+$ cells. Determining whether or where TCDD-$CD4^+$ cells traffic in vivo is currently being studied, and could help to identify where the generation of similar T-reg like cells occurs in other models with TCDD exposure.

In this GVH model, we found no evidence for the expansion or de-novo generation of $Foxp3^+$ cells in either the donor or host $CD4^+$ T cell populations exposed to TCDD. Furthermore, depletion of $CD25^+$ cells from the donor inoculum does not alter the T-reg phenotype of TCDD-$CD4^+$ cells (Funatake et al., 2005). Thus, because the phenotype and suppressive function of TCDD-$CD4^+$ cells appear to be independent of Foxp3 expression, it is possible that ligand-activated AhR acts

as an alternative to Foxp3 in naïve T cells exposed to TCDD during activation and differentiation into effectors. Although Foxp3 does not appear to be involved in T-reg generation during GVH, a recent report links suppression of EAE by TCDD treatment with increased $Foxp3^+$ T-regs (Quintana et al., 2008). Similarly, recent data from our laboratory links suppression of diabetes in NOD mice treated with TCDD to an expanded population of $Foxp3^+$ $CD4^+$ cells (N. I. Kerkvliet, L. B. Steppan, W. R. Vorachek, S. Oda, C. Wong, D. Pham, and D. V. Mourich, manuscript in preparation). Thus the role of AhR activation by TCDD in T-reg development appears to depend on the conditions of T cell activation; in some conditions it may drive de novo induction of adaptive T-regs, or in other conditions it may support $Foxp3^+$ T-reg expansion.

One of the questions that needs to be answered is: if the normal pattern of gene expression required for activation-induced differentiation of a naïve T cell into an effector T cell is interrupted, is the default differentiation into a regulatory T cell? Furthermore, what are the specific genetic changes that may cause this? For example, a deacetylase inhibitor has been shown to promote the generation and function of T-regs (Tao et al., 2007) as a result of interrupting normal chromatin remodeling during T cell activation. Similarly, perhaps the inappropriate activation by TCDD of a transcription factor such as AhR during T cell activation causes a default differentiation into a T-reg, as the "normal" gene expression pattern is altered. Thus, it is important to further identify the epigenetic changes that occur in T cells exposed to TCDD to understand how the AhR pathway may provide new insight into regulatory T cell induction. Ultimately, this may introduce a novel

therapeutic role for the AhR and certain other agonist AhR ligands.

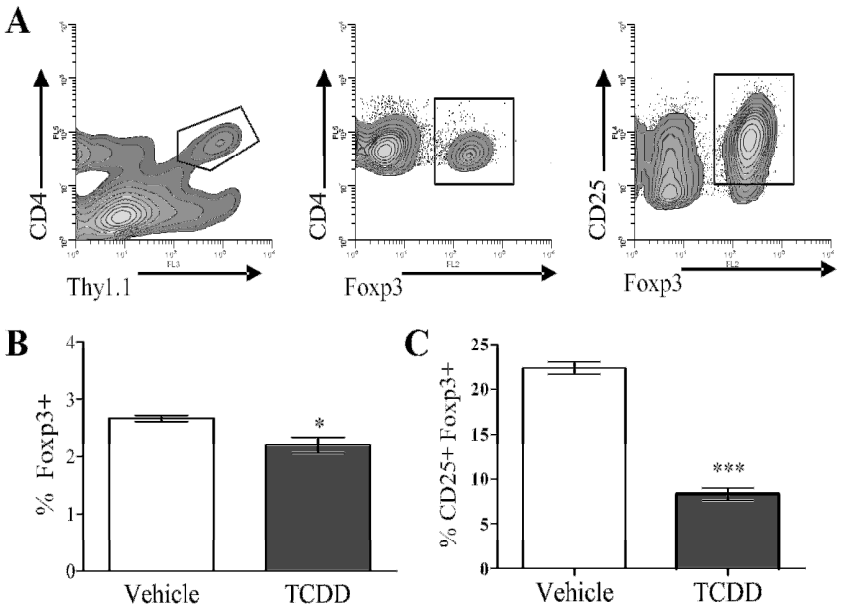

Figure 2.1. The frequency of Foxp3$^+$ donor CD4$^+$ cells is decreased in mice exposed to TCDD during acute GVH response.
A, Using flow cytometry, B6 donor CD4$^+$ cells were identified in vehicle- or TCDD-treated F1 host mice at 48 h after adoptive transfer by their expression of the congenic marker Thy 1.1, from which Foxp3, and/or CD25 were measured. *B* and *C*, The percentage of Thy1.1$^+$ CD4$^+$ cells (*B*), and percentage of Thy1.1$^+$CD4$^+$ CD25$^+$ cells (*C*) expressing Foxp3 is shown. These data are representative of two separate experiments (n = 3 mice per treatment group). Asterisks indicate statistically significant difference in the percent of Foxp3$^+$ cells compared with vehicle control (t test; *, $p < 0.05$; ***, $p < 0.0005$).

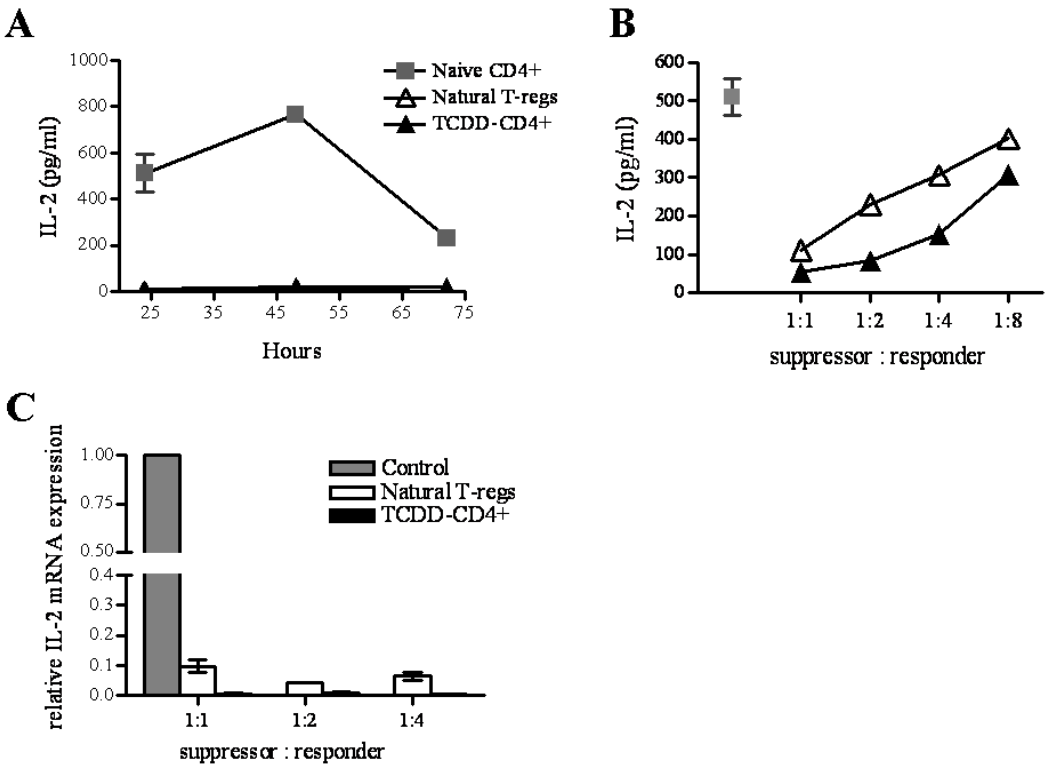

Figure 2.2. TCDD-CD4$^+$ cells suppress IL-2 production by responder CD4$^+$ T cells. *A*, IL-2 protein levels were measured by ELISA in supernatants from cultures containing anti-CD3 Ab and irradiated ACs cocultured with either naïve CD4$^+$ cells, natural T-regs, or magnetically sorted TCDD-CD4$^+$ cells at 24, 48, and 72 h (triplicates). *B*, IL-2 was measured in suppression assay supernatants harvested at 24 h containing naïve CD4$^+$ responder cells alone or co-cultured with either natural T-regs or TCDD-CD4$^+$ cells titrated in at 1:1 to 1:8 suppressor to responder ratios. *C*, The relative expression of *IL-2* was determined by qRT-PCR (normalized for 18S ribosomal subunit expression) in cells harvested from a suppression assay at 14 h including naïve CD4$^+$ responders cultured alone or cocultured with TCDD-CD4$^+$ cells or natural T-regs at 1:1 to 1:4 suppressor to responder ratios.

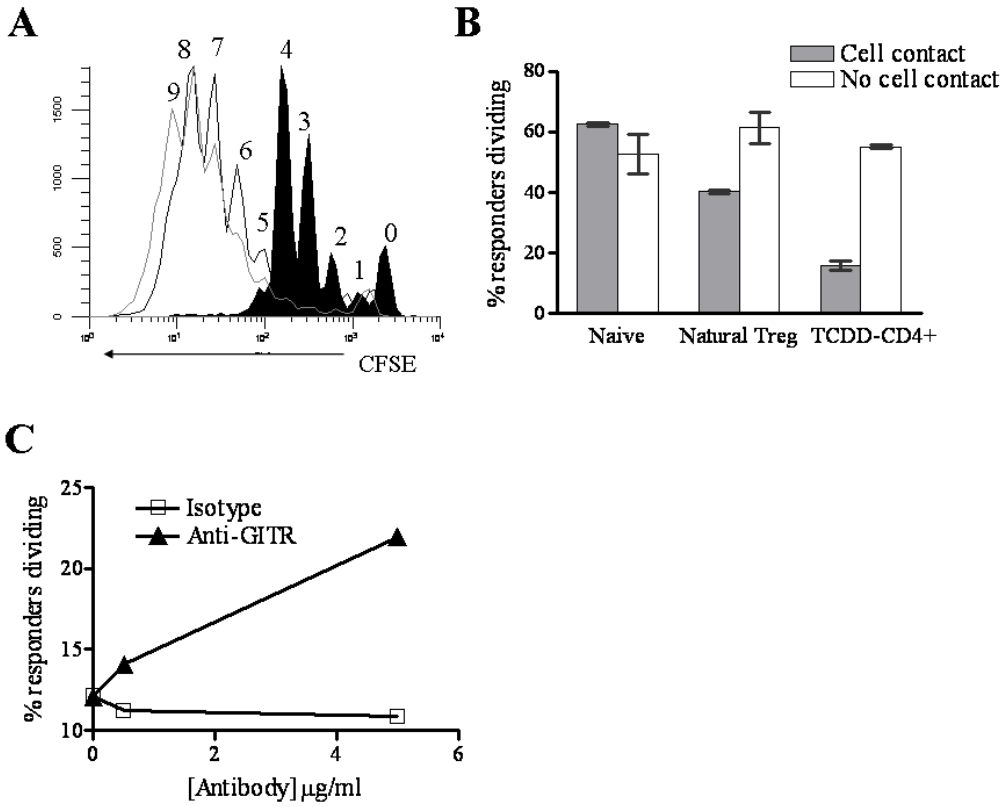

Figure 2.3. TCDD-CD4$^+$ cells proliferate in culture and require cell contact for suppressive function that is released by ligating GITR.
A, TCDD-CD4$^+$ cells were magnetically purified from pooled F1 host spleens (filled histogram) and cultured for 40 h with 50 U/ml IL-2 (black line histogram), or plate-bound anti-CD3 Ab (5 µg/ml) (gray line histogram). Cell divisions are numbered as per CFSE dilution, and are representative of three separate experiments. *B*, For cell-contact studies, TCDD-CD4$^+$ cells or B6 natural T-regs were magnetically purified and then cultured with anti-CD3 Ab (0.5 µg/ml) and irradiated ACs together with ("cell contact") or separated from ("no cell contact") CFSE-labeled naïve CD4$^+$ responders by using a 96-well Transwell system for 72 h; "Naïve" indicates wells that contained no suppressors. *C*, TCDD-CD4$^+$ cells were cocultured with CFSE-labeled CD4$^+$ CD25$^-$ T cells, anti-CD3 Ab (0.25 µg/ml) and irradiated ACs for 72 h with 0, 0.5, or 5 µg/ml anti–GITR (clone DTA-1) or rat IgG2b isotype control Abs.

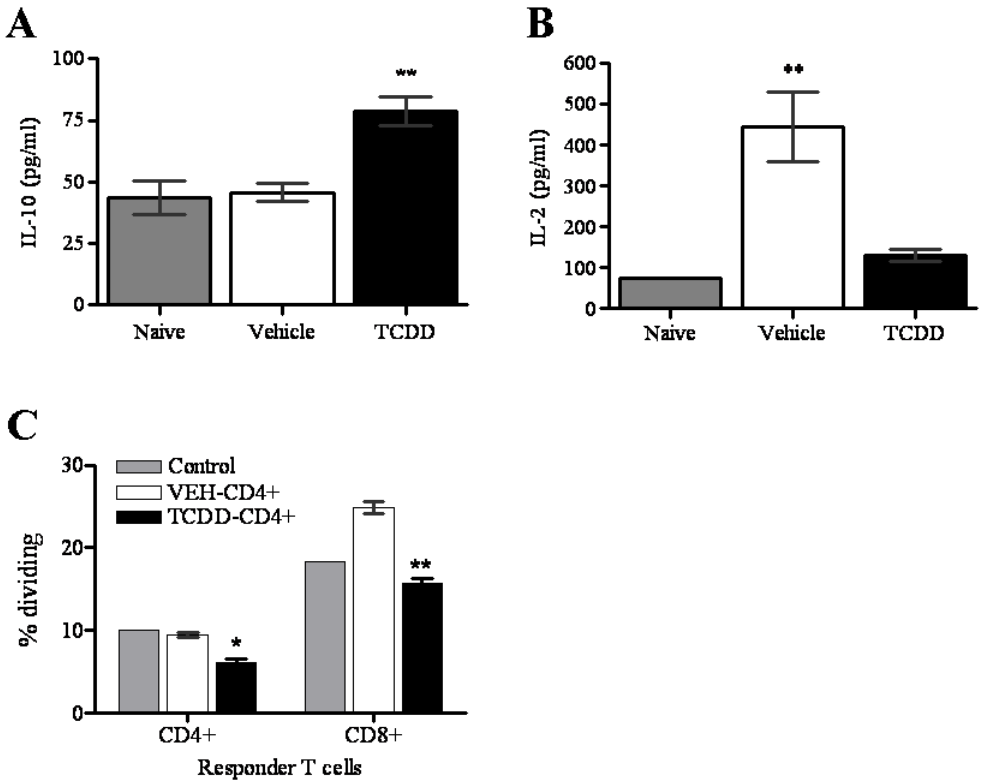

Figure 2.4. Allostimulation discriminates TCDD-CD4$^+$ and VEH-CD4$^+$ cytokine production and suppressive function.
A and *B*, Splenocytes were harvested from either naïve B6 mice, TCDD-treated, or vehicle-treated F1 host mice 48 h after adoptive transfer of B6 T cells (n = 3 mice) and then cultured at 1 X 10^7/ml for 24 h before the harvest of supernatants and assaying for cytokines *C*, Magnetically purified TCDD-CD4$^+$ or VEH-CD4$^+$ cells (1 X 10^5) were cultured for 72 h with 2 X 10^5 CFSE-labeled responder T cells (combination of CD4$^+$ and CD8$^+$) and 3.2 X 10^4 LPS-matured bone marrow-derived F1 DCs; the percentage of responder T cells dividing was measured by CFSE dilution. Control indicates no donor cells added (adjusted for cell density). Statistical significance compared with vehicle is indicated (t test; *, $p < 0.05$; ** < 0.005).

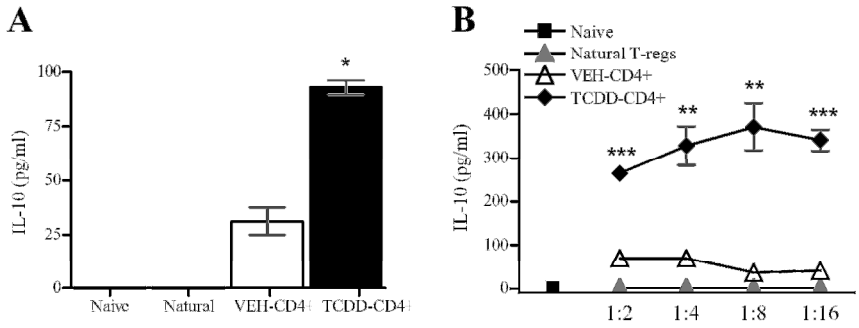

Figure 2.5. TCDD-CD4$^+$ cells secrete significant levels of IL-10.
Naïve CD4$^+$ responders, natural T-regs, VEH-CD4$^+$ cells or TCDD-CD4$^+$ cells were cultured separately with irradiated ACs and anti-CD3 Ab (5 µg/ml plate-bound) (A) or titrated in with CD4$^+$ responders (B); supernatants were harvested at 72 h and assayed for IL-10 (triplicates). Statistically significant differences are indicated in comparison to VEH-CD4$^+$ cells (*t* tests; *, $p < 0.05$; **, $p < 0.005$; $p < 0.0005$).

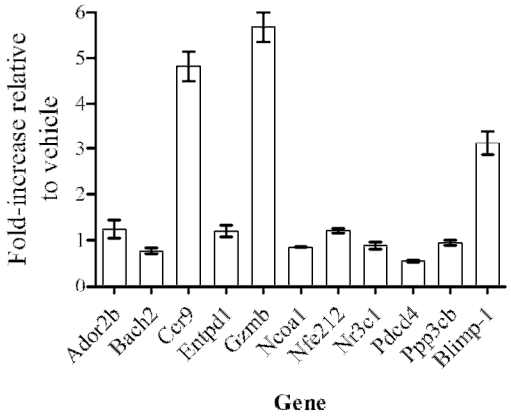

Figure 2.6. qPCR validation of gene expression in TCDD-CD4$^+$ cells.
Up-regulated genes of interest identified on a DNA microarray chip were validated by qPCR using gene-specific primers and normalized for β-actin expression. Results are expressed as fold increase in gene expression in TCDD-CD4$^+$ cells relative to VEH-CD4$^+$ cells; $n = 3$ per treatment ($n = 2$ pooled mouse spleens).

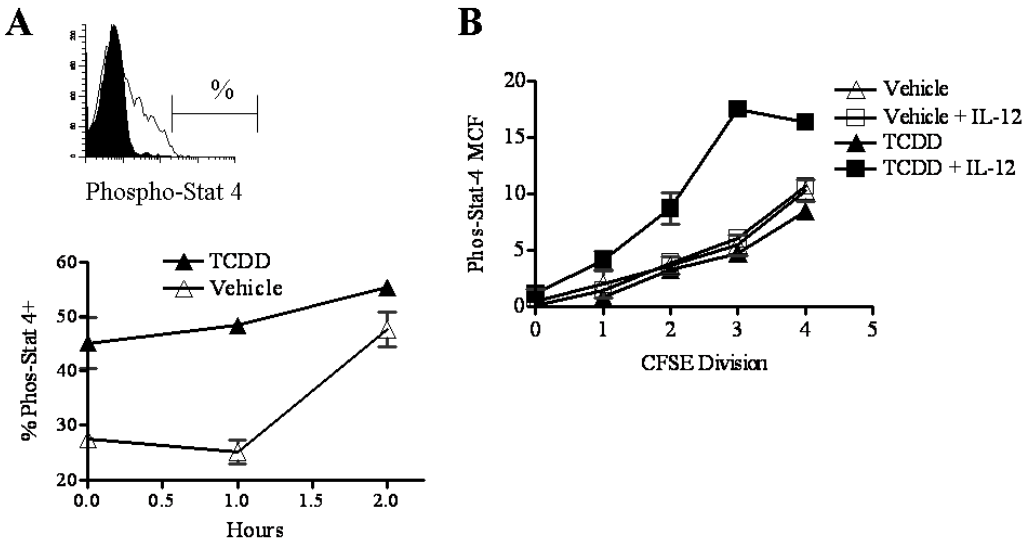

Figure 2.7. TCDD-CD4$^+$ cells express enhanced STAT4 phosphorylation and responsiveness to IL-12.
A, Splenocytes harvested from vehicle- or TCDD-treated F1 hosts (n = 2) at 48 h after the adoptive transfer of donor cells were cultured in cRPMI with rIL-12 (2 ng/ml) at room temperature (duplicate cultures). The percentage of donor CD4$^+$ cells expressing phosphorylated STAT4 was measured by flow cytometry (*top*) immediately after harvest from the mice (0) (representative of 3 separate experiments) or after 1-2 h of culture (*bottom*). *B*, STAT4 phosphorylation (MCF, mean channel fluorescence) was measured in VEH-CD4$^+$ cells or TCDD-CD4$^+$ cells per cell division (indicated by CFSE-dilution) after 1 h of culture at room temperature with or without IL-12 (2 ng/ml).

Table 2.1. Significant changes in gene expression in TCDD-CD4$^+$ cells relative to VEH-CD4$^+$ cells after 48 h of acute GVH response[a]

Gene	Average Fold Difference (TCDD vs. Vehicle)
Tgf-b3	13.1
IL12-rb2	9.8
Ccr4	4.7
Stat4	3.3
Ccr5	3.0
Socs3	2.7
Cd30	2.6
Bcl3	2.4
Ctla4	2.3
Cd25	1.9
IL-10	1.8
Gata3	1.8
Icos	1.5
Cd28	1.4
Jak2	1.3
Ox40L	-2.9
IL13-ra	-2.3
Cd86	-2.2
Bcl6	-1.5
IL-5	-1.4
Nfkb1	-1.4
Ccl5	-1.4

[a]The expression of genes associated with Th1, Th2, and Th3 classes of T cells were measured in VEH-CD4$^+$ and TCDD-CD4$^+$ cDNA samples (n = 3, two pooled mouse spleens per n) by PCR array. Only genes that were significantly changed (t test, $p < 0.05$) are indicated.

Table 2.2. Summary of protein expression changes in/on TCDD-CD4$^+$ cells relative to VEH-CD4$^+$ cells after 48 h of acute GVH response

Protein[a]	Change in Expression Relative to Vehicle[b]
4-1BB	ND
CCR5	ND
CD5	Decrease (MCF)
CD25	Increase
CD28	ND
CD30	ND
CD62-L	Decrease
CD86	ND
CD103	ND
CTLA-4	Increase
FasL	ND
Foxp3	Decrease (%)
GITR	Increase
Granzyme B	ND
Phosphorylated-STAT4	Increase

[a]The expression of proteins either identified as changed at the transcript level or reported to be associated with regulatory T cells were measured in/on TCDD-CD4$^+$ cells by flow cytometry.
[b]ND indicates expression was not different between VEH-CD4$^+$ cells and TCDD-CD4$^+$ cells. Significant change in expression relative to VEH-CD4$^+$ cells is indicated as an increase or decrease in percentage of cells and the mean channel fluorescence (MCF) measured by flow cytometry unless specifically indicated ($n \geq 3$; t test, $p < 0.05$).

Chapter 3

Arginine-rich Cell Penetrating Peptides Facilitate Delivery of Antisense Oligomers into Murine Leukocytes and Alter Pre-mRNA Splicing

Authors: Nikki B. Marshall

Shannon K. Oda

Carla A. London

Hong M. Moulton

Patrick L. Iversen

Nancy I. Kerkvliet

Dan V. Mourich

Journal of Immunological Methods

Elsevier Publishing

August 31 2007; 325:114-126

Abstract

Phosphorodiamidate morpholino oligomers (PMO) are synthetic antisense molecules that interfere with translation, pre-mRNA splicing and RNA synthesis. Like other gene-silencing technologies, PMO are poorly taken up by primary leukocytes without the use of physical or chemical delivery techniques. We sought an alternative delivery mechanism of PMO into immune cells that eliminates the need for such manipulations. Here we demonstrate the first use of arginine-rich cell penetrating peptides (CPPs) to deliver PMO (P-PMO) directly into primary murine leukocytes for inhibition of gene expression and promotion of altered pre-mRNA splicing. We compared the P-PMO delivery efficacy of four arginine-rich CPPs including HIV Tat and penetratin, and one histidine rich CPP, and found that the $(RXR)_4$ peptide was the most efficacious for PMO delivery and targeted antisense effect. The delivery and antisense effects of P-PMO are time- and dose-dependent and influenced by the activation and maturation states of T cells and dendritic cells, respectively. Targeted expression of several genes using P-PMO is shown including surface signaling proteins (CD45 and OX-40), a cytokine (interleukin-2), and a nuclear transcription factor (Foxp3). Considering the abundance of naturally occurring alternatively spliced gene products involved in immune regulation, P-PMO offer an effective method for modulating gene activity for immunological research and applications beyond traditional antisense approaches.

Introduction

Antisense is a method of altering gene expression by introducing RNA, DNA or synthetic oligomers that complement sequences within a targeted mRNA molecule. There are two traditional approaches to disrupting mRNA translation using antisense: (i) targeting of the AUG start site and thus sterically blocking ribosomal assembly or scanning and (ii) targeting the mRNA for nuclease degradation using RNase H or siRNA and target prediction algorithms. Applying antisense technologies in leukocytes has been challenging given that delivery requires physical or chemical manipulations that often damage cells, confounding the results of inhibiting a specific gene's expression (Ghosh and Iversen, 2000). Furthermore, pattern recognition molecules expressed by most lymphoid cells allows for exquisite sensitivity to the introduction of nucleotide oligomers. Therefore, if antisense is to be useful in the field of immunology, methods are needed to deliver molecules that are effective and specific for altering targeted gene expression, can be monitored by a positive read-out, and do not perturb the activity of cultured primary cells so that effects of gene silencing are not misinterpreted.

The synthetic antisense molecules phosphorodiamidate morpholino oligomers (PMO), are structurally similar to RNA but the phosphorodiester linkage is replaced with a neutral phosphorodiamidate linkage, and the ribose ring is substituted with a 6-membered Morpholino ring (Summerton and Weller, 1993; Summerton and Weller, 1997). As a result of these modifications, PMO are chemically stable and resistant to nucleases and other cellular enzymes including

RNase H (Hudziak et al., 1996; Stein et al., 1997; Youngblood et al., 2007). PMO have been used to alter gene expression in primary leukocytes, however the cellular membranes were physically or chemically perturbed to facilitate delivery into the cells (Ehlers et al., 2003; Kryczek et al., 2006; Vaknin-Dembinsky et al., 2006).

Cell penetrating peptides (CPPs) rich in basic cationic amino acids like arginine have well-documented use as intracellular delivery vectors for cargo including peptides, proteins, nucleic acids, and oligonucleotides (Wagstaff and Jans, 2006). The efficacy of PMO conjugated to arginine-rich CPPs (P-PMO) targeted against infectious agents has been repeatedly demonstrated in cell culture (Deas et al., 2005; Enterlein et al., 2006; Ge et al., 2006; Kinney et al., 2005; Tilley et al., 2006) and in-vivo (Burrer et al., 2007; Tilley et al., 2007; Yuan et al., 2006). It was not known whether P-PMO could deliver into primary leukocytes and target gene expression in a highly specific manner.

PMO alter gene expression by inhibiting translation, disrupting RNA secondary structure, or interfering with pre-mRNA splicing. The classic antisense target has been the sequence surrounding the AUG start codon, however there are other effective targeting strategies. For example, it has been demonstrated that P-PMO prevent IRES function by binding to sites of RNA secondary structure (Yuan et al., 2006). Gene expression can also be disrupted by targeting sequences that flank exon-intron boundaries of pre-mRNA (Kole and Sazani, 2001; Kole et al., 2004). PMO interfere with the recognition of splice sites by the splicesome machinery which determines proper assembly of a mature mRNA transcript. The best examples of this approach include the correction of aberrant splicing of the

mutated β-globin gene (Lacerra et al., 2000; Suwanmanee et al., 2002), and the induction of exon-skipping of pretermination codons in the mutated dystrophin gene (Alter et al., 2006; McClorey et al., 2006). The advantage to modulating gene expression through the process of "redirecting splicing" is the detection of novel or under-expressed splice forms by sensitive RT-PCR assay. This provides a positive read-out for effectiveness rather than just inhibition of protein expression alone, which can often be confounded by cytotoxicity or other global inhibitory effects due to treatment. Oligonucleotide-induced redirecting of exon utilization of pre-mRNA in lymphoid cells has not yet been shown.

We demonstrate here that by employing CPP-assisted delivery, P-PMO molecules can be added directly to cultures of primary murine leukocytes to specifically affect gene expression through redirecting the splicing of targeted mRNAs. Immunologically-relevant gene targets such as cell surface receptors, cytokines and transcription factors are given as examples to demonstrate the breadth and utility made possible by this approach.

Materials and Methods

Mice

8-12 week old female C57Bl/6 mice (Jackson Laboratories) were housed in microisolator cages under pathogen-free conditions and treated according to animal use protocols approved by the Institutional Animal Care and Use Committee of Oregon State University.

Cell isolation and culture

Isolation and culture of murine splenocytes

Splenic cell suspensions were obtained by passing splenocytes through a 100 µM nylon cell strainer (BD Biosciences) in Dulbeccos' Minimum Modified Media (DMEM) supplemented with 1% fetal bovine serum (FBS) and 1X antibiotic-antimycotic solution (Cellgro). Erythrocytes were hypotonically lysed with sterile deionized water. Cells were cultured in cRPMI (RPMI 1640 including 10% FBS, 5 mM L-glutamine, 1X antibiotic-antimycotic solution, and 50 µM beta-mercaptoethanol) at 5 X 10^6 cells/ml. In some cases, the cells were stimulated overnight with either 5 µg/ml plate-bound anti-CD3 and 2 µg/ml soluble anti-CD28 (eBioscience) or 5 µg/ml concanavalin-A (Con-A, Sigma).

Isolation and culture of dendritic cells and macrophages

Bone marrow-derived dendritic cells (DCs) and macrophages were isolated by flushing tibias with DMEM supplemented with 1% FBS and 1X antibiotic-antimycotic solution using a 25-gauge needle. The cells were dissociated through a 100 µM nylon mesh cell strainer and cultured in non-TC treated 100 x 15 mm Petri dishes in cRPMI containing either 25 ng/ml GM-CSF (eBioscience) and 100 U/ml IL-4 (eBioscience) to produce DCs or 20 ng/ml M-CSF (R&D Systems) to produce macrophages. For DCs, after 3 days of culture the floating and loosely adherent cells were collected and re-cultured in fresh cRPMI supplemented with GM-CSF and IL-4 in a new dish and used within an additional 3-7 days of culture. For macrophages, after 4 days in culture the media was replenished and the cells were used within an

additional 2-7 days. Removal of adherent cells was performed with a 15 minute incubation at 4˚C in 5 mM EDTA followed by gentle trituration. Cells were seeded in cRPMI at 5 X 10^5 cells/well in 24-well plates for P-PMO treatments. Maturation of DCs was achieved by incubation with 500 ng/ml LPS (*E. coli* 0111:B4, Sigma) for 24 h prior to P-PMO treatment.

PMO treatments

Lyophilized P-PMO were dissolved in sterile deionized water at 1-2 mM to produce stock solutions. An intermediate dilution of PMO stock in media was made prior to adding it directly to the experimental media. Cells were treated for 0.5 to 72 h at a final PMO concentration from 0.5 μM to 5 μM as indicated.

Microscopy

Macrophages were incubated for 3 h with 2 μM fluorescein-conjugated P-PMO in cRPMI and washed twice in Dulbecco's Phosphate-Buffered Saline (DPBS). Cells were visualized with a Nikon Diaphot 300 microscope (Tokyo) and images were captured with an Olympus digital camera using Magnafire software (Optronics).

Flow Cytometry

Cultured splenocytes were washed and stained on ice in DPBS containing 1% FBS and 0.2% sodium azide. Cells were first incubated with anti-mouse CD16/32 for FC-blocking (eBioscience) and in some cases also incubated with anti-

fluorescein rabbit polyclonal IgG (Molecular Probes) to decrease surface-bound fluorescein-PMO signal. Cells were then stained with different combinations of anti-mouse MAbs including PE-Cy7-CD8a (clone 53-6.7), PE-OX40 (clone OX-86), or PE-CD45 (clone 30-F11) from eBioscience, APC-Cy7-CD4 (clone GK1.5) from BD Biosciences, or PE-Cy5.5-CD11c (clone N418) from Caltag Laboratories. Foxp3 (clone FJK-16s) was measured with eBioscience's PE anti-mouse/rat Foxp3 staining kit. Viability of live cells was measured with 7-Amino-Actinomycin D (7-AAD, Calbiochem), or with Ethidium Monoazide (EMA, Sigma) for fixed cells. Intracellular IL-2 was measured with PE-IL-2 (eBioscience, clone JES6-5H4) in cells fixed and permeabilized with BD Bioscience's Cytofix/Cytoperm kit. A minimum of 20,000 $CD4^+$, $CD8^+$, or $CD11c^+$ events were collected per sample on a Beckman Coulter FC-500 flow cytometer. Data analysis and software compensation were performed using WinList (Verity Software).

Peptide and PMO preparation

The sequences and nomenclature of cell penetrating peptides (CPPs) and PMO are listed in Tables 3.1 and 3.2. PMO were designed to target either sequence encompassing the AUG start codon, or sequence concentrated around the 5´ and/or 3´ ends of coding exons to redirect splicing. Compounds were then screened for effectiveness using flow cytometry and/or RT-PCR. Both CPPs and PMO were synthesized at AVI BioPharma to >90% purity. PMO syntheses have been described previously (Summerton and Weller, 1993; Summerton and Weller, 1997), while the solid-phase synthesis of the CPPs was done using Fluorenylmethoxycarbonyl

(Fmoc) chemistry (Chan and White, 2000). Strong cation exchange HPLC utilizing Source 15S resin (Amersham Biosciences) was used for purification, followed by a reversed phase desalt employing Amberchrom 300M resin (Tosoh Bioscience). Desalted peptides were lyophilized and analyzed for identity and purity by MALDI-TOF MS, SCX HPLC. The method of conjugation of CPPs and PMO through a thioether linkage (R_9F_2, rTat, penetratin, His1) or amide linker $(RXR)_4$ have also been described previously (Abes et al., 2006; Moulton et al., 2004). In some cases the 3´ end of the PMO was modified with activated carboxyfluorescein (Moulton et al., 2003).

RT-PCR and sequencing

Total RNA was extracted from cultured cells (Qiagen RNeasy mini kit) and used as template material for RT-PCR (Invitrogen SuperScript III One-Step RT-PCR System with Platinum *Taq* DNA Polymerase) using sequence specific primers. Primers were designed using Vector NTI software (Invitrogen) and synthesized by Biosource Int. (Camarillo, CA). Mouse OX-40 primer sequences include: OX40-FWD 5´- TATGGTGAGCCGCTGTGATC- 3´, OX40-REV 5´-ACAGTCAAGGGAGCCAGCAG -3´ (annealed 54°C).

Foxp3 was amplified using nested PCR. The primers used for the first amplification include: Foxp3-FWD 5´-TATTGAGGGTGGGTGTCAG- 3´, Foxp3-REV 5´-AGCTCTTGTCCATTGAGGC- 3´ (annealed 66°C). Nested PCR primers encompassing a fragment internal to the first amplified product include Foxp3Nest-FWD 5´-CAGCTGCCTACAGTGCCCCTAG- 3´, Foxp3Nest-REV 5´-

CATTTGCCAGCAGTGGGTAG- 3´ (annealed 55°C). All PCR reactions were performed using a Biorad I-Cycler instrument.

The PCR cDNA products were visualized by gel electrophoresis. A 100 bp DNA ladder served as a molecular weight marker (New England Biolabs). Selected bands were excised and purified (Qiagen QIAquick Gel Extraction Kit). The fragments were cloned into pCR4-TOPO vector (Invitrogen TOPO TA Cloning Kit) and plasmid DNA was purified (Qiagen QIAprep Spin Miniprep Kit). DNA was sequenced using an ABI Prism 3730 Genetic Analyzer at the CGRB Core Laboratories at Oregon State University (Corvallis, OR).

Statistics

Results are expressed as mean ± SEM for each group of duplicate or triplicate samples.

Results

Peptide-conjugation facilitates delivery of PMO into primary leukocytes

Five different CPPs were selected in this study to examine their relative utility for delivering PMO into primary macrophages, T cells and dendritic cells (Table 3.1). Two of the sequences are naturally occurring and well-known CPPs: a reverse sequence derived from the transduction domain of HIV Tat protein (rTat) and the other is derived from the *Drosophila* antennapedia homeodomain (penetratin) (Derossi et al., 1994; Vives et al., 1997). Two other sequences were

previously shown to deliver PMO into HeLa cells: one consisting of a series of nine arginines and two phenylalanines (R_9F_2), and the other consisting of eight arginines alternating between 6-aminohexanoic acids (X), $(RXR)_4$ (Abes et al., 2006; Moulton et al., 2004). The fifth peptide we tested was rich in another basic amino acid, histidine (His1), a residue also demonstrated to penetrate cells (Midoux et al., 1998).

An initial survey of the relative delivery effectiveness of these different P-PMO conjugates was conducted using fluorescent microscopy. Bone marrow-derived macrophages were cultured with 2 μM P-PMOs tagged with carboxyfluorescein at the 3' end (P-PMO-fl) allowing uptake of the molecules into the cells to be visualized and photographed. We observed cell-associated P-PMO-fl in His1-, rTat-, and $(RXR)_4$- treated cells at three h (Fig 3.1A). R_9F_2 was associated primarily with cellular debris upon light microscope visualization (data not shown). Little to no fluorescent signal was observable for penetratin or PMO without a conjugated peptide.

To next quantify the intensity of P-PMO-fl that delivered into viable T cells, we utilized flow cytometry. To eliminate fluorescein signal associated just with the cell surface, we treated cells with anti-fluorescein antibody after incubation with the P-PMO-fl prior to analysis as the cells were sensitive to normal cell surface removal or quenching methods such as trypsin or trypan blue treatment. Anti-CD3 stimulated $CD4^+$ splenic-derived T cells showed a similar uptake profile as observed by microscopy for macrophages. A ranking of the mean fluorescence intensity (MFI) measured at 24 h for the different treatments in descending order is as follows: $(RXR)_4$ > rTat > His1 > no peptide/penetratin/R_9F_2 (Fig 3.1B). Together, these

results suggested that with the given culture conditions, His1, $(RXR)_4$ and rTat were the most efficient CPPs for delivery of PMO into primary leukocytes.

Delivery of P-PMO into splenic T cells is dose-, time-, and activation-dependent

We were interested in how factors including dose, time, and activation influenced the amount of P-PMO delivered into cells. Resting or activated splenic T cells were treated with the panel of different P-PMO-fl conjugates for 3 h at concentrations of 0, 0.5, 2, or 5 μM, and the fluorescein intensities were measured by flow cytometry for viable (7-AAD negative) $CD4^+$ cells (Fig. 3.2 inset). The fluorescein signal intensity for cells treated with 5 μM His1-PMO was off scale for the cytometer's detector settings so it was removed from these analyses, and is discussed later. Signs of cellular toxicity were observed at concentrations approaching 10 μM, thus we did not treat with P-PMO at concentrations greater than 5 μM (data not shown). There was little effect on the viability of cells treated with P-PMO for 27 h at concentrations between 0.5-5 μM when compared to untreated cells (Fig. 3.2A); this remained true even after 72 h of treatment (data not shown). The two remaining P-PMO conjugates that delivered best into T cells, rTat-PMO and $(RXR)_4$-PMO, did so in a dose-dependent manner into both resting and activated T cells (Fig. 3.2B). Stimulating the T cells with anti-CD3 to induce activation before P-PMO treatment led to strikingly enhanced uptake. In fact, at 5 μM, the MFI for activated $CD4^+$ cells was 4-fold greater for rTat and almost 22-fold greater for $(RXR)_4$ compared to that of resting $CD4^+$ cells. The MFI for $(RXR)_4$ was 9-fold greater than rTat at this dose. We saw little uptake of R_9F_2-, penetratin-, or no

peptide-PMO even at 5 μM, however stimulating the cells did double the weak fluorescein signals suggesting activation enhanced the mechanism(s) of uptake for all the CPPs we tested.

To measure the effect of incubation time on delivery, we treated the splenocytes for 0.5, 2, 6, or 27 h with the different P-PMO-fl conjugates. Ultimately those P-PMO that showed poor delivery at 5 μM still showed little delivery after 27 h, even into activated cells. The delivery of rTat- and $(RXR)_4$-PMO was time-dependent, and was enhanced by addition of stimulus to the cultured cells (Fig. 3.2C). Within 30 minutes there was twice as much $(RXR)_4$, and within 2 h twice as much rTat-PMO internalized by activated $CD4^+$ cells compared to resting $CD4^+$ cells. This increased to 7-fold more for both peptide conjugates after 27 h though the signal was 1.7-fold higher for $(RXR)_4$- than rTat-PMO. The MFIs for both conjugates were still climbing at 27 h suggesting neither had reached saturation levels prior to the initiation of cell proliferation.

These results also show a differential in P-PMO uptake between $CD4^+$ and $CD8^+$ cells. At 6 h, there was more internalized $(RXR)_4$- and rTat-PMO-fl in activated $CD4^+$ cells than activated $CD8^+$ cells, and by 27 h this equated to 1.8- and 1.5-fold more respectively. This showed that the extent of P-PMO internalization is dependent on cell type as well as activation status.

Delivery of P-PMO into DCs is not enhanced after LPS-induced maturation

We next examined the same conditions of P-PMO delivery for bone marrow-derived dendritic cells (BM-DCs). The uptake profile of the P-PMO-fl conjugates

into $CD11c^+$ BM-DCs was similar to that seen in splenic T cells as both time-dependent (Fig. 3.3A) and dose-dependent (data not shown). RTat- and $(RXR)_4$-PMO demonstrated equivalent internalization, while R_9F_2-, penetratin-, and no peptide-PMO uptake was minimal (Fig. 3.3A). Because activation status of a T cell influenced P-PMO uptake, we also determined whether the maturation status of DCs had a similar effect. We were surprised to find that LPS-induced maturation of the BM-DCs did not enhance uptake except in the case of penetratin (Fig. 3.3B). Rather, cells treated with the other peptide conjugates showed a minor reduction in fluorescein signal after LPS treatment indicating maturation did not enhance uptake of P-PMO into DCs.

Cellular uptake does not directly correlate with delivery of antisense activity

His1-PMO appeared to internalize into splenic T cells much like $(RXR)_4$- and rTat-PMO (Fig. 3.1B), even at levels such that the cell-associated fluorescein signal was too intense for our instrument at higher concentrations. It has been previously demonstrated that the antisense activity of $(RXR)_4$ peptide-PMO is more potent than that of Tat peptide-PMO (Abes et al., 2006), thus we chose to focus on whether His1- and/or $(RXR)_4$-PMO could access their mRNA target and target gene expression in leukocytes. We chose a member of the TNF receptor family, OX-40, as our target. OX-40 is expressed predominantly on activated $CD4^+$ T cells and involved in cellular activation and survival (Birkeland et al., 1995). We targeted sequences specific for the AUG start codon and suspected splice-acceptor site on the 5´ end of exon 3 with both His1- and $(RXR)_4$-PMO (Table 3.2, Fig. 3.4A). There

was marked uptake of both His1- and $(RXR)_4$-PMO-fl into Con-A-stimulated splenic $CD4^+$ cells (Fig. 3.4B). After an overnight stimulation with Con-A, the cells were incubated with OX-40-specific P-PMO for 18 h, followed by isolation of whole RNA and RT-PCR using OX-40 specific primers. We confirmed detection of full-length OX-40 amplified PCR product of the expected size (845 bp) (Fig. 3.4C), and sequence (data not shown). An alternative splice product was seen only for cells treated with $(RXR)_4$-$OX40_{3SA}$ of anticipated size (742 bp), if exon three was precisely spliced out (Fig. 3.4A,C). To confirm this, we verified by the sequence traces for the two splice products that exon 3 was present in the full-length band for $(RXR)_4$-$OX40_{AUG}$-treated cells, but was replaced with exon 4 sequence in the alternative splice product from $(RXR)_4$-$OX40_{3SA}$-treated cells indicating exon 3 had been spliced out (Fig. 3.4D). Though His1 appeared to internalize into splenic T cells as well as $(RXR)_4$, the alternative splice product was not present in His1-$OX40_{SA3}$-treated cells (Fig. 3.4C).

We were also able to detect changes in OX-40 expression following P-PMO treatment using flow cytometry. OX-40 protein expression was induced on the surface of activated $CD4^+$ T cells due to Con-A stimulation, and remained unchanged after His1-$OX40_{3SA}$ treatment. Both $(RXR)_4$-$OX40_{AUG}$ and $(RXR)_4$-$OX40_{3SA}$ reduced the OX-40 MFI by 64% and 46% respectively (Fig. 3.4D). The lack of binding by the OX-40 detection antibody to $OX40_{3SA}$-treated cells indicates the spliced gene product prevented expression of normal OX40 protein. Determining the consequences of this altered expression for OX40 protein function was beyond the scope of this study. Taken together, these results indicated His1 did not deliver

PMO to its mRNA target, thus we used $(RXR)_4$-PMO conjugates in all further experiments.

The duration of an antisense effect is target-dependent

We were also interested in the duration of antisense-effects after $(RXR)_4$-PMO was washed out of the culture. Splenic T cells were stimulated and then treated overnight with 4 μM $(RXR)_4$-PMO, washed, and targeted gene expression was measured at 0, 6, 24, and 48 h by RT-PCR and/or flow cytometry (Fig. 3.5). We assumed the duration of effect would vary according to the target so we looked at multiple genes important for different aspects of T cell function.

Targeting cytokines with $(RXR)_4$-PMO

Our first gene target was a cytokine critical for proper T cell function: interleukin-2 (IL-2). IL-2 is secreted by T cells and is involved with their activation, proliferation, and survival. We targeted the AUG start codon of the IL-2 gene with $(RXR)_4$-IL-2_{AUG} (Table 3.2), and measured intracellular IL-2 by flow cytometry. At the time of wash-out, the IL-2 MFI for viable $CD4^+$ cells was markedly reduced compared to control (Fig. 3.5A). This reduction was maintained for at least 6 h after P-PMO was removed, however within 24 h, IL-2 levels returned to control levels. When we measured the percent of $CD4^+$ cells that were IL-2 positive at 6 h, there were markedly less, but by 24 h the effect was lost (Fig. 3.5B). The duration of the reduction in IL-2 expression after removal of P-PMO from the media was considerably less than we would later see for other gene targets.

Targeting surface signaling proteins with $(RXR)_4$-PMO

We also targeted cell surface signaling proteins important for proper T cell function. We chose to target a highly abundant protein, CD45, which can account for up to 10% of the total surface area on a leukocyte, and is important for regulation of T cell receptor signaling (Sasaki et al., 2001). After treating with $(RXR)_4$-$CD45_{AUG}$ targeting the start codon (Table 3.2), we saw marked reduction in surface CD45 expression compared to control (Fig. 3.5C). We were surprised to see the duration of this initial reduction was maintained through 48 h after P-PMO was washed out. We also looked again at the cell surface signaling protein OX-40, and the duration of the effect after $(RXR)_4$-$OX\text{-}40_{SA3}$ treatment. There was marked reduction in the OX-40 MFI after PMO was removed, and a reduction could still be seen 24 h later (Fig. 3.5D). However, we were able to still detect the splice-altered OX-40 gene product at 48 h even as endogenous OX-40 protein levels decreased (Fig. 3.5E). For both cell surface targets the antisense effect lasted at least 48 h after P-PMO treatment was removed; considerably longer than the effect we saw for IL-2 which was lost within 24 h.

Targeting a nuclear transcription factor with $(RXR)_4$-PMO

Finally, we targeted the nuclear transcription factor Foxp3 which confers T-regulatory function to $CD4^+$ T cells (Hori et al., 2003). The Foxp3 gene consists of 11 coding exons (Brunkow et al., 2001) of which, we chose to target a suspected splice-acceptor site on the 5´ end of exon 7 (Table 3.2). The percent of $CD4^+$ cells expressing Foxp3 was reduced after $(RXR)_4$-$Foxp3_{7SA}$ treatment (Fig. 3.5F), and the

effect lasted a minimum of 24 h. At 48 h, the percent of the treated cells that were Foxp3$^+$ was equivalent to that seen of control cells at time zero, while the percent of control-treated Foxp3$^+$ cells had declined. However, the control-treated cells had higher Foxp3 MFIs at all time-points examined (data not shown). We determined by RT-PCR that treating with $(RXR)_4$-$Foxp3_{7SA}$ caused exon 7 to be spliced out, resulting in the joining of exons 6 and 8 (data not shown). We were able to detect this altered Foxp3 splice product through 48 h (Fig. 3.5G). To our knowledge this is the first demonstration of inducing exon-skipping in a T-regulatory cell. The effect on T-regulatory cell function is beyond the scope of this study and will be reported elsewhere.

Discussion

We demonstrate here a novel method for delivery of antisense molecules into primary leukocytes that can effectively alter gene expression. The use of cell penetrating peptides for delivery of molecular cargo into cells has been described for several cell types, and here we report for the first time their utility in delivering antisense oligomers into primary leukocytes. Of the five CPPS we tested, $(RXR)_4$-, rTat- and His1-peptide conjugates exhibited the greatest uptake properties, however when gene expression was examined, only $(RXR)_4$-PMO, and not His1-PMO, successfully altered the targeted mRNA. We assessed $(RXR)_4$-PMO targeting of several genes important for T cell function including IL-2, CD45, OX-40, and Foxp3 to explore the breadth in utility of this technology. Sequences encompassing

either the start codon or potential consensus splice sites within exon/intron boundaries were chosen to confirm the ability of $(RXR)_4$-PMO to access the nucleus of primary murine leukocytes and alter target mRNA in a sequence-specific manner. We found that conditions such as dose, time, and activation status influenced the amount of P-PMO internalized into T cells in the first 27 h. RTat- and $(RXR)_4$-PMO delivery was both time- and dose-dependent for both resting and activated splenic T cells, however a state of activation enhanced the uptake of all the P-PMO tested suggesting activation enhances the mechanism(s) of uptake. Enhanced uptake of P-PMO by $CD4^+$ T cells compared to $CD8^+$ T cells suggests the internalization mechanisms could be regulated differently by $CD4^+$ and $CD8^+$ cells. We did not see saturation of cells with P-PMO at 27 h however at 72 h, at which time stimulated lymphocytes were proliferating in culture, a steady-state level of internalized P-PMO was observed (data not shown). The ability to deliver PMO into resting T cells and immature thymic T cells (data not shown) and alter targeted gene expression is an important observation given that RNA interference technologies like siRNA require that primary T cells be activated for successful delivery and interference (McManus et al., 2002).

Most of the peptides tested as vectors for delivery of PMO into leukocytes were rich in arginine, and cellular uptake of arginine-rich peptides is reportedly, for other cell types, an energy-dependent process (Vives et al., 2003). We found that after treating cells with the actin polymerization inhibitor cytochalasin-D, the internalization of $(RXR)_4$-PMO was severely impaired (data not shown) supporting the idea that uptake of P-PMO into leukocytes is still primarily energy-

dependent. We found that after LPS-induced maturation, uptake into DCs was not enhanced, rather a minor inhibition of uptake was seen. Given that phagocytic activity decreases with maturity of a DC (Kitajima et al., 1996), phagocytosis may contribute to some uptake of P-PMO but is not the primary mechanism since uptake is minimally affected after DCs are matured. We also found that blocking FC receptors with IgG did not reduce uptake suggesting P-PMO is not internalized through FC-receptor-binding (data not shown). Considering mechanisms of endocytosis, caveolae are absent in lymphoid cells eliminating caveolin-mediated endocytosis as a possible uptake mechanism. Penetratin is suspected to be taken into cells through clathrin-mediated endocytosis (Nakase et al., 2004), but demonstrated poor uptake into leukocytes, and was also differentially affected by LPS-maturation when compared to the other P-PMO conjugates suggesting its internalization could be weighted towards different uptake mechanism(s) than other peptide-PMO conjugates.

There is evidence suggesting membrane lipid raft-mediated macropinocytosis is involved in the internalization of HIV Tat into T cells (Futaki, 2006; Kaplan et al., 2005; Wadia et al., 2004). During the process of macropinocytosis, actin filaments polymerize to form a protrusion from the cell membrane to engulf extracellular material for internalization through macropinosomes. Macropinosomes do not fuse with lysosomes like other endosomal compartments, and are used by antigen-presenting cells for the presentation of exogenous antigen on class I MHC molecules (Norbury et al., 1995). Condensation of the membrane at sites of activation or at immunological

synapses may facilitate lipid raft-building (Gaus et al., 2005; Shaw, 2006), and that could participate in the macropinocytotic process. However, clathrin-coated pits are also found clustered near the synapse in non-raft domains (Dustin, 2002), and their involvement in uptake cannot be dismissed either. Thus it is plausible that in some capacity, the formation of the synapse enhances uptake mechanisms to explain why the internalization of P-PMO into T cells is strikingly increased during a state of activation.

A polymer of nine arginines in the R_9F_2 peptide facilitates good delivery into HeLa cells (Abes et al., 2006; Moulton et al., 2004), but did not support robust uptake into primary T cells regardless of their activation status. Eight arginines alternating between 6-amino-hexanoic acids in the $(RXR)_4$ peptide did facilitate uptake suggesting two things; one is that the degree different mechanisms of uptake contribute to the internalization of CPPs likely differ between HeLa cells and leukocytes, and secondly, the spacing between arginines is important for internalization into leukocytes. The importance of alternative spacing of arginine residues for delivery has been previously demonstrated in Jurkat cells (Rothbard et al., 2002). Considering that β-actin has been shown to be post-translationally arginylated which prevents filament aggregation due to charge repulsions between the equally-spaced positively charged arginines (Karakozova et al., 2006); charge repulsion may play a role in the requirement for arginine spacing in CPPs for internalization into leukocytes. The role of arginine-spacing for the stimulation of uptake mechanisms is not yet known.

The duration of the antisense effect varied depending on the gene target.

Issues including rates of mRNA and protein production, turnover, and degradation, likely contribute to the maintenance and/or loss of the effect we measured. We saw in the case of an abundantly expressed protein like CD45, the initial reduction in surface CD45 protein expression was maintained at least 48 h after P-PMO was removed. For a cytokine like IL-2 that has a more rapid turnover rate, a reduction was maintained for at least 6 h but rebounded within 24 h. We found that by implementing two different methods of detection simultaneously: flow cytometry, and RT-PCR, we were able to monitor both the rebound in normal protein expression, and the presence of the induced-splice product after P-PMO removal. From this we learned a reduction in OX-40 protein expression was maintained past 24 h, but rebounded within 48 h at which time the induced OX-40 splice product could still be detected. The induced Foxp3 splice product was detected for 48 h, however the percent of cells expressing Foxp3 had rebounded. Surprisingly, the percent of $Foxp3^+$ cells in control-treated samples had declined suggesting the Foxp3 P-PMO treatment had enhanced the later survival of $Foxp3^+$ cells in culture. In total, these duration experiments give insight into potential in-vivo dosing strategies such that a cytokine would require more frequent dosing to maintain a steady antisense effect compared to a target with slower recovery of total expression like CD45. Additionally, a P-PMO-induced splice product could persist well past a resumption of normal protein expression and continue to produce biological effects.

A potential concern over treating leukocytes with arginine-rich P-PMO is that degradation of peptides rich in L-arginine in the culture could presumably modulate cell function. Some L-arginine is required in the growth media to support

the cells in culture; however with increasing concentrations, leukocytes can metabolize L-arginine to produce nitric oxide and/or L-ornithine and urea which are known to inhibit T cell proliferation. Conversely, it has been shown that $CD8^+$ T cells in whole splenic cell cultures stimulated in the presence of 100μM L-arginine showed enhanced proliferation (Ochoa et al., 2001). On occasion we have observed minor changes in the percent of splenic T cells actively cycling when treated with $(RXR)_4$-PMO compared to controls, however the effect has not been consistent. We found that a control $(RXR)_4$-PMO conjugate alone could not induce activation of T cells and did not affect the expression of a key activation molecule CD25 (data not shown). These issues should be considered when either mixed cultures of leukocytes or purified sub-populations are utilized.

Having the ability to selectively manipulate splicing of mRNA is important given that it is estimated >70% of human genes are alternatively spliced. Genes of both the immune and nervous systems in particular are predisposed to undergoing alternative splicing (Lynch, 2004). Mutations in alternatively or constitutively spliced genes can cause aberrant splicing of pre-mRNA and this has been associated with disease susceptibility (Faustino and Cooper, 2003; Lynch and Weiss, 2001; Ueda et al., 2003). Given that RT-PCR is a sensitive, positive read-out for a target-specific antisense effect, inducing a novel splice product by directing exon-skipping with P-PMO can create either a splice form that performs a desired biological function, or create a nonfunctional product. Targeting splice sites may be a preferred approach given that the readout after targeting the start codon, though an effective means for reducing gene expression, is measured by lack of gene product which is

more difficult to fully interpret. Additionally, the detection of the altered splice product in vivo would provide further demonstration the P-PMO is having the desired effect on the gene target of interest to explain resultant biological effects.

In conclusion, given that current recombinant techniques used to examine the functional activity of various molecules and their respective splice forms can be time- and labor-intensive, this P-PMO antisense technology allows for specific splice forms to be readily induced with minimal manipulation of cells. As we recognize the increasing importance of alternative splice forms in immune function, P-PMO can fill an important niche for the field of immunology.

A

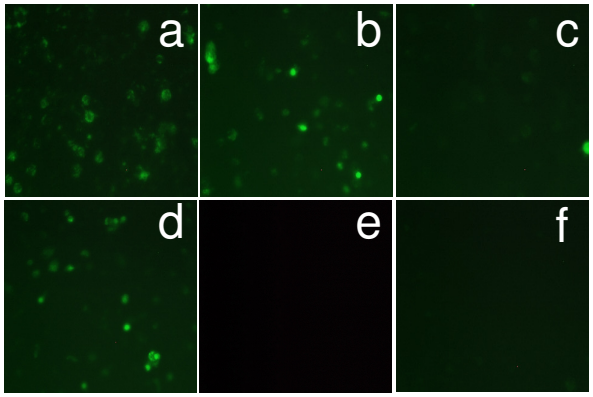

B

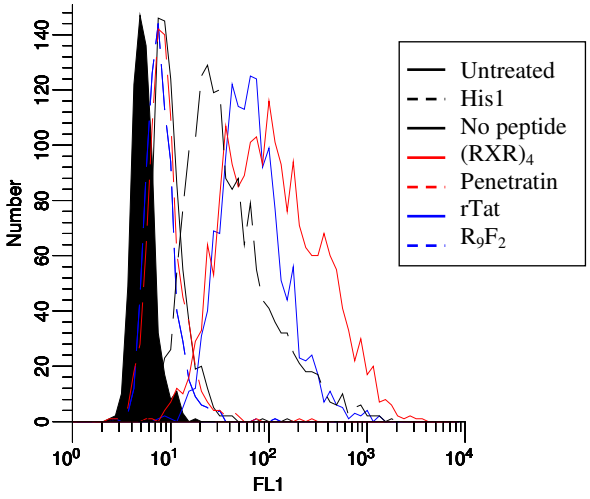

Figure 3.1. P-PMO deliver into primary leukocytes.
Bone marrow-derived macrophages were treated with 2 µM fluorescein-tagged P-PMO (P-PMO-fl) conjugated to His1 (a), rTat (b), R_9F_2 (c), $(RXR)_4$ (d), penetratin (e), or no peptide (f) for 3 h and visualized by fluorescent microscopy (A). Uptake of the panel of P-PMO-fl (2 µM) into anti-CD3 stimulated splenic $CD4^+$ T cells was measured by flow cytometry at 24 h; the mean fluorescence intensities (MFIs) were as follows: penetratin (5.39 ± 0.14), R_9F_2 (12.88 ± 0.04), no peptide (13.76 ± 0.09), His1 (85.48 ± 4.10), rTat (92.23 ± 2.04), and $(RXR)_4$ (202.8 ± 23.65) (B).

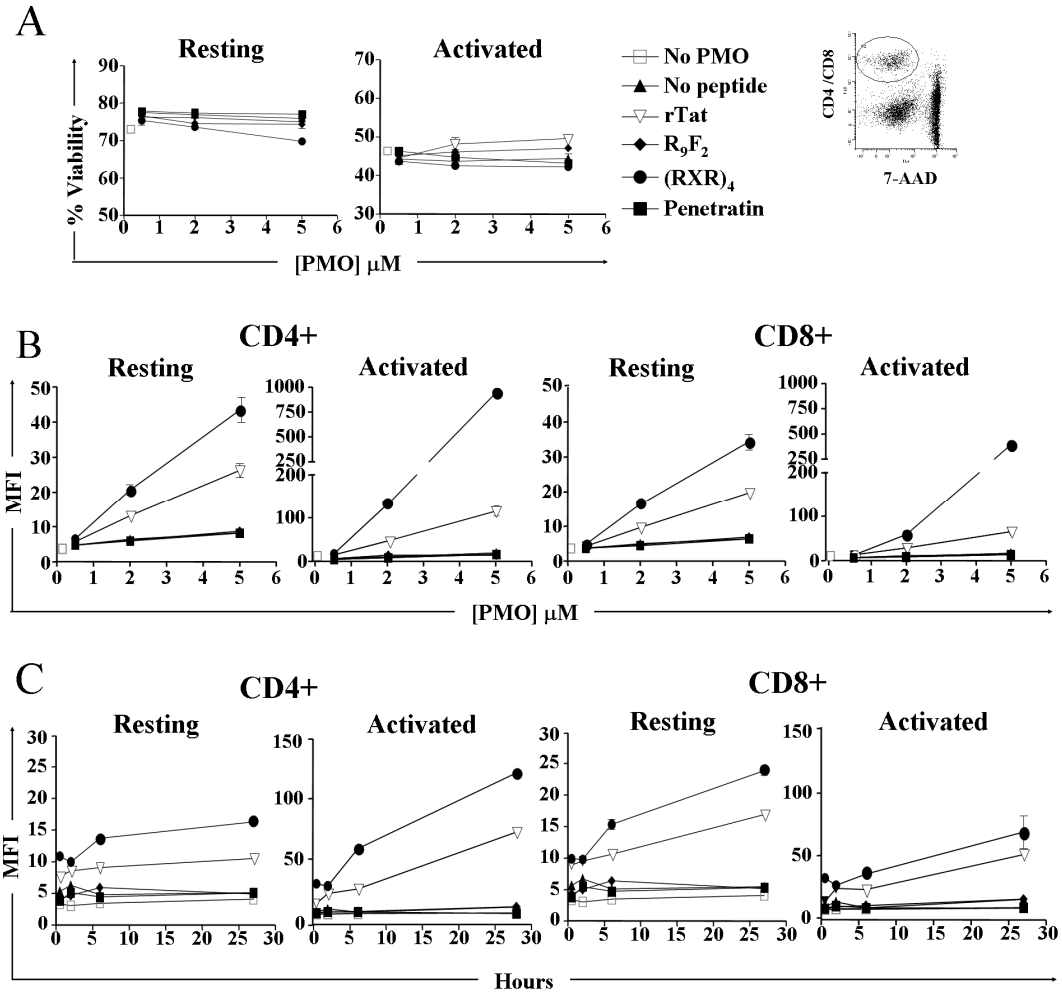

Figure 3.2. Uptake of P-PMO in splenic T cells is dose, time, and activation-dependent.

The MFI of P-PMO-fl was measured by flow cytometry for viable (7-AAD negative) mouse splenic $CD4^+$ or $CD8^+$ T cells cultured in cRPMI at 27 h (A, A inset). A symbol legend for the different P-PMO treatments is indicated (A). Cells were treated with 0, 0.5, 2, or 5 μM P-PMO–fl at 4 h (B), or treated with 2 μM P-PMO–fl for 0.5, 2, 6, or 27 h (C). A portion of the cells were stimulated with plate-bound anti-CD3 (5 μg/ml) and soluble anti-CD28 (2 μg/ml) for 24 h prior to beginning P-PMO treatment (Activated) (B & C).

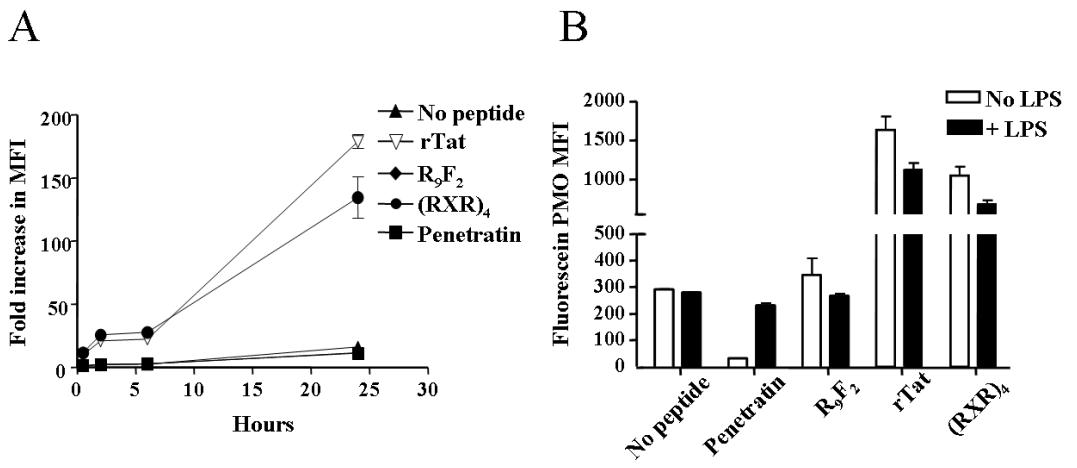

Figure 3.3. Uptake of P-PMO into dendritic cells is not enhanced after LPS-maturation.
Bone marrow-derived dendritic cells were incubated with 2 μM P-PMO-fl in cRPMI and harvested at 0.5, 2, 6, or 24 h (A). MFIs are expressed as fold-increase over untreated. (A). A portion of cells were pre-incubated for 24 h with 500 ng/ml LPS and then treated for 4 h with P-PMO-fl (B). Uptake was measured by flow cytometry and is expressed as the P-PMO-fl MFI for $CD11c^+$ 7-AAD negative cells (A & B).

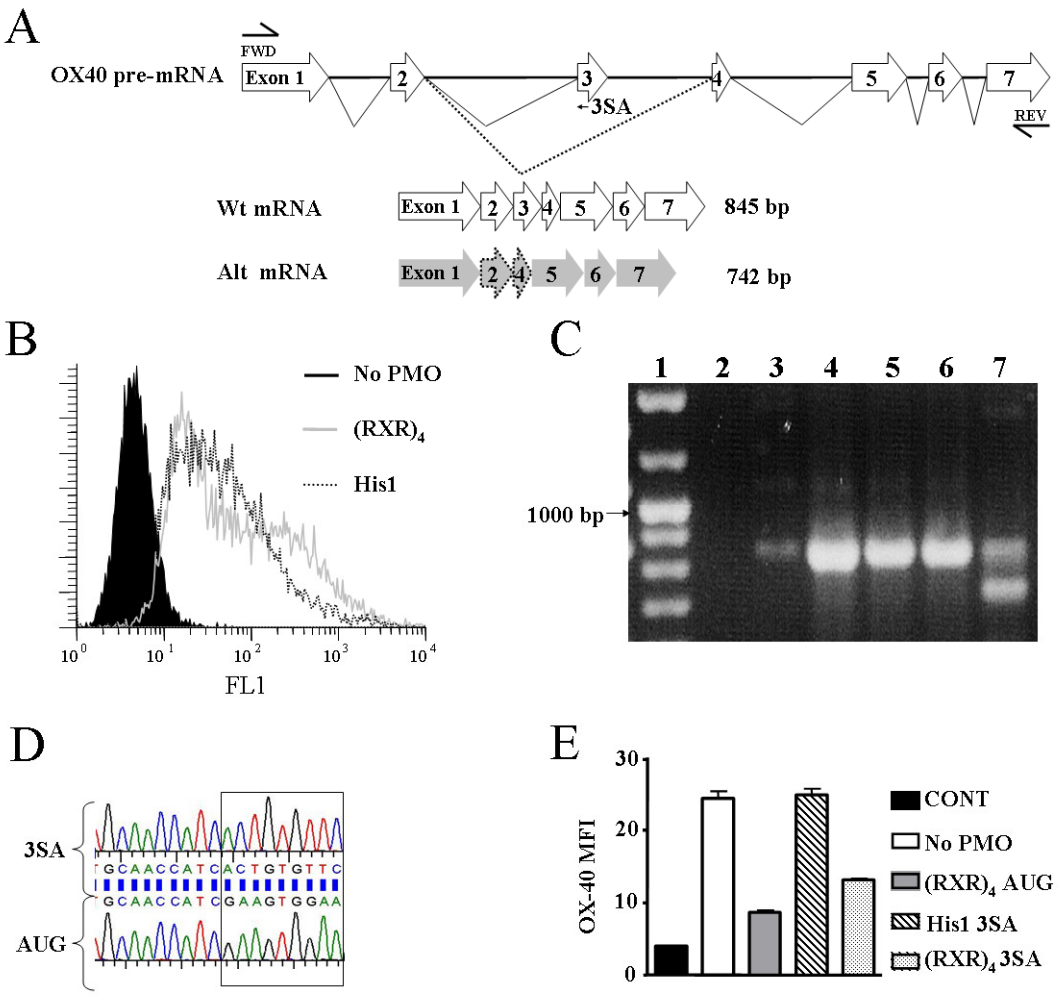

Figure 3.4. Cellular uptake does not directly correlate with delivery of antisense activity.

A map is shown of the intron/exon organization of wild-type OX-40 pre-mRNA and mRNA (Wt) and expected mRNA product after $(RXR)_4$-$OX\text{-}40_{3SA}$-treatment (Alt) including the position of the forward (FWD) and reverse (REV) PCR primers (A). His1- or $(RXR)_4$-PMO-fl fluorescence was measured for previously Con-A stimulated 7-AAD negative splenic $CD4^+$ cells after 6 h of 2 µM treatment (B). Whole RNA was isolated from cells treated with P-PMO for 18 h, OX-40-specific cDNA products were identified by RT-PCR and agarose gel electrophoresis; DNA ladder (lane 1), blank (lane 2), no Con-A stimulation (lane 3), no P-PMO treatment (lane 4), $(RXR)_4$-$OX40_{AUG}$ (lane 5), His1–$OX40_{3SA}$ (lane 6), $(RXR)_4$-$OX40_{3SA}$ (lane 7) (C). PCR fragments for $(RXR)_4$-$OX40_{AUG}$ or -$OX40_{3SA}$-treated cells were cloned and sequenced; the square encompasses sequence at what should be the start of exon 3 (D). Surface OX-40 expression was measured by flow cytometry for 7-AAD negative splenic $CD4^+$ cells treated with no P-PMO, or 5 µM His-$OX40_{3SA}$, $(RXR)_4$-$OX40_{AUG}$ or –$OX40_{3SA}$ at 18 h. Control was not stimulated with Con-A (E).

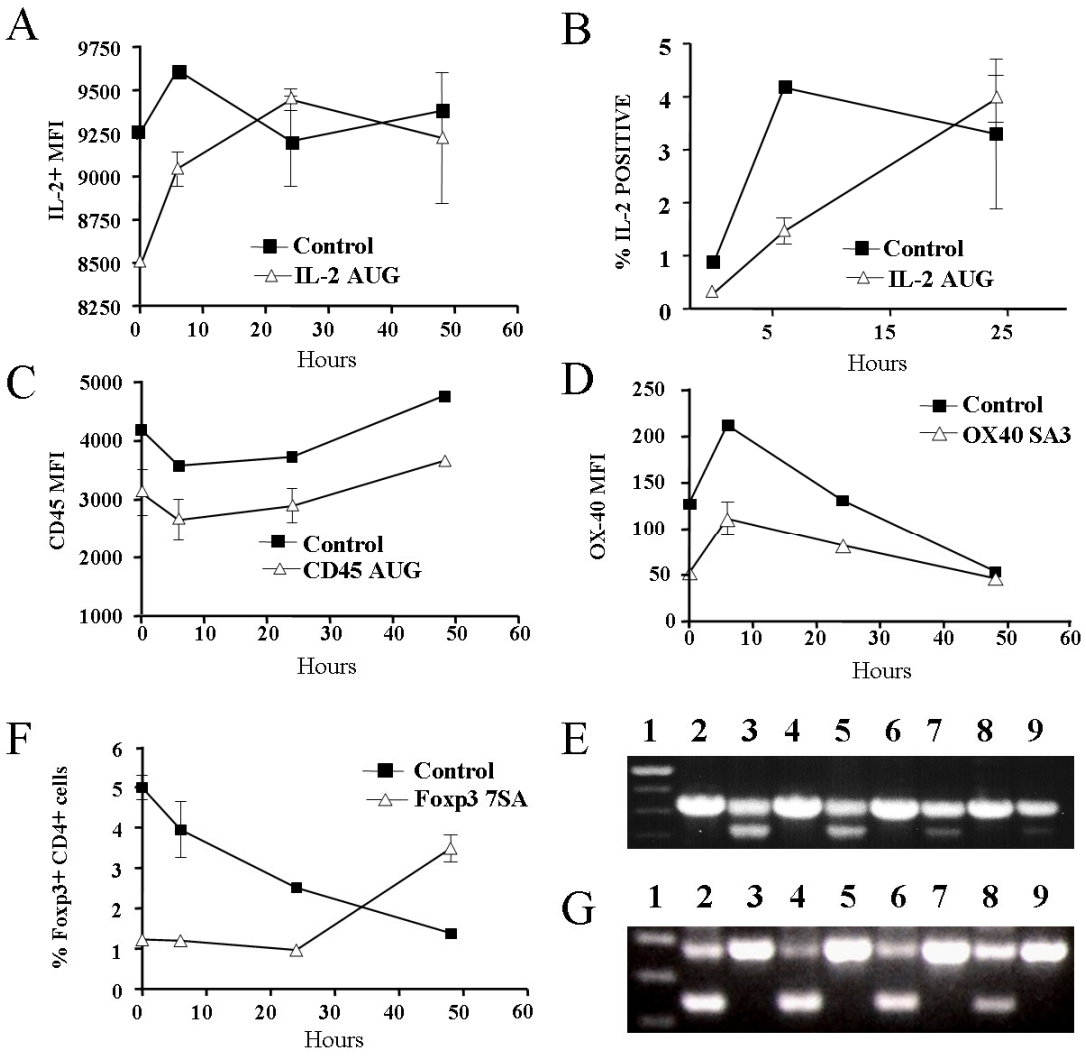

Figure 3.5. The duration of an antisense effect is target-specific.
Target gene expression was measured by flow cytometry for 7-AAD or EMA negative splenic $CD4^+$ T cells treated with specific $(RXR)_4$-PMO (4 µM) for 24 h in cRPMI at 0, 6, 24, or 48 h after removal of treatment and is expressed as percent of cells or MFI (A-F). The AUG start codon of interleukin-2 (A & B) and CD45 (C), splice-acceptor sites on exon 3 of OX40 (D) and of exon 7 of Foxp3 (F) were targeted with specific $(RXR)_4$-PMO. Gene-specific cDNA was also prepared from $(RXR)_4$-OX-40_{3SA}-treated cells (lanes 3, 5, 7, and 9) (E) and $(RXR)_4$-$Foxp3_{7SA}$-treated cells (lanes 2, 4, 6, 8 respectively) (G) from RNA harvested at 0 h (lanes 2 & 3), 6 h (lanes 4 & 5), 24 h (lanes 6 & 7) and 48 h (lanes 8 & 9) to detect OX40 (E) and Foxp3 (G) PCR products.

Table 2.2. Cell-penetrating peptides

Name	Amino acid sequence
R_9F_2	NH_2-RRRRRRRRRFFC-$CONH_2$
rTat	NH_2-RRRQRRKKRC-$CONH_2$
Penetratin	NH_2 DRQIKIWFQNRRMKWKKC-$CONH_2$
$(RXR)_4$	NH_2-RXRRXRRXRRXRXB-COOH
His1	NH_2-HLFHAIAHFIHHGWHGLHHC-$CONH_2$

The peptide sequences are expressed using standard amino acid symbols in order from N to C terminus. The symbol X represents 6-aminohexanoic acid, and B represents β-alanine.

Table 3.2. PMO Sequences

Gene target	PMO Sequence
Control / fluorescein conjugate	CCT CTT ACC TCA GTT ACA
OX-40 splice acceptor site on exon 3	GCT TGA GTT CAC TTC CAC TTC
OX-40 AUG	GAA CCC ACA CAT ACA TCC TTG
CD45 AUG	CCA CAA ACC CAT GGT CAT ATC
IL-2 AUG	CTG CAT GCT GTA CAT GCC TG
Foxp3 splice acceptor site on exon 7	CAT CCA CAG TGG AGA GCT GG

The PMO sequences are shown in order from 5’ to 3’.

Chapter 4

The roles of IL-10 and IL-12Rb2 in the induction of regulatory T cell phenotypes induced by activation of the aryl hydrocarbon receptor during a GVH response

Authors: Nikki B. Marshall

Diana C. Rohlman

Mark Leid

Dan V. Mourich

Nancy I. Kerkvliet

Abstract

Activation of the aryl hydrocarbon receptor by 2,3,7,8-Tetrachlorodibenzo-*p*-dioxin (TCDD) has been linked to the induction of regulatory T cells (Tregs). Gene expression changes induced by TCDD that promote Treg generation have not been identified. IL-12Rb2 and IL-10 were upregulated in $CD25^{high}$CD4+ Tregs induced in TCDD-treated mice during an acute graft-vs.-host (GVH) response. In the present studies, the role of these genes in Treg development is addressed. The results suggest that IL-12Rb2 is a direct AhR-mediated target of TCDD in T cells, but is not required for induction of the Treg phenotype. However, a lack of IL-12Rb2 expression significantly reduced the frequency of T-bet^+ donor CD4+ T cells in TCDD-treated mice. Treatment with IL-10-specific morpholino antisense conjugated to a cell-penetrating peptide (P-PMO) suppressed IL-10 expression in-vivo, but also did not affect the Treg phenotype. To determine the effects of early IL-10 expression on CTL development, we examined the donor T cells on day 6 and found significantly increased populations of $CD69^+$CD4+ and $CD69^+CD122^+$CD8+ donor T cells in TCDD-treated mice, phenotypes associated with regulatory function. Inhibition of IL-10 expression in TCDD-treated mice significantly decreased the frequency of these populations and increased the frequency of $perforin^+$ T cells. Thus increased expression of IL-10 in TCDD-treated mice appears to promote the development of CD8+ T cells with a regulatory-type phenotype that emerge in place of CTL.

Introduction

The aryl hydrocarbon receptor (AhR) ligand TCDD is a ubiquitous environmental contaminant shown to potently suppress T cell-mediated immune responses in mice. Studies suggest that T cell activation and early clonal expansion are preserved, however the T cells fail to differentiate into appropriate effectors, as their numbers drop off prematurely (Camacho et al., 2002; Funatake et al., 2004; Shepherd et al., 2000). Most recently, TCDD has also been linked to the generation and/or preservation of $Foxp3^-$ and $Foxp3^+$ regulatory T cells, respectively (Marshall and Kerkvliet, 2009). The AhR-mediated effects of TCDD that cause T cells to lose proper effector differentiation and/or develop into Tregs are still not well understood. Two of the important observations that have been made in this regard thus far are that TCDD must be present during early events in T cell activation to inhibit a response (Kerkvliet et al., 1996) and secondly, T cells are direct AhR-mediated targets of TCDD (Funatake et al., 2008; Kerkvliet, 2002). Increasing our understanding of the effects of AhR-mediated gene changes on T cell phenotype and function will help elucidate how T cell-mediated immune responses are suppressed by TCDD.

Interestingly, donor CD4+ T cells in mice exposed to TCDD during an acute GVH response gain transient regulatory phenotype ($CD25^{high}$, $CD62L^{low}$, $CTLA\text{-}4^+$, $GITR^+$, $IL\text{-}10^+$) and suppressive function that are not dependent on Foxp3 expression (Funatake et al., 2005; Marshall et al., 2008). These changes are however, dependent on AhR expression in the T cell (Funatake et al., 2008;

Funatake et al., 2005). During a GVH response, the activation of AhR in T cells by TCDD appears to either cause a T cell to acquire regulatory characteristics, or to default to a regulatory-type T cell due to the lack of appropriate signals for proper effector development. GVH is a classic Th1-type response mediated by CD4+ T cells that promote CD8+ cytotoxic T lymphocyte (CTL) development. In the presence of TCDD, both the CD4+ and CD8+ alloreactive donor T cells were shown to acquire regulatory characteristics, however the Treg phenotype of the donor CD8+ T cells was dependent on AhR-mediated events in the donor CD4+ T cells (Funatake et al., 2008; Funatake et al., 2005; Marshall et al., 2008), Gene expression changes induced by TCDD in the alloreactive T cells that are involved in the induction of Treg phenotype are not yet known.

Th1 differentiation is induced by the sequential involvement of IFN-g, IL-12 and the transcription factor T-bet (Schulz et al., 2009). The IL-12 receptor (IL-12R) is a heterodimeric type I cytokine receptor that is composed of a beta 1 and beta 2 subunit (IL-12Rb2), of which the latter is upregulated during T cell activation (Szabo et al., 1997). The binding of IL-12 initiates a signaling cascade that results in the phosphorylation and nuclear translocation of STAT4 which alters the transcription of IL-12-responsive genes. Both *Il-12rb2* and *Stat4* transcripts were upregulated 10-fold and 3-fold in the donor CD4+ T cells from TCDD-treated mice at 48 h, respectively (Marshall et al., 2008). Furthermore, the IL-12R was functional as evidenced by increased STAT4 protein phosphorylation in cells exposed to IL-12 from TCDD-treated mice. Since TCDD suppresses CD4+ T cell-mediated CD8+ CTL effector development (Kerkvliet et al., 1996; Kerkvliet et al., 2002; Oughton

and Kerkvliet, 1999), it was surprising to find that genes involved with the priming of Th1 cells were upregulated in the Tregs.

Recently, the distinctions between Th1 and regulatory T cells have become increasingly blurred. IL-12Rb2 signaling has not only been linked to the generation of Th1 cells, as it has also been linked recently to the development of Tregs (Zhao et al., 2008), and spontaneous autoimmunity (Airoldi et al., 2005). Tregs have also been shown to express T-bet under certain conditions (Gabrysova et al., 2009; Koch et al., 2009; Wei et al., 2009; Zeng et al., 2009). IL-10, produced as an effector cytokine by some regulatory T cells (Roncarolo et al., 2006), can also be produced by Th1 cells to limit the response (Trinchieri, 2007). Since TCDD-induced adaptive CD4+ Tregs express significantly increased levels of IL-10 at both the transcript and protein levels (Marshall et al., 2008), IL-10 may play an important role in Treg induction and suppression of the GVH response in TCDD-treated mice.

The purpose of these studies was to determine the role of IL-12Rb2 and IL-10 in the induction of adaptive regulatory T cells in TCDD-treated mice during the GVH response. The results suggest that IL-12Rb2 is regulated by AhR in activated T cells exposed to TCDD in the presence of IL-12, however the transfer of IL-12Rb2 KO donor T cells into TCDD-treated hosts showed that IL-12Rb2 is not required for the induction of Treg phenotype. The inhibition of IL-10 expression on days 0-1 of the GVH response also did not affect the Treg phenotype in TCDD-treated mice. Upon examination of donor T cells on day 6, we found an increased frequency of $CD69^{+}CD122^{+}$CD8+ and $CD69^{+}$CD4+ donor T cells in TCDD-treated mice, phenotypes that have been associated with regulatory function. When IL-10

expression was inhibited on days 0-3, these populations were significantly decreased, and the frequency of perforin^{+} CD8+ T cells was increased. Thus the early production of IL-10, produced in part by the CD4+ Tregs in TCDD-treated mice, promotes the development of CD8+ T cells with regulatory-type phenotypes in place of alloreactive CTL.

Materials and Methods

Mice

C57BL/6J (donor) and B6D2F$_1$/J (host) mice were purchased from The Jackson Laboratory; B6.PL-Thy1^{a}/CyJ (Thy 1.1^{+}), B6.129S1-Il12rb2^{tm1Jm}/J (IL-12Rb2 KO) and B6.129-AhR^{tm1Bra}/J (AhR$^{-/-}$) mice were originally purchased from The Jackson Laboratory and maintained as a breeding colony in a pathogen-free animal facility at Oregon State University (Corvallis, OR.). Animals were treated according to animal use protocols approved by the Institutional Animal Care and Use Committee at Oregon State University.

TCDD treatment

For in-vivo use, TCDD (99% purity; Cambridge Isotope Laboratories) was dissolved in anisole and diluted in peanut oil (vehicle). Host B6D2F$_1$ mice were dosed with vehicle or TCDD (15 µg/kg) by gavage within 24 h before the adoptive transfer of donor T cells. For in vitro use, TCDD was dissolved in DMSO (vehicle) and added to culture media at a final concentration of 10 nM.

Graft-versus-host response

Splenocytes were prepared by dissociation of spleens between frosted slides in HBSS buffer containing 2.5% FBS, 50 µg/ml gentamicin, and 20 mM HEPES, followed by a 10-s hypotonic lysis of red blood cells. Donor CD4+ and CD8+ T cells were purified from pooled splenocytes on an autoMACS separator using a Pan T cell isolation kit (Miltenyi Biotec) to >90% purity according to manufacturer's instructions. T cells were labeled with 2 µM CFSE in PBS (Invitrogen), and 2 X 10^7 T cells were injected into the tail vein or retro orbital sinus of vehicle- or TCDD-treated B6D2F_1/J hosts (day 0).

Cell culture

Splenocytes or purified T cells (method described above) were cultured in RPMI 1640 medium containing 10% FBS, 50 µg/ml gentamicin and 50 µM 2-ME (cRPMI) at 37°C with 5% CO_2 and protected from light. To some cultures, anti-CD3 (0.5 µg/ml) anti-CD28 (1 µg /ml) or recombinant IL-12 (2 ng/ml) or IL-2 (50 U/ml) (eBioscience) were added. For intracellular staining, splenocytes were cultured ex-vivo for 21 h, the last 5 h in the presence of GolgiPlug (Brefeldin A, BD Biosciences).

Chromatin ImmunoPrecipitation (ChIP)

Spleen cells were stimulated with 0.25 µg/ml soluble anti-CD3 and 0.5 µg/ml anti-CD28 for 24 h with vehicle (DMSO) or 10 nM TCDD. Cells were

harvested, fixed in 1% formaldehyde, and quenched with 0.125 M glycine. Chromatin was isolated and sheared with MNase (New England Biolabs) and sonicated into fragments < 0.5 kb. AhR-bound DNA was immunoprecipitated using 150 µg of chromatin DNA incubated overnight at 4°C with 1 µg of an anti-AhR antibody (Biomol) that has been previously reported to work in ChIP assays (Beischlag et al., 2008; Hestermann and Brown, 2003; Quintana et al., 2008). A 10% aliquot was set aside and used as the relative input fraction. Samples were then incubated with a 50% sepherose bead slurry (PBS + 0.05% NP-40) to eliminate non-specific binding and then transferred to a protein G bead slurry (GE Healthcare) and incubated at 4°C for 4 h. After extensive washing, samples were eluted off the beads in 50 mM Tris-HCl (pH 8.1) with 1 mM EDTA, 1% SDS, and 50 mM $NAHCO_3$. Crosslinks were reversed overnight at 65°C, and protein digested with 20 µg/ml proteinase K. The DNA was purified using a Qiagen PCR clean-up kit, and used as template for real-time PCR reactions.

PCR

Semi-quantitative real-time PCR reactions of ChIP-DNA were carried out using SYBR® Green JumpStart Taq ReadyMix (Sigma) on an ABI 7500 Real-Time PCR system. The primers specific for the DRE-rich region upstream of the IL-12Rb2 gene: fwd: 5'-AGTACTCTGCACAGGGAAACAGCA-3' and rev: 5'-TGAGAAA GGAACCAAGGCGTGTGA-3' were synthesized by Integrated DNA Technologies (IDT). IL-10 RT-PCR was conducted using total RNA isolated from cultured splenocytes (Qiagen RNeasy mini kit) used as template material with the

Invitrogen SuperScript III One-Step RT-PCR System with Platinum Taq DNA Polymerase. IL-10-specific primers: IL-10 fwd: 5'-GGAA - GACAATAACTGCACCC-3' and IL-10 rev: 5'-CATTCATGGCCTTGTAGACA - C-3' were synthesized by IDT.

Flow cytometry

Splenocytes were washed and stained on ice in Dulbecco's PBS containing 1% BSA and 0.1% sodium azide. Fc receptors were blocked with rat IgG (Jackson ImmunoResearch Laboratories), and stained with combinations of optimal concentrations of anti-mouse mAbs. Primary anti-mouse staining antibodies included CD25-APC (PC61), CD54-PE (3E2), CD44-Cychrome (IM7) from BD Biosciences/Pharmingen, CD8-efluor605/780 (53-6.7), Thy1.1-efluor605 (HIS51) and CD4-APC-eFluor780 (RM4-5) from eBioscience and CD69-PE from BioLegend. Some primary antibodies including purified hamster anti-mouse IL-12Rb2 (BD Biosciences) and anti-mouse CD122-biotin were followed up with the labeled-secondary reagents anti-Armenian hamster IgG-PE (eBioscience) and streptavidin-APC (eBioscience), respectively. Intranuclear T-bet-PE (eBio4B10) was measured using the anti-mouse/rat Foxp3 staining buffer set (eBioscience). Intracellular IFN-g-APC (XMG1.2, BioLegend) and perforin-PE (JAW246, eBioscience) were measured using BD Bioscience's Cytofix/Cytoperm Kit. Samples lacking an individual stain (fluorescence minus one, FMO) were used as controls for gating. Cellular viability of cultured cells was measured with ethidium monoazide (Sigma-Aldrich). IL-10 was measured in cell supernatants with a FlowCytomic

Simplex kit (Bender MedSystems) according to manufacturer's instructions. Samples were collected on a Beckman Coulter FC-500 flow cytometer. Data analysis and software compensation were performed using WinList (Verity Software).

Peptide-conjugated Phosphorodiamidate Morpholino Oligomers (P-PMO)

Peptide-conjugated PMO were formulated at AVI BioPharma Inc. as previously described (Marshall 2008). The Arginine-rich cell penetrating peptide NH_2-RXRRXRRXRRXRXB-COOH (where X represents 6-aminohexanoic acid and B represents Beta-alanine) was conjugated to either control sequence non-specific for mouse: 5'-CCTCTTACCTCAGTTACA-3' or IL-10 sequence targeting the 5' end of exon 4 within the open reading frame of IL-10: (Gene ID: 16153) 5'-GGAGAAATCGATGCTGAAGAA-3'. In vitro, P-PMO was added to splenocytes in culture media at a final concentration of 5 µM, and incubated for 48 h at 37°C, 5% CO_2. In some cases the 3' end of the P-PMO was modified with activated carboxyfluorescein as previously described (Moulton et al. 2003). In vivo, P-PMO was prepared by diluting 200 µg of P-PMO in 250 µl PBS and injected intraperitoneally every 24 hrs.

Statistical analyses

Error bars represent the mean ± SEM for individual mice or culture well replicates. Unpaired *t* tests were performed using GraphPad software where statistically significant differences are either indicated by $p < 0.05$ (*) and $p < 0.005$

(**), or if $p < 0.05$, the letters a, b, c indicate that statistically, $a \neq b \neq c$.

Results

IL-12Rb2 expression is regulated by AhR in activated T cells exposed to TCDD

Previous studies showed that IL-12Rb2 transcript was increased 10-fold in alloreactive CD4+ Tregs on day 2 of a GVH response in TCDD-treated mice (Marshall et al., 2008). Whether IL-12Rb2 is directly regulated by AhR in T cells in the presence of TCDD is not known. To determine this, IL-12Rb2 expression was measured by flow cytometry on purified CD4+ T cells treated with TCDD (10 nM) or vehicle (DMSO) and stimulated with anti-CD3/CD28 antibodies in the presence of IL-12. At 24 h, there was a significant increase (3-fold) in the percentage of TCDD-treated T cells expressing IL-12Rb2 compared to vehicle (Figure 4.1A). When purified T cells were cultured without IL-12, IL-12Rb2 was not significantly impacted by TCDD treatment (data not shown). Since there are 6 dioxin-response elements (DREs) clustered within a span of 700 base pairs upstream of the IL-12Rb2 gene transcriptional start site (Table 4.1), chromatin immunoprecipitation (ChIP) was used to measure AhR occupancy of this DRE-rich region. $AhR^{+/+}$ or $AhR^{-/-}$ mouse splenocytes were stimulated with anti-CD3/CD28 and treated with 10 nM TCDD for 24 h. Under these conditions, treatment with TCDD increased AhR binding of the DRE-rich region upstream of IL-12Rb2 (2-fold), but not as strongly as the promoter of Cyp1a1 (8-fold) (Figure 1B). The significant increase in AhR-binding with TCDD treatment compared to vehicle was not observed for the open

reading frame of IL-12Rb2 or of actin (data not shown). Thus, AhR occupancy of the DRE-rich region upstream of the IL-Rb2 gene may partially explain the upregulation of IL-12Rb2 in T cells.

The effects of IL-12Rb2 signaling on donor T cell phenotype in TCDD-treated mice

The role of IL-12Rb2 expression in generating the Treg phenotype induced by TCDD during the GVH response was addressed using donor T cells from IL-12Rb2-deficient (IL-12Rb2 KO) or WT mice. Donor CD4+ and CD8+ T cells (H-2^{b}) were labeled with the cytosolic dye CFSE, injected into TCDD- or vehicle-treated F1 hosts (H-$2^{b/d}$) (n = 3), and analyzed by flow cytometry at 48 h. CD25 is highly expressed on TCDD-induced CD4+ and CD8+ Tregs and although the expression is dependent on AhR-mediated events in the donor CD4+ T cells (Funatake et al., 2008), a lack of known DREs suggest it may be indirectly regulated by TCDD. Since CD25 is an IL-12-responsive gene (O'Sullivan et al., 2004), we examined whether a lack of IL-12Rb2 signaling affected the CD25 expression. Surprisingly, the frequency of donor $CD25^{high}$CD4+ donor T cells in TCDD-treated mice was not affected by the lack of IL-12Rb2 signaling (Figure 4.2A), nor was the intensity of CD25 that was expressed per cell (data not shown). There was only a small (5%) albeit significant decrease in the percentage of donor CD8+ T cells that expressed CD25 when the donor T cells were IL-12Rb2 KO (Figure 4.2A). The IL-12Rb2 KO donor CD4+ and CD8+ T cells also expressed the same CD62-L^{low} CTLA-4^{high} phenotype as WT cells treated with TCDD (Figure 4.2A).

Signaling through IL-12Rb2 maintains the expression of Th1-related genes

including the transcription factor T-bet, which plays an essential role in regulating Th1 differentiation (Szabo et al., 2000), but can also be expressed by Tregs. We found that the percentage of proliferating donor CD4+ T cells that expressed T-bet on day 2 of the response varied between 30-60% depending on the particular experiment, and was not affected by TCDD treatment. However, the frequency of proliferating IL-12Rb2 KO donor CD4+ T cells that expressed T-bet was significantly decreased in TCDD-treated mice compared to WT T cells (Figure 4.2B). As T-bet and IFN-g feed back to reinforce expression of the other (Schulz et al., 2009), the concentrations of secreted IFN-g in the supernatants of cultured splenocytes from TCDD-treated mice were also measured, and although high levels of IFN-g were detected, the concentrations were not different for splenocyte cultures containing IL-12Rb2 KO donor T cells compared to WT donor T cells (Figure 4.2C). The concentrations of secreted IL-10 in the supernatants were also not affected by the adoptive transfer of IL-12Rb2 KO donor T cells compared to WT T cells (Figure 4.2C). Taken together, these data suggest that although signaling through IL-12Rb2 increases the frequency of T-bet^{+} donor CD4+ T cells, IL-12Rb2 is not required for the induction of Treg phenotype in TCDD-treated mice.

The effects of IL-10 on donor T cell phenotype in TCDD-treated mice

IL-10 transcript was increased 2-fold in donor CD4+ T cells from TCDD-treated mice which translated into a significant increase in secreted IL-10 protein (Marshall et al., 2008). To determine if this early increased expression of IL-10 in donor CD4+ T cells influenced the conversion of alloreactive donor CD4+ and

CD8+ T cells into Tregs, we inhibited IL-10 expression with an IL-10-specific phosphorodiamidate morpholino oligomer conjugated to an Arginine-rich cell penetrating peptide (P-PMO). This antisense chemistry effectively alters specific gene expression in primary leukocytes both in vitro and in vivo (Marshall et al., 2007; Mourich et al., 2009). The IL-10 P-PMO was designed to target the 5' intron/exon junction of exon 4 of the IL-10 pre-mRNA transcript to mask splice recognition sequence and alter pre-mRNA splicing for a loss of functional protein (Figure 4.3A). The control P-PMO sequence was non-specific for mouse. Mouse splenocytes were stimulated with anti-CD3/CD28 antibodies and treated for 48 h with control or IL-10 P-PMO. The IL-10 P-PMO-treated cells produced both a full-length and truncated IL-10 mRNA transcript detected by RT-PCR (Figure 4.3B). The truncated RT-PCR product was confirmed to lack exon 4 sequence (data not shown). Furthermore, the splice redirection of the pre-mRNA also translated into decreased IL-10 protein in the cell supernatants (Figure 4.3C). The P-PMO (conjugated to fluorescein) was also readily taken up by the activated donor T cells ex-vivo (Figure 4.3D). The in-vivo efficacy of this specific IL-10 P-PMO compound was recently demonstrated by its ability to protect mice from lethal challenge with mouse-adapted *Ebola* virus (Iversen, 2009).

Groups of vehicle- or TCDD-treated mice (n = 4) were dosed with 200 µg of control P-PMO at the time of adoptive transfer of donor T cells (day 0), and again at 24 h (day 1). Another group of mice treated with TCDD were dosed with 200 µg of IL-10 P-PMO at the same intervals. The experiment was then terminated on day 2. As shown in Figure 4.4A, there was a marked decrease in the concentrations of IL-

10 in the supernatants of cultured splenocytes from TCDD-treated mice dosed with IL-10 P-PMO compared to control P-PMO indicating that the IL-10 P-PMO effectively inhibited IL-10 expression in-vivo. The Treg phenotype of the donor T cells was also evaluated by flow cytometry on day 2. The expected increase in the percentages of CD4+ and CD8+ donor T cells in TCDD-treated mice expressing high levels of CD25 compared to vehicle-treated mice was not affected by IL-10 P-PMO (Figure 4.4B). The significant increase in CTLA-4^+ donor CD4+ and CD8+ T cell frequency and significant increase in IL-12Rb2^+ donor CD4+ T cell frequency in TCDD-treated mice were also not affected by IL-10 P-PMO treatment (data not shown). Intracellular IFN-g was also measured in the donor CD4+ and CD8+ T cells to determine if these cells were a source of IFN-g detected in the supernatants from cultured host splenocytes (Figure 4.2C), and whether this was affected by IL-10. IFN-g^+ donor CD4+ and CD8+ T cells were detected and were found to have undergone at least five cellular divisions according to CFSE dilution. There were significantly more IFN-g^+ donor CD8+ T cells in the vehicle control P-PMO group (7.3 ± 0.8%) compared to the TCDD control P-PMO (2.4 ± 0.08%; $p = 0.01$) or TCDD + IL-10 P-PMO group (3.6 ± 0.4%; $p = 0.01$) (Figure 4.4C). The increase in the percentage of donor CD8+ T cells expressing IFN-g in TCDD-treated mice dosed with IL-10 P-PMO versus control P-PMO was suggestive, but not significant. This same trend was observed for donor CD4+ T cells at a similar frequency although the effect was also not statistically significant. Interestingly, the concentration of IFN-g in the supernatants of cultured host splenocytes from vehicle-treated mice was not different from TCDD-treated mice despite the

significant increase in IFN-g$^+$ donor T cells suggesting other cell types in the spleen are producing IFN-g (data not shown). Taken together, these results suggest that the early expression of IL-10 is not required for the generation of the Treg phenotype on day 2 in TCDD-treated mice, but may partially inhibit the development of IFN-g$^+$ donor CD4+ and CD8+ T cells.

The effects of early IL-10 expression on CTL precursor development in TCDD-treated mice

Although inhibition of IL-10 expression did not affect Treg phenotype on day 2 of the GVH response, we hypothesized that the early IL-10 expression may suppress the development of alloreactive CTL in TCDD-treated mice. Thus, host mice were treated with vehicle or TCDD and dosed with 200 µg of IL-10 P-PMO or control P-PMO every 24 h on days 0-3 relative to adoptive transfer of donor T cells (n = 3-4). The donor T cells were identified in the spleen by their expression of the congenic marker Thy1.1. The frequency and phenotype of donor T cells were then measured on day 6 of the GVH response at a time when differentiated CTL precursors begin to emerge (Oughton and Kerkvliet, 1999). On day 6, the Thy1.1$^+$ donor T cells comprised approximately 9% of the total cells in the host spleen regardless of treatment. The Treg phenotype, including high CD25 expression that is measurable on day 2, is no longer detected beginning on day 3 of the GVH response in TCDD-treated mice (Funatake et al., 2005). This suggests that either the Tregs have trafficked out of the spleen, or that the cells have down-regulated these markers. However, a subset of activated CTL precursors was shown to express

CD25 in a tumor allograft model (Oughton and Kerkvliet, 1999), thus we measured CD25 expression on donor T cells again on day 6 of the response. The percentage of donor CD8+ T cells that expressed CD25 was significantly decreased in TCDD-treated mice (2-fold) compared to vehicle-treated mice (Figure 4.5A); and the frequency of $CD25^{+}$CD8+ T cells was not affected by IL-10 P-PMO treatment. Few (<1%) donor CD4+ T cells expressed CD25, which was expressed at low levels. Consistent with other CTL precursors that have been described (Oughton and Kerkvliet, 1999), the donor $CD25^{+}$CD8+ T cells also co-expressed CD44 and CD54 (ICAM-1). These two adhesion receptors were expressed on >90% of the donor CD4+ and CD8+ T cells on day 6 regardless of treatment. The percentage of donor CD4+ T cells that were $CD44^{high}$ $CD54^{+}$ was significantly upregulated in TCDD-treated mice (66.2% ± 2.6, $p = 0.01$) compared to vehicle-treated (47.1% ± 1.2), and was not affected by treatment with IL-10 P-PMO. The significant increase in $CD44^{high}CD54^{+}$ phenotype was not observed for the donor CD8+ T cells.

CTL precursors have also been previously shown to express the membrane-bound receptor CD69 (Oughton and Kerkvliet, 1999). Although normally recognized as a temporal early T cell activation marker, data has begun to emerge linking CD69 expression with regulatory function (Han et al., 2009; Radstake et al., 2009; Sancho et al., 2005). Surprisingly, there was a significant increase in the frequency of donor CD8+ and CD4+ T cells expressing CD69 in TCDD-treated mice on day 6, which was significantly reversed by early IL-10 P-PMO treatment. (Figure 4.5B). Approximately 80% of the donor CD8+ cells, and less than 4% of the donor CD4+ T cells also expressed the beta subunit of the IL-2 receptor (CD122),

and like CD69, the frequency of $CD122^+$ donor CD8+ T cells was significantly decreased by IL-10 P-PMO in TCDD-treated mice (Figure 4.5C). These results suggest that early IL-10 production on days 0-3 in TCDD-treated mice is linked to an increase in the $CD69^+CD4^+$ and $CD69^+CD122^+CD8^+$ T cell populations in TCDD-treated mice on day 6.

The expression of IFN-g, both intracellularly in the donor T cells, and in soluble form in supernatants from cultured host splenocytes was also measured on day 6 of the GVH response. Less than 1% of the donor CD4+ T cells expressed IFN-g^+ on day 6 however the frequency of IFN-g^+ donor CD8+ T cells was significantly increased in TCDD-treated mice compared to vehicle-treated mice, however this effect was not seen in TCDD-treated mice dosed with IL-10 P-PMO (Figure 4.6A). Concentrations of IFN-g were also measured in supernatants from cultured splenocytes from host mice. A significant increase in concentrations of IFN-g was observed in the splenocyte supernatants from TCDD-treated mice dosed with control P-PMO compared to IL-10 P-PMO and compared to vehicle-treated mice (Figure 4.6B). This was consistent with the increased intracellular IFN-g expression

The expression of the cytolytic protein perforin was also measured in donor T cells on day 6 as it is a known mediator of CTL effector function. Although there was no significant effect of TCDD treatment on perforin expression, the frequency of perforin$^+$ donor CD8+ T cells was significantly increased in TCDD-treated mice dosed with IL-10 P-PMO compared to all other groups (from approximately 9% to 22%) (Figure 4.6C). There was also a significant increase in the frequency of perforin$^+$ donor CD8+ T cells in vehicle-treated mice dosed with IL-10 P-PMO

compared to control P-PMO. An increase in a small subset of donor CD4+ T cells that expressed perforin was also seen in TCDD-treated mice dosed with IL-10 P-PMO (from 1% to 6%). The subset of CD8+ T cells that expressed perforin were found not to co-express IFN-g (Figure 4.6D). Taken together, these results suggest that the early expression of IL-10 in TCDD-treated mice during GVH promotes the development of IFN-g^{+}CD8+ T cells and suppresses the development of perforin^{+} CD8+ T cells.

Discussion

These studies were performed to determine the role of IL-12Rb2 and IL-10 in the generation of alloreactive Tregs in TCDD-treated mice. The data suggest that IL-12Rb2 is a direct AhR-mediated target of TCDD in T cells as has been shown for other cell types (Kinehara et al., 2008). The upregulation of IL-12Rb2 in purified T cells required the presence of IL-12 suggesting that other IL-12-dependent factor(s) are necessary for TCDD-mediated upregulation of IL-12Rb2 expression. It is interesting that AhR occupies this DRE-rich region upstream of IL-12Rb2 as well as the Cyp1a1 promoter even 24 h after the cells were first exposed to TCDD. Most often ChIP studies are performed with samples harvested within 2 h of the initial TCDD exposure, however this may not accurately reflect the AhR occupancy that occurs over the course of activation and differentiation of a T cell. Further studies of the occupancy of the DRE-rich region upstream of the IL-12Rb2 gene by AhR are needed to further determine the direct mechanisms of TCDD-induced upregulation

of IL-12Rb2 gene expression.

Although IL-12Rb2 expression is upregulated by TCDD, signaling through IL-12Rb2 was not required for the generation of the $CD25^{high}$ $CD62\text{-}L^{low}$ $CTLA\text{-}4^{+}$ $IL\text{-}10^{+}$ Treg phenotype. Approximately 30-60% of the proliferating donor CD4+ T cells expressed T-bet on day 2 regardless of TCDD exposure, however this frequency was significantly reduced when the donor T cells were IL-12Rb2-deficient. It appears then that Treg induction in TCDD-treated mice does not occur at the expense of Th1 priming, rather a suppressive T cell with both Th1 and Treg characteristics is produced. Interestingly, $Foxp3^{+}$ Tregs were shown to express T-bet during a Th1-response which enhanced their suppressive function (Koch et al., 2009). Thus gene expression controlled by T-bet may enhance the ability of a Treg to respond and traffic alongside Th1 cells, making the Tregs particularly suited for suppressing Th1 responses. Whether Tregs generated in TCDD-treated mice during a GVH response can be transferred to suppress a subsequent GVH response or other Th1-type responses is not yet known.

We also examined the role of IL-10 in induction of Treg phenotype and suppression of CTL development. To suppress IL-10 expression in-vivo, we utilized an IL-10-specific morpholino oligomer conjugated to a cell-penetrating peptide (P-PMO). Activated T cells are particularly sensitive to uptake of these antisense compounds (Marshall et al., 2007), and have been successfully used in-vivo for targeted splice-altering of CTLA-4 in non-obese diabetic mice (Mourich, D.V., personal communication). TCDD-treated mice dosed with IL-10 P-PMO on days 0-1 had suppressed splenic IL-10 production, but the donor T cell Treg phenotype was

not altered indicating that IL-10 is not required for the induction of Tregs by TCDD. We further determined the consequences of the early IL-10 expression on downstream CTL precursor development. Even as early as day 6, suppression of CTL development was suggested in TCDD-treated mice by a significant decrease in the frequency of emerging donor $CD25^{+}CD8+$ T cells. After dosing with IL-10 P-PMO on days 0-3, the $CD25^{+}CD8+$ population remained suppressed in TCDD-treated mice on day 6. Concomitantly, increased populations of $CD69^{+}CD4+$ and $CD69^{+}CD122^{+}CD8+$ T cells emerged in TCDD-treated mice on day 6 that were significantly reduced by early dosing with IL-10 P-PMO. Interestingly, populations of $CD122^{+}CD8+$ T cells and $CD69^{+}CD4+$ T cells with regulatory function have been previously described (Endharti et al., 2005; Han et al., 2009; Rifa'i et al., 2004), although these studies are the first to suggest that they are induced by IL-10. Whether the loss of $CD69^{+}$ T cells in TCDD-treated mice dosed with IL-10 P-PMO partially restores CTL activity will be addressed in future studies.

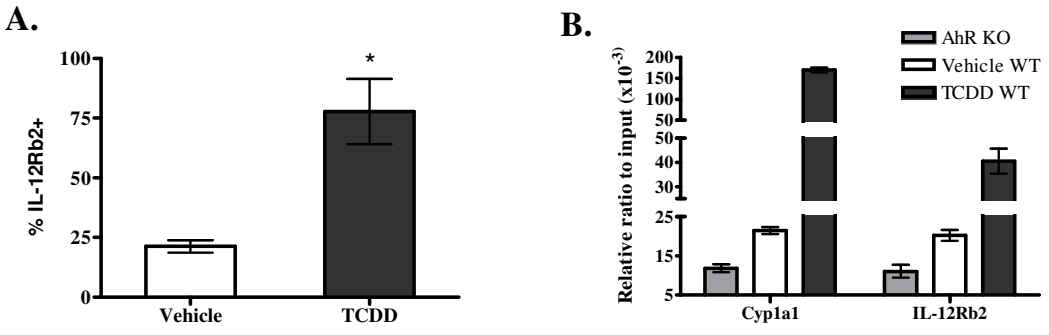

Figure 4.1. IL-12Rb2 expression is regulated by AhR in T cells exposed to TCDD in the presence of IL-12.
Pan-T purified splenic T cells were stimulated with anti-CD3/CD28 antibodies and 2 ng/ml IL-12 for 24 h in the presence of vehicle (DMSO) or 10 nM TCDD. Surface IL-12Rb2 protein expression was measured on CD4+ T cells by flow cytometry (A). Splenocytes from $AhR^{+/+}$ or $AhR^{-/-}$ mice were stimulated with anti-CD3/CD28 antibodies for 24 h, chromatin was isolated, immunoprecipitated with anti-AhR antibody, and used as genomic DNA template for semi-quantitative real time-PCR with primers specific for the DRE-rich region upstream of the IL-12Rb2 gene (B).

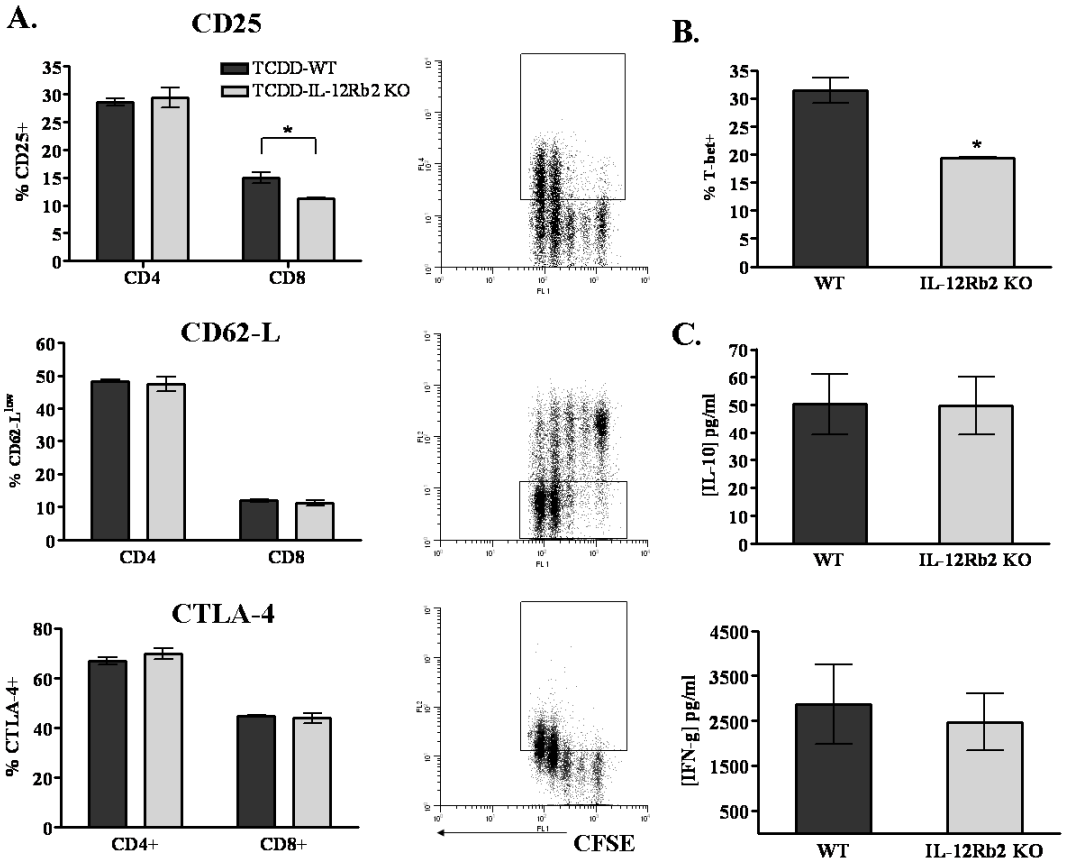

Figure 4.2. A lack of IL-12Rb2 signaling affects T-bet^{+} donor T cell frequency but not the Treg phenotype in TCDD-treated mice on day 2 of the GVH response. WT or IL-12Rb2 KO pan-T purified T cells (H-2^{b}) were labeled with CFSE and adoptively transferred into B6D2F$_1$/J (H-2$^{b/d}$) hosts treated with vehicle or 15 µg/kg TCDD. Spleens were harvested at 48 h. The expression of CD25, CD62-L and intracellular CTLA-4 was measured on/in splenic donor CD4+ and CD8+ T cells by flow cytometry (A). Splenocytes were fixed and permeabilized to measure nuclear expression of T-bet protein in donor CD4+ T cells by flow cytometry (B). Host splenocytes were also cultured for 24 h and supernatants were harvested and used to measure soluble IFN-g and IL-10 concentrations using bead-based cytokine assays (C).

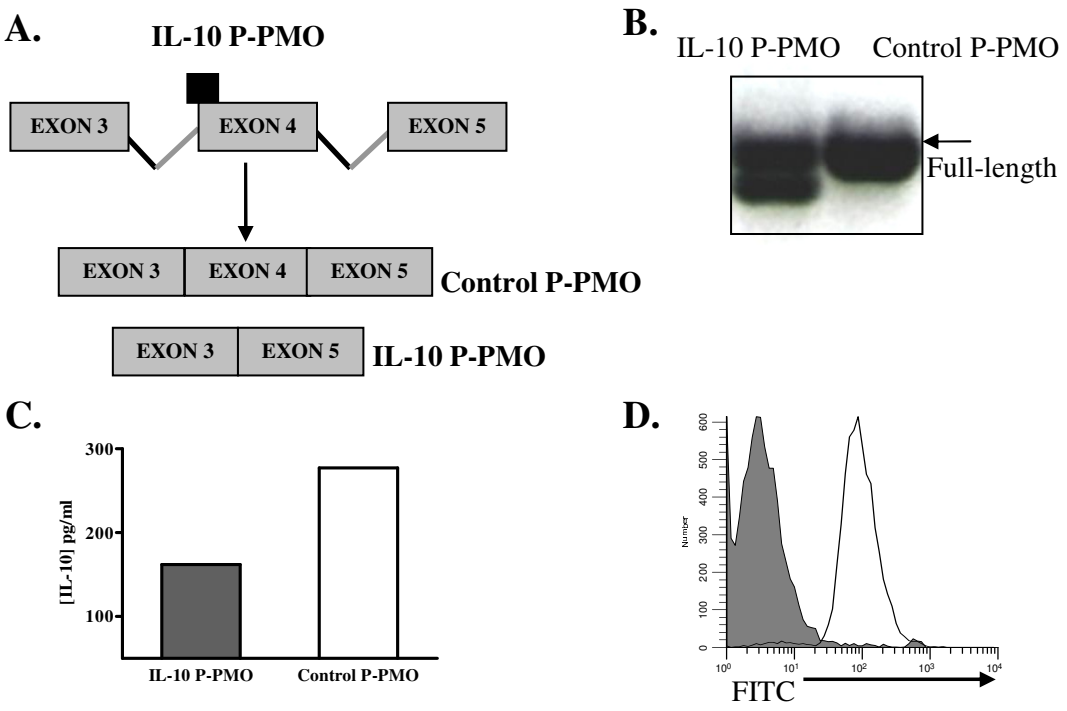

Figure 4.3. IL-10 P-PMO delivers into leukocytes and induces splice-altering of the IL-10 pre-mRNA transcript to inhibit protein expression.
IL-10 P-PMO was designed to target the 5' intron/exon boundary of exon 4 of the coding sequence of the IL-10 gene to produce an altered IL-10 pre-mRNA transcript (A). The altered transcript was measured by RT-PCR in IL-10 P-PMO-treated splenocytes at 48 h (B). Soluble IL-10 protein expression in P-PMO-treated splenocyte supernatants were measured by bead-based cytokine assay (C). Uptake of P-PMO (solid histogram), or P-PMO conjugated to fluorescein (dotted histogram) was measured in donor T cells cultured in cRPMI supplemented with 50 U/ml IL-2 for 24 h (D).

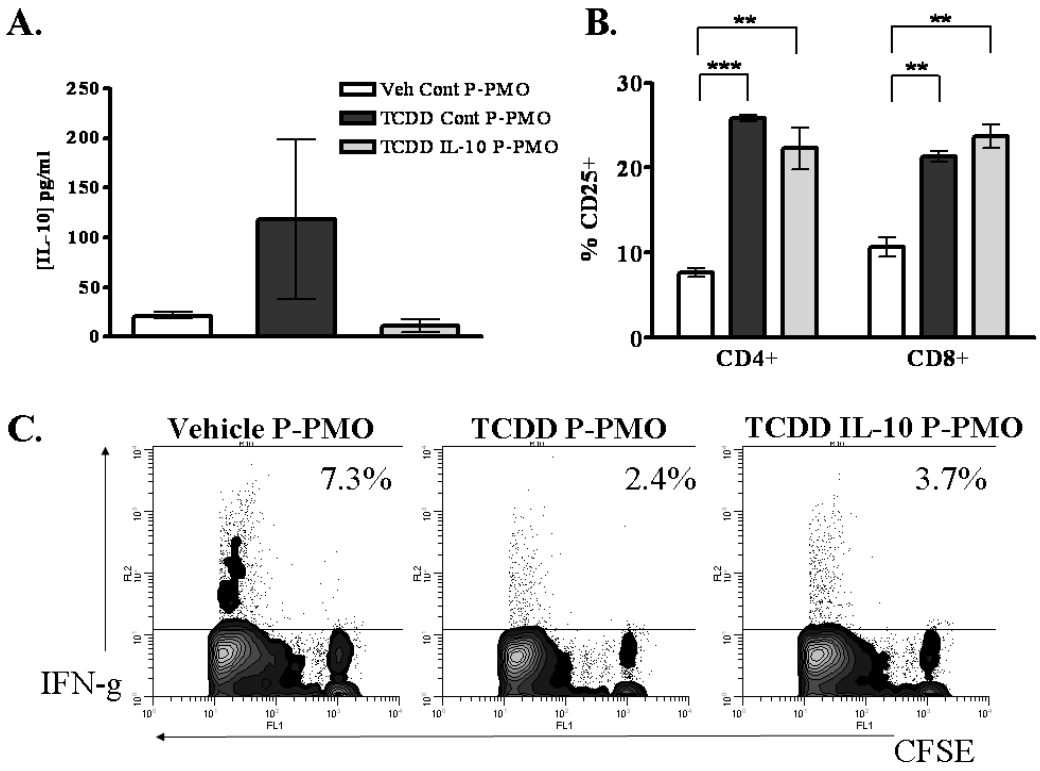

Figure 4.4. Treatment with IL-10 P-PMO inhibits IL-10 protein expression but does not affect Treg phenotype or IFN-g$^+$ donor CD8+ T cell frequency in TCDD-treated mice on day 2 of the GVH response.
Pan-T purified T cells from C57Bl/6 mice were labeled with CFSE and adoptively transferred into B6D2F$_1$/J host mice treated with vehicle or 15 µg/kg TCDD and dosed with 200 µg of control or IL-10 P-PMO intraperitoneally days 0-1. Host spleens were harvested at 48 h. IL-10 was measured in the supernatants of host splenocytes cultured for 24 h, and adjusted for donor T cell frequency (A). CD25 expression was measured on donor CD4+ and CD8+ T cells by flow cytometry (B). Intracellular IFN-g was measured in donor CD8+ T cells from host splenocytes cultured 24 h with the last 5 h in the presence of brefeldin A(C).

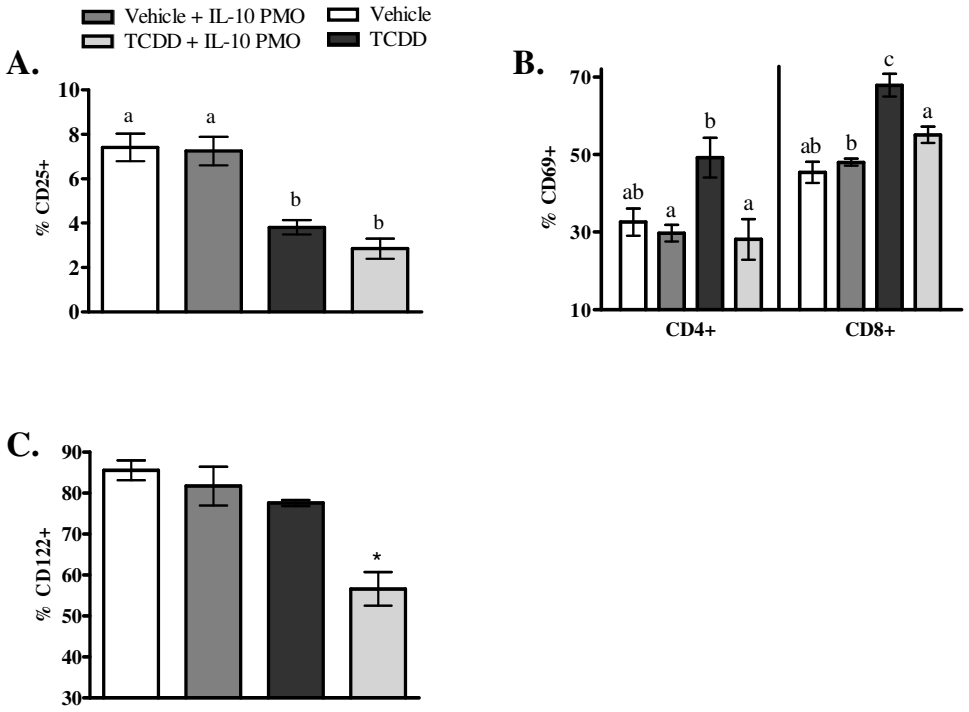

Figure 4.5. TCDD suppresses CD25$^+$CD8+ donor T cell frequency, and increases the IL-10-dependent frequency of CD69$^+$CD4+ and CD69$^+$CD122$^+$CD8+ T cells on day 6 of the GVH response.
Pan-T purified T cells from Thy1.1$^+$ mice were adoptively transferred into B6D2F$_1$/J host mice treated with vehicle or 15 µg/kg TCDD and dosed with 200 µg of control or IL-10 P-PMO intraperitoneally on days 0-3. Host spleens were harvested on day 6. Using flow cytometry, the percentage of Thy1.1$^+$CD8+ T cells that expressed CD25 (A), the percentage of Thy1.1$^+$CD4+ and Thy1.1$^+$CD8+ T cells that expressed CD69 (B), and the percentage Thy1.1$^+$CD8+ T cells that expressed CD122 were measured (C).

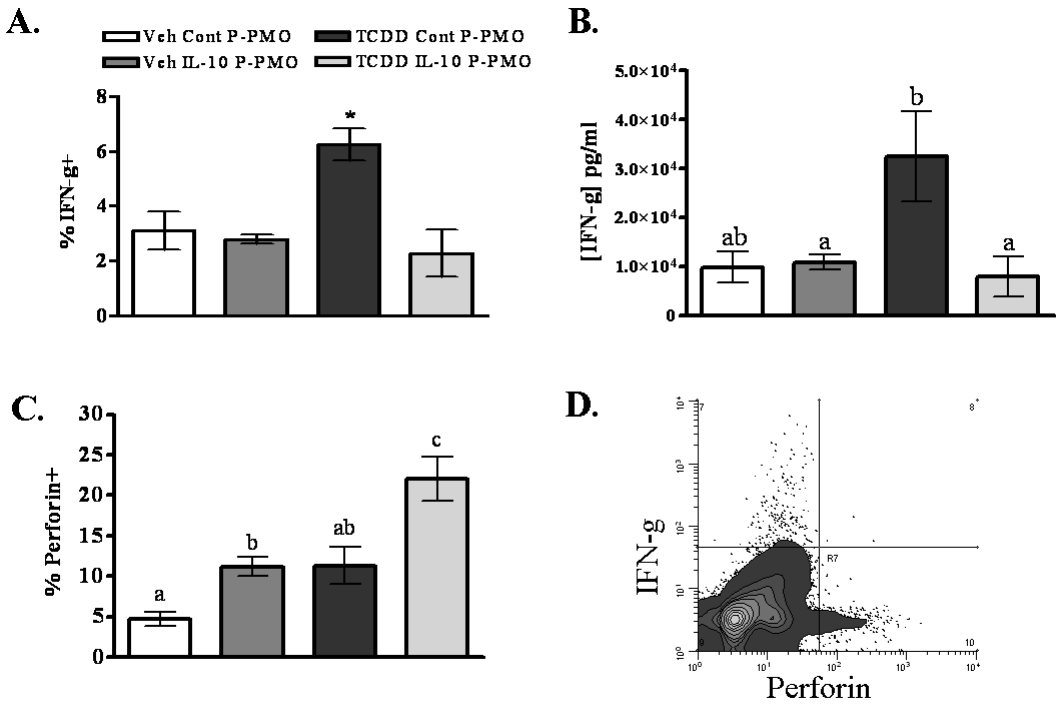

Figure 4.6. Early IL-10 P-PMO treatment suppresses IFN-g$^+$ but increases perforin$^+$ donor CD8+ T cell frequency on day 6 of the GVH response.
Pan-T purified T cells from Thy1.1$^+$ mice were adoptively transferred into B6D2F$_1$/J host mice treated with vehicle or 15 µg/kg TCDD and dosed with 200 µg of control or IL-10 P-PMO intraperitoneally days 0-3. Host spleens were harvested on day 6. Intracellular IFN-g and perforin was measured by flow cytometry in Thy1.1$^+$CD8+ T cells from host splenocytes cultured for 24 h and treated with brefeldin A for the last 5 h (A,C,D). Host splenocytes were cultured for 24 h and supernatants were harvested and used to measure IFN-g by bead-based cytokine assay (B).

Table 4.1. DREs in/upstream of the IL-12Rb2 gene*

Site	DRE sequence	Strand
-203	gcaggagGCGTGtgccaca	-
-153	gcacccaGCGTGcttagtg	-
-126	aaccaagGCGTGtgacccc	-
-69	gtggcggGCGTGgtgagag	+
23	cactgccGCGTGgactcca	+
461	gaatcagGCGTGggggatg	-

*Identified by Sun et al. (2004)

Chapter 5

Conclusions

The recent publication of two pivotal articles, Funatake et al. (2005) and Quintana et al. (2008) that demonstrate a role for TCDD-activated AhR in regulatory T cell development, has stimulated considerable interest in the role of AhR ligands in modulating T cell effector differentiation. Adaptive $CD25^{+}CTLA\text{-}4^{+}$ $CD62\text{-}L^{low}CD4^{+}$ Tregs that were identified and characterized in TCDD-treated mice by our lab on day 2 of the GVH response has provided important new insights into the direct AhR-mediated effects of TCDD on T cells. It is challenging to characterize a novel type of regulatory T cell that does not express the widely accepted marker of most Tregs, transcription factor Foxp3. However various populations of $Foxp3^{-}$ Tregs continue to be described in the literature, and AhR may play a role in their induction.

A Treg by the simplest definition is a T cell with suppressive function. We demonstrated suppression of naïve responder T cells by TCDD-induced CD4+ Tregs ex-vivo in the presence of anti-CD3 in the standard assay for Treg function, but also in the presence of semi-allogeneic DC stimulation. Also, consistent with the function of natural $Foxp3^{+}$ Tregs, the cells did not produce IL-2, and suppression by the TCDD-induced Tregs was shown to be cell-contact dependent, and relieved by ligating the costimulatory molecule GITR. The cells also differed from natural Tregs in that they were not anergic in culture, did not sequester IL-2 from the media, and

produced high levels of IL-10. Collectively, the results suggest that TCDD-activated AhR may act as an alternative transcription factor to Foxp3 for the induction of a Treg with suppressive function and a unique phenotype.

To help elucidate the direct AhR-mediated effects of TCDD on T cells involved in Treg induction, we chose to examine the role of IL-12Rb2 in the generation of Treg phenotype. IL-12Rb2 was selected because it was upregulated 10-fold at the transcript level and because CD25, which was highly expressed by the Tregs, is an IL-12-responsive gene. Upon further study, we found that TCDD enhanced IL-12Rb2 protein expression in purified T cells in the presence of IL-12, and using ChIP, we found that AhR binds a DRE-rich region of DNA upstream of the IL-12Rb2 gene. However, IL-12Rb2 was not required for the generation of the $CD25^{high}$ Treg phenotype in TCDD-treated mice. This demonstrates that significant gene changes induced by TCDD-activated AhR, although seemingly important, may only be ancillary to a biological response. The role of TCDD-induced IL-12Rb2 upregulation in other immune responses is not yet known, but should be examined.

A major theme of the studies presented in this dissertation is the complex temporal nature of gene expression changes and gene-specific effects that occur over the course of T cell effector development during an alloresponse. We found that inhibiting IL-10 expression on days 0-1 with IL-10-specific $(RXR)_4$-conjugated morpholino antisense did not affect the $CD25^{high}$ Treg phenotype on day 2. By treating the mice on days 0-3 with antisense and then examining the donor T cells on day 6 during CTL precursor development, we identified an increased frequency of $CD69^{+}$ CD4+ and CD8+ T cells in TCDD-treated mice that were suppressed in mice

dosed with IL-10-specific antisense. The use of a reagent that temporally inhibits expression of a gene as opposed to using gene-deficient cell lines or animals allows us to study the timing of gene expression and when subsequent effects occur. Given that the transcripts of cytokines like IL-2 and IL-10 are rapidly degraded (Stoecklin et al., 2008), and that IL-2 expression rebounded within 6-24 h after we treated with antisense, the expression of IL-10 in-vivo would have likely rebounded on day 4. Thus it appears that the IL-10 present on days 0-3 was adequate to drive the increase in day 6 $CD69^+$ donor T cell phenotype in TCDD-treated mice. These studies demonstrate that $(RXR)_4$-conjugated morpholino antisense can be used in-vivo to target genes in immune cells for the study of temporal gene expression to further our understanding of immune responses.

Whether $Foxp3^+$ Tregs are induced de novo by TCDD is not yet clear. TCDD treatment did not increase the frequency of $Foxp3^+$ Tregs during the GVH response, in fact there was a small but significant decrease in donor $Foxp3^+$ Treg frequency. ChIP studies by Quintana et al. (2008) have shown that AhR interacts directly with the Foxp3 gene to enhance transcription. Interestingly, an increased frequency of $Foxp3^+$ Tregs was found in mouse models of EAE (Quintana et al,. 2008) and type 1 diabetes (Kerkvliet et al., 2009) with TCDD treatment. It is possible that $Foxp3^+$ Tregs exported from the thymus are naturally more resistant to AhR-mediated effects as they are more fully differentiated compared to other developing effector T cells and express fewer gene transcripts. It is this same reason that unactivated, naive T cells appear more resistant to the effects of TCDD. Thus increased $Foxp3^+$ Treg frequency may reflect Treg preservation due to the inhibition

of other T cell effectors that are more sensitive to the effects of TCDD. Further studies of the effects of TCDD on Foxp3$^+$ Tregs are still needed to determine whether induction or preservation occurs and why enhanced frequency of Foxp3$^+$ Tregs is only observed in certain disease models.

The findings by Quintana et al. (2008) and Veldhoen et al. (2008) that the naturally-occurring high-affinity AhR ligand FICZ promotes Th17 instead of Treg development has led some in the field to suggest TCDD is not an optimal tool for studying AhR signaling. I believe that TCDD is one of the best tools for the study of AhR for 2 reasons: (1) If the goal is to enhance our understanding of the role of AhR in biological systems, I would argue that the use of a high affinity ligand that is not metabolized by the battery of enzymes that AhR induces, despite its anthropogenic origin, offers the most straightforward approach to studying AhR function. To this, alternative AhR ligands can then be compared. (2) The link between Treg induction and TCDD suggests that AhR ligands may have therapeutic potential for conditions such as transplant rejection and autoimmune disease. Thus studies of the AhR-mediated effects of TCDD on biological responses may help us to identify and develop alternative AhR ligands or other compounds that produce comparable effects that could be used to improve human health.

Bibliography

Abes S, Moulton HM, Clair P, Prevot P, Youngblood DS, Wu RP, et al. Vectorization of morpholino oligomers by the (R-Ahx-R)4 peptide allows efficient splicing correction in the absence of endosomolytic agents. J Control Release 2006; 116: 304-13.

Airoldi I, Di Carlo E, Cocco C, Sorrentino C, Fais F, Cilli M, et al. Lack of Il12rb2 signaling predisposes to spontaneous autoimmunity and malignancy. Blood 2005; 106: 3846-53.

Allan LL, Sherr DH. Constitutive activation and environmental chemical induction of the aryl hydrocarbon receptor/transcription factor in activated human B lymphocytes. Mol Pharmacol 2005; 67: 1740-50.

Alter J, Lou F, Rabinowitz A, Yin H, Rosenfeld J, Wilton SD, et al. Systemic delivery of morpholino oligonucleotide restores dystrophin expression bodywide and improves dystrophic pathology. Nat Med 2006; 12: 175-7.

Amakura Y, Tsutsumi T, Sasaki K, Nakamura M, Yoshida T, Maitani T. Influence of food polyphenols on aryl hydrocarbon receptor-signaling pathway estimated by in vitro bioassay. Phytochemistry 2008; 69: 3117-30.

Apostolou I, von Boehmer H. In vivo instruction of suppressor commitment in naive T cells. J Exp Med 2004; 199: 1401-8.

Awasthi A, Kuchroo VK. Th17 cells: from precursors to players in inflammation and infection. Int Immunol 2009; 21: 489-98.

Aylward LL, Hays SM. Temporal trends in human TCDD body burden: decreases over three decades and implications for exposure levels. J Expo Anal Environ Epidemiol 2002; 12: 319-28.

Bandyopadhyay B, Fan J, Guan S, Li Y, Chen M, Woodley DT, et al. A "traffic control" role for TGFbeta3: orchestrating dermal and epidermal cell motility during wound healing. J Cell Biol 2006; 172: 1093-105.

Barrat FJ, Cua DJ, Boonstra A, Richards DF, Crain C, Savelkoul HF, et al. In vitro generation of interleukin 10-producing regulatory CD4(+) T cells is induced by immunosuppressive drugs and inhibited by T helper type 1 (Th1)- and Th2-inducing cytokines. J Exp Med 2002; 195: 603-16.

Battaglia M, Gregori S, Bacchetta R, Roncarolo MG. Tr1 cells: from discovery to

their clinical application. Semin Immunol 2006; 18: 120-7.

Bauer TM, Jiga LP, Chuang JJ, Randazzo M, Opelz G, Terness P. Studying the immunosuppressive role of indoleamine 2,3-dioxygenase: tryptophan metabolites suppress rat allogeneic T-cell responses in vitro and in vivo. Transpl Int 2005; 18: 95-100.

Beischlag TV, Luis Morales J, Hollingshead BD, Perdew GH. The aryl hydrocarbon receptor complex and the control of gene expression. Crit Rev Eukaryot Gene Expr 2008; 18: 207-50.

Belladonna ML, Puccetti P, Orabona C, Fallarino F, Vacca C, Volpi C, et al. Immunosuppression via tryptophan catabolism: the role of kynurenine pathway enzymes. Transplantation 2007; 84: S17-20.

Bettelli E, Carrier Y, Gao W, Korn T, Strom TB, Oukka M, et al. Reciprocal developmental pathways for the generation of pathogenic effector TH17 and regulatory T cells. Nature 2006; 441: 235-8.

Birkeland ML, Copeland NG, Gilbert DJ, Jenkins NA, Barclay AN. Gene structure and chromosomal localization of the mouse homologue of rat OX40 protein. Eur J Immunol 1995; 25: 926-30.

Birnbaum LS, Tuomisto J. Non-carcinogenic effects of TCDD in animals. Food Addit Contam 2000; 17: 275-88.

Bjeldanes LF, Kim JY, Grose KR, Bartholomew JC, Bradfield CA. Aromatic hydrocarbon responsiveness-receptor agonists generated from indole-3-carbinol in vitro and in vivo: comparisons with 2,3,7,8-tetrachlorodibenzo-p-dioxin. Proc Natl Acad Sci U S A 1991; 88: 9543-7.

Bowers OJ, Sommersted KB, Sowell RT, Boling GE, Hanneman WH, Titus RG, et al. 2,3,7,8-tetrachlorodibenzo-p-dioxin (TCDD) reduces Leishmania major burdens in C57BL/6 mice. Am J Trop Med Hyg 2006; 75: 749-52.

Brunkow ME, Jeffery EW, Hjerrild KA, Paeper B, Clark LB, Yasayko SA, et al. Disruption of a new forkhead/winged-helix protein, scurfin, results in the fatal lymphoproliferative disorder of the scurfy mouse. Nat Genet 2001; 27: 68-73.

Bunger MK, Glover E, Moran SM, Walisser JA, Lahvis GP, Hsu EL, et al. Abnormal liver development and resistance to 2,3,7,8-tetrachlorodibenzo-p-dioxin toxicity in mice carrying a mutation in the DNA-binding domain of the aryl hydrocarbon receptor. Toxicol Sci 2008; 106: 83-92.

Burbach KM, Poland A, Bradfield CA. Cloning of the Ah-receptor cDNA reveals a

distinctive ligand-activated transcription factor. Proc Natl Acad Sci U S A 1992; 89: 8185-9.

Burleson GR, Lebrec H, Yang YG, Ibanes JD, Pennington KN, Birnbaum LS. Effect of 2,3,7,8-tetrachlorodibenzo-p-dioxin (TCDD) on influenza virus host resistance in mice. Fundam Appl Toxicol 1996; 29: 40-7.

Burrer R, Neuman BW, Ting JP, Stein DA, Moulton HM, Iversen PL, et al. Antiviral effects of antisense morpholino oligomers in murine coronavirus infection models. J Virol 2007; 81: 5637-48.

Camacho IA, Hassuneh MR, Nagarkatti M, Nagarkatti PS. Enhanced activation-induced cell death as a mechanism of 2,3,7,8-tetrachlorodibenzo-p-dioxin (TCDD)-induced immunotoxicity in peripheral T cells. Toxicology 2001; 165: 51-63.

Camacho IA, Nagarkatti M, Nagarkatti PS. 2,3,7,8-Tetrachlorodibenzo-p-dioxin (TCDD) induces Fas-dependent activation-induced cell death in superantigen-primed T cells. Arch Toxicol 2002; 76: 570-80.

Camacho IA, Singh N, Hegde VL, Nagarkatti M, Nagarkatti PS. Treatment of mice with 2,3,7,8-tetrachlorodibenzo-p-dioxin leads to aryl hydrocarbon receptor-dependent nuclear translocation of NF-kappaB and expression of Fas ligand in thymic stromal cells and consequent apoptosis in T cells. J Immunol 2005; 175: 90-103.

Campbell JJ, O'Connell DJ, Wurbel MA. Cutting Edge: Chemokine receptor CCR4 is necessary for antigen-driven cutaneous accumulation of CD4 T cells under physiological conditions. J Immunol 2007; 178: 3358-62.

Chan W, White P. Fmoc solid phase peptide synthesis; A practical approach.: Oxford University Press, New York, 2000.

Chang HD, Helbig C, Tykocinski L, Kreher S, Koeck J, Niesner U, et al. Expression of IL-10 in Th memory lymphocytes is conditional on IL-12 or IL-4, unless the IL-10 gene is imprinted by GATA-3. Eur J Immunol 2007; 37: 807-17.

Chen TC, Cobbold SP, Fairchild PJ, Waldmann H. Generation of anergic and regulatory T cells following prolonged exposure to a harmless antigen. J Immunol 2004; 172: 5900-7.

Chen W, Jin W, Hardegen N, Lei KJ, Li L, Marinos N, et al. Conversion of peripheral CD4+CD25- naive T cells to CD4+CD25+ regulatory T cells by TGF-beta induction of transcription factor Foxp3. J Exp Med 2003; 198: 1875-86.

Chiaro CR, Patel RD, Perdew GH. 12(R)-Hydroxy-5(Z),8(Z),10(E),14(Z)-eicosatetraenoic acid [12(R)-HETE], an arachidonic acid derivative, is an activator of the aryl hydrocarbon receptor. Mol Pharmacol 2008; 74: 1649-56.

Clark DA, Sweeney G, Safe S, Hancock E, Kilburn DG, Gauldie J. Cellular and genetic basis for suppression of cytotoxic T cell generation by haloaromatic hydrocarbons. Immunopharmacology 1983; 6: 143-53.

Coumailleau P, Poellinger L, Gustafsson JA, Whitelaw ML. Definition of a minimal domain of the dioxin receptor that is associated with Hsp90 and maintains wild type ligand binding affinity and specificity. J Biol Chem 1995; 270: 25291-300.

Curti A, Pandolfi S, Valzasina B, Aluigi M, Isidori A, Ferri E, et al. Modulation of tryptophan catabolism by human leukemic cells results in the conversion of CD25- into CD25+ T regulatory cells. Blood 2007; 109: 2871-7.

Deas TS, Binduga-Gajewska I, Tilgner M, Ren P, Stein DA, Moulton HM, et al. Inhibition of flavivirus infections by antisense oligomers specifically suppressing viral translation and RNA replication. J Virol 2005; 79: 4599-609.

Derossi D, Joliot AH, Chassaing G, Prochiantz A. The third helix of the Antennapedia homeodomain translocates through biological membranes. J Biol Chem 1994; 269: 10444-50.

Dooley RK, Holsapple MP. Elucidation of cellular targets responsible for tetrachlorodibenzo-p-dioxin (TCDD)-induced suppression of antibody responses: I. The role of the B lymphocyte. Immunopharmacology 1988; 16: 167-80.

Durakovic N, Radojcic V, Powell J, Luznik L. Rapamycin promotes emergence of IL-10-secreting donor lymphocyte infusion-derived T cells without compromising their graft-versus-leukemia reactivity. Transplantation 2007; 83: 631-40.

Dustin ML. Membrane domains and the immunological synapse: keeping T cells resting and ready. J Clin Invest 2002; 109: 155-60.

Ehlers M, Laule-Kilian K, Petter M, Aldrian CJ, Grueter B, Wurch A, et al. Morpholino antisense oligonucleotide-mediated gene knockdown during thymocyte development reveals role for Runx3 transcription factor in CD4 silencing during development of CD4-/CD8+ thymocytes. J Immunol 2003; 171: 3594-604.

Ema M, Ohe N, Suzuki M, Mimura J, Sogawa K, Ikawa S, et al. Dioxin binding activities of polymorphic forms of mouse and human arylhydrocarbon receptors. J Biol Chem 1994; 269: 27337-43.

Endharti AT, Rifa IM, Shi Z, Fukuoka Y, Nakahara Y, Kawamoto Y, et al. Cutting edge: CD8+CD122+ regulatory T cells produce IL-10 to suppress IFN-gamma production and proliferation of CD8+ T cells. J Immunol 2005; 175: 7093-7.

Enterlein S, Warfield KL, Swenson DL, Stein DA, Smith JL, Gamble CS, et al. VP35 knockdown inhibits Ebola virus amplification and protects against lethal infection in mice. Antimicrob Agents Chemother 2006; 50: 984-93.

Fallarino F, Grohmann U, Hwang KW, Orabona C, Vacca C, Bianchi R, et al. Modulation of tryptophan catabolism by regulatory T cells. Nat Immunol 2003; 4: 1206-12.

Fallarino F, Grohmann U, You S, McGrath BC, Cavener DR, Vacca C, et al. The combined effects of tryptophan starvation and tryptophan catabolites down-regulate T cell receptor zeta-chain and induce a regulatory phenotype in naive T cells. J Immunol 2006; 176: 6752-61.

Faustino NA, Cooper TA. Pre-mRNA splicing and human disease. Genes Dev 2003; 17: 419-37.

Fernandez-Salguero PM, Hilbert DM, Rudikoff S, Ward JM, Gonzalez FJ. Aryl-hydrocarbon receptor-deficient mice are resistant to 2,3,7,8-tetrachlorodibenzo-p-dioxin-induced toxicity. Toxicol Appl Pharmacol 1996; 140: 173-9.

Fontenot JD, Gavin MA, Rudensky AY. Foxp3 programs the development and function of CD4+CD25+ regulatory T cells. Nat Immunol 2003; 4: 330-6.

Frericks M, Meissner M, Esser C. Microarray analysis of the AHR system: tissue-specific flexibility in signal and target genes. Toxicol Appl Pharmacol 2007; 220: 320-32.

Frumento G, Rotondo R, Tonetti M, Damonte G, Benatti U, Ferrara GB. Tryptophan-derived catabolites are responsible for inhibition of T and natural killer cell proliferation induced by indoleamine 2,3-dioxygenase. J Exp Med 2002; 196: 459-68.

Fujimaki H, Nohara K, Kobayashi T, Suzuki K, Eguchi-Kasai K, Tsukumo S, et al. Effect of a single oral dose of 2,3,7,8-tetrachlorodibenzo-p-dioxin on immune function in male NC/Nga mice. Toxicol Sci 2002; 66: 117-24.

Fukunaga BN, Probst MR, Reisz-Porszasz S, Hankinson O. Identification of functional domains of the aryl hydrocarbon receptor. J Biol Chem 1995; 270: 29270-8.

Funatake CJ, Ao K, Suzuki T, Murai H, Yamamoto M, Fujii-Kuriyama Y, et al. Expression of constitutively-active aryl hydrocarbon receptor in T-cells enhances the down-regulation of CD62L, but does not alter expression of CD25 or suppress the allogeneic CTL response. J Immunotoxicol 2009; 6: 194-203.

Funatake CJ, Dearstyne EA, Steppan LB, Shepherd DM, Spanjaard ES, Marshak-Rothstein A, et al. Early consequences of 2,3,7,8-tetrachlorodibenzo-p-dioxin exposure on the activation and survival of antigen-specific T cells. Toxicol Sci 2004; 82: 129-42.

Funatake CJ, Marshall NB, Kerkvliet NI. 2,3,7,8-Tetrachlorodibenzo-p-dioxin alters the differentiation of alloreactive CD8+ T cells toward a regulatory T cell phenotype by a mechanism that is dependent on aryl hydrocarbon receptor in CD4+ T cells. J Immunotoxicol 2008; 5: 81-91.

Funatake CJ, Marshall NB, Steppan LB, Mourich DV, Kerkvliet NI. Cutting edge: activation of the aryl hydrocarbon receptor by 2,3,7,8-tetrachlorodibenzo-p-dioxin generates a population of CD4+ CD25+ cells with characteristics of regulatory T cells. J Immunol 2005; 175: 4184-8.

Futaki S. Oligoarginine vectors for intracellular delivery: design and cellular-uptake mechanisms. Biopolymers 2006; 84: 241-9.

Gabrysova L, Nicolson KS, Streeter HB, Verhagen J, Sabatos-Peyton CA, Morgan DJ, et al. Negative feedback control of the autoimmune response through antigen-induced differentiation of IL-10-secreting Th1 cells. J Exp Med 2009; 206: 1755-67.

Gaus K, Chklovskaia E, Fazekas de St Groth B, Jessup W, Harder T. Condensation of the plasma membrane at the site of T lymphocyte activation. J Cell Biol 2005; 171: 121-31.

Ge Q, Pastey M, Kobasa D, Puthavathana P, Lupfer C, Bestwick RK, et al. Inhibition of multiple subtypes of influenza A virus in cell cultures with morpholino oligomers. Antimicrob Agents Chemother 2006; 50: 3724-33.

Gershon RK, Cohen P, Hencin R, Liebhaber SA. Suppressor T cells. J Immunol 1972; 108: 586-90.

Geusau A, Abraham K, Geissler K, Sator MO, Stingl G, Tschachler E. Severe 2,3,7,8-tetrachlorodibenzo-p-dioxin (TCDD) intoxication: clinical and

laboratory effects. Environ Health Perspect 2001; 109: 865-9.

Ghosh C, Iversen PL. Intracellular delivery strategies for antisense phosphorodiamidate morpholino oligomers. Antisense Nucleic Acid Drug Dev 2000; 10: 263-74.

Gielen JE, Goujon FM, Nebert DW. Genetic regulation of aryl hydrocarbon hydroxylase induction. II. Simple Mendelian expression in mouse tissues in vivo. J Biol Chem 1972; 247: 1125-37.

Gomez-Duran A, Carvajal-Gonzalez JM, Mulero-Navarro S, Santiago-Josefat B, Puga A, Fernandez-Salguero PM. Fitting a xenobiotic receptor into cell homeostasis: how the dioxin receptor interacts with TGFbeta signaling. Biochem Pharmacol 2009; 77: 700-12.

Gondek DC, Lu LF, Quezada SA, Sakaguchi S, Noelle RJ. Cutting edge: contact-mediated suppression by CD4+CD25+ regulatory cells involves a granzyme B-dependent, perforin-independent mechanism. J Immunol 2005; 174: 1783-6.

Gong D, Malek TR. Cytokine-dependent Blimp-1 expression in activated T cells inhibits IL-2 production. J Immunol 2007; 178: 242-52.

Goryo K, Suzuki A, Del Carpio CA, Siizaki K, Kuriyama E, Mikami Y, et al. Identification of amino acid residues in the Ah receptor involved in ligand binding. Biochem Biophys Res Commun 2007; 354: 396-402.

Grohmann U, Volpi C, Fallarino F, Bozza S, Bianchi R, Vacca C, et al. Reverse signaling through GITR ligand enables dexamethasone to activate IDO in allergy. Nat Med 2007; 13: 579-86.

Grossman WJ, Verbsky JW, Barchet W, Colonna M, Atkinson JP, Ley TJ. Human T regulatory cells can use the perforin pathway to cause autologous target cell death. Immunity 2004; 21: 589-601.

Haarmann-Stemmann T, Bothe H, Abel J. Growth factors, cytokines and their receptors as downstream targets of arylhydrocarbon receptor (AhR) signaling pathways. Biochem Pharmacol 2009; 77: 508-20.

Hahn ME, Allan LL, Sherr DH. Regulation of constitutive and inducible AHR signaling: complex interactions involving the AHR repressor. Biochem Pharmacol 2009; 77: 485-97.

Han Y, Guo Q, Zhang M, Chen Z, Cao X. CD69+ CD4+ CD25- T cells, a new subset of regulatory T cells, suppress T cell proliferation through membrane-bound TGF-beta 1. J Immunol 2009; 182: 111-20.

Hansen W, Westendorf AM, Reinwald S, Bruder D, Deppenmeier S, Groebe L, et al. Chronic Antigen Stimulation In Vivo Induces a Distinct Population of Antigen-Specific Foxp3 CD25 Regulatory T Cells. J Immunol 2007; 179: 8059-68.

Hauben E, Gregori S, Draghici E, Migliavacca B, Olivieri S, Woisetschlager M, et al. Activation of the aryl hydrocarbon receptor promotes allograft-specific tolerance through direct and dendritic cell-mediated effects on regulatory T cells. Blood 2008; 112: 1214-22.

Hayashio S, Okabe-Kado J, Honma Y, Kawajiri K. Expression of Ah receptor (TCDD receptor) during human monocytic differentiation. Carcinogenesis 1995; 16: 1403-1409.

Head JL, Lawrence BP. The aryl hydrocarbon receptor is a modulator of anti-viral immunity. Biochem Pharmacol 2009; 77: 642-53.

Heath-Pagliuso S, Rogers WJ, Tullis K, Seidel SD, Cenijn PH, Brouwer A, et al. Activation of the Ah receptor by tryptophan and tryptophan metabolites. Biochemistry 1998; 37: 11508-15.

Hestermann EV, Brown M. Agonist and chemopreventative ligands induce differential transcriptional cofactor recruitment by aryl hydrocarbon receptor. Mol Cell Biol 2003; 23: 7920-5.

Hill JA, Feuerer M, Tash K, Haxhinasto S, Perez J, Melamed R, et al. Foxp3 transcription-factor-dependent and -independent regulation of the regulatory T cell transcriptional signature. Immunity 2007; 27: 786-800.

Hinsdill RD, Couch DL, Speirs RS. Immunosuppression in mice induced by dioxin (TCDD) in feed. J Environ Pathol Toxicol 1980; 4: 401-25.

Hirahara K, Liu L, Clark RA, Yamanaka K, Fuhlbrigge RC, Kupper TS. The majority of human peripheral blood CD4+CD25highFoxp3+ regulatory T cells bear functional skin-homing receptors. J Immunol 2006; 177: 4488-94.

Hollingshead BD, Beischlag TV, Dinatale BC, Ramadoss P, Perdew GH. Inflammatory signaling and aryl hydrocarbon receptor mediate synergistic induction of interleukin 6 in MCF-7 cells. Cancer Res 2008; 68: 3609-17.

Hori S, Nomura T, Sakaguchi S. Control of regulatory T cell development by the transcription factor Foxp3. Science 2003; 299: 1057-61.

House RV, Lauer LD, Murray MJ, Thomas PT, Ehrlich JP, Burleson GR, et al. Examination of immune parameters and host resistance mechanisms in B6C3F1 mice following adult exposure to 2,3,7,8-tetrachlorodibenzo-p-

dioxin. J Toxicol Environ Health 1990; 31: 203-15.

Hudziak RM, Barofsky E, Barofsky DF, Weller DL, Huang SB, Weller DD. Resistance of morpholino phosphorodiamidate oligomers to enzymatic degradation. Antisense Nucleic Acid Drug Dev 1996; 6: 267-72.

Huff J, Lucier G, Tritscher A. Carcinogenicity of TCDD: experimental, mechanistic, and epidemiologic evidence. Annu Rev Pharmacol Toxicol 1994; 34: 343-72.

Huwe JK. Dioxins in food: a modern agricultural perspective. J Agric Food Chem 2002; 50: 1739-50.

Inouye K, Pan X, Imai N, Ito T, Takei T, Tohyama C, et al. T cell-derived IL-5 production is a sensitive target of 2,3,7,8-tetrachlorodibenzo-p-dioxin (TCDD). Chemosphere 2005; 60: 907-13.

Ito T, Inouye K, Fujimaki H, Tohyama C, Nohara K. Mechanism of TCDD-induced suppression of antibody production: effect on T cell-derived cytokine production in the primary immune reaction of mice. Toxicol Sci 2002; 70: 46-54.

Iversen PL. Screening for effective host gene targets to identify therapeutic leads for hemorrhagic viral infections. Interscience Conference on Antimicrobial Agents and Chemotherapy. San Francisco, 2009.

Jensen BA, Leeman RJ, Schlezinger JJ, Sherr DH. Aryl hydrocarbon receptor (AhR) agonists suppress interleukin-6 expression by bone marrow stromal cells: an immunotoxicology study. Environ Health 2003; 2: 16.

Jeon MS, Esser C. The murine IL-2 promoter contains distal regulatory elements responsive to the Ah receptor, a member of the evolutionarily conserved bHLH-PAS transcription factor family. J Immunol 2000; 165: 6975-83.

Jones S. An overview of the basic helix-loop-helix proteins. Genome Biol 2004; 5: 226.

Kaartinen V, Cui XM, Heisterkamp N, Groffen J, Shuler CF. Transforming growth factor-beta3 regulates transdifferentiation of medial edge epithelium during palatal fusion and associated degradation of the basement membrane. Dev Dyn 1997; 209: 255-60.

Kallies A, Hawkins ED, Belz GT, Metcalf D, Hommel M, Corcoran LM, et al. Transcriptional repressor Blimp-1 is essential for T cell homeostasis and self-tolerance. Nat Immunol 2006; 7: 466-74.

Kaplan IM, Wadia JS, Dowdy SF. Cationic TAT peptide transduction domain enters

cells by macropinocytosis. J Control Release 2005; 102: 247-53.

Karakozova M, Kozak M, Wong CC, Bailey AO, Yates JR, 3rd, Mogilner A, et al. Arginylation of beta-actin regulates actin cytoskeleton and cell motility. Science 2006; 313: 192-6.

Karras JG, Holsapple MP. Inhibition of calcium-dependent B cell activation by 2,3,7,8-tetrachlorodibenzo-p-dioxin. Toxicol Appl Pharmacol 1994a; 125: 264-70.

Karras JG, Holsapple MP. Mechanisms of 2,3,7,8-tetrachlorodibenzo-p-dioxin (TCDD)-induced disruption of B-lymphocyte signaling in the mouse: a current perspective. Exp Clin Immunogenet 1994b; 11: 110-8.

Kerkvliet NI. Immunotoxicology of Dioxins and Related Chemicals. In: Schecter A, editor. Dioxins and Health. New York: Plenum Press, 1994.

Kerkvliet NI. Recent advances in understanding the mechanisms of TCDD immunotoxicity. Int Immunopharmacol 2002; 2: 277-91.

Kerkvliet NI. AHR-mediated immunomodulation: the role of altered gene transcription. Biochem Pharmacol 2009; 77: 746-60.

Kerkvliet NI, Baecher-Steppan L, Shepherd DM, Oughton JA, Vorderstrasse BA, DeKrey GK. Inhibition of TC-1 cytokine production, effector cytotoxic T lymphocyte development and alloantibody production by 2,3,7,8-tetrachlorodibenzo-p-dioxin. J Immunol 1996; 157: 2310-9.

Kerkvliet NI, Shepherd DM, Baecher-Steppan L. T lymphocytes are direct, aryl hydrocarbon receptor (AhR)-dependent targets of 2,3,7,8-tetrachlorodibenzo-p-dioxin (TCDD): AhR expression in both CD4+ and CD8+ T cells is necessary for full suppression of a cytotoxic T lymphocyte response by TCDD. Toxicol Appl Pharmacol 2002; 185: 146-52.

Kerkvliet NI, Steppan LB, Vorachek WR, Oda SK, Farrer D, Wong CP, et al. Activation of aryl hydrocarbon receptor by TCDD prevents diabetes in NOD mice and increases Foxp3+ T cells in pancreatic lymph nodes. Immunotherapy 2009; 1: 539-547.

Kim DW, Gazourian L, Quadri SA, Romieu-Mourez R, Sherr DH, Sonenshein GE. The RelA NF-kappaB subunit and the aryl hydrocarbon receptor (AhR) cooperate to transactivate the c-myc promoter in mammary cells. Oncogene 2000; 19: 5498-506.

Kimura A, Naka T, Nakahama T, Chinen I, Masuda K, Nohara K, et al. Aryl hydrocarbon receptor in combination with Stat1 regulates LPS-induced

inflammatory responses. J Exp Med 2009; 206: 2027-35.

Kimura A, Naka T, Nohara K, Fujii-Kuriyama Y, Kishimoto T. Aryl hydrocarbon receptor regulates Stat1 activation and participates in the development of Th17 cells. Proc Natl Acad Sci U S A 2008; 105: 9721-6.

Kinehara M, Fukuda I, Yoshida K, Ashida H. High-throughput evaluation of aryl hydrocarbon receptor-binding sites selected via chromatin immunoprecipitation-based screening in Hepa-1c1c7 cells stimulated with 2,3,7,8-tetrachlorodibenzo-p-dioxin. Genes Genet Syst 2008; 83: 455-68.

Kinney RM, Huang CY, Rose BC, Kroeker AD, Dreher TW, Iversen PL, et al. Inhibition of dengue virus serotypes 1 to 4 in vero cell cultures with morpholino oligomers. J Virol 2005; 79: 5116-28.

Kitajima T, Caceres-Dittmar G, Tapia FJ, Jester J, Bergstresser PR, Takashima A. T cell-mediated terminal maturation of dendritic cells: loss of adhesive and phagocytotic capacities. J Immunol 1996; 157: 2340-7.

Klinge CM, Kaur K, Swanson HI. The aryl hydrocarbon receptor interacts with estrogen receptor alpha and orphan receptors COUP-TFI and ERRalpha1. Arch Biochem Biophys 2000; 373: 163-74.

Koch MA, Tucker-Heard G, Perdue NR, Killebrew JR, Urdahl KB, Campbell DJ. The transcription factor T-bet controls regulatory T cell homeostasis and function during type 1 inflammation. Nat Immunol 2009; 10: 595-602.

Kole R, Sazani P. Antisense effects in the cell nucleus: modification of splicing. Curr Opin Mol Ther 2001; 3: 229-34.

Kole R, Vacek M, Williams T. Modification of alternative splicing by antisense therapeutics. Oligonucleotides 2004; 14: 65-74.

Kretschmer K, Apostolou I, Hawiger D, Khazaie K, Nussenzweig MC, von Boehmer H. Inducing and expanding regulatory T cell populations by foreign antigen. Nat Immunol 2005; 6: 1219-27.

Kryczek I, Wei S, Zou L, Zhu G, Mottram P, Xu H, et al. Cutting edge: induction of B7-H4 on APCs through IL-10: novel suppressive mode for regulatory T cells. J Immunol 2006; 177: 40-4.

Kumar MB, Ramadoss P, Reen RK, Vanden Heuvel JP, Perdew GH. The Q-rich subdomain of the human Ah receptor transactivation domain is required for dioxin-mediated transcriptional activity. J Biol Chem 2001; 276: 42302-10.

Lacerra G, Sierakowska H, Carestia C, Fucharoen S, Summerton J, Weller D, et al. Restoration of hemoglobin A synthesis in erythroid cells from peripheral

blood of thalassemic patients. Proc Natl Acad Sci U S A 2000; 97: 9591-6.

Lai ZW, Hundeiker C, Gleichmann E, Esser C. Cytokine gene expression during ontogeny in murine thymus on activation of the aryl hydrocarbon receptor by 2,3,7,8-tetrachlorodibenzo-p-dioxin. Mol Pharmacol 1997; 52: 30-7.

Lai ZW, Pineau T, Esser C. Identification of dioxin-responsive elements (DREs) in the 5' regions of putative dioxin-inducible genes. Chem Biol Interact 1996; 100: 97-112.

Lawrence BP, Denison MS, Novak H, Vorderstrasse BA, Harrer N, Neruda W, et al. Activation of the aryl hydrocarbon receptor is essential for mediating the anti-inflammatory effects of a novel low-molecular-weight compound. Blood 2008; 112: 1158-65.

Lawrence BP, Kerkvliet NI. Immune modulation by TCDD and related polyhalogenated aromatic hydrocarbons. In: Luebke R, House R and Kimber I, editors. Immunotoxicology and Immunopharmacology. Boca Raton FL: CRC Press, 2007: 239-258.

Lawrence BP, Roberts AD, Neumiller JJ, Cundiff JA, Woodland DL. Aryl hydrocarbon receptor activation impairs the priming but not the recall of influenza virus-specific CD8+ T cells in the lung. J Immunol 2006; 177: 5819-28.

Lawrence BP, Vorderstrasse BA. Activation of the aryl hydrocarbon receptor diminishes the memory response to homotypic influenza virus infection but does not impair host resistance. Toxicol Sci 2004; 79: 304-14.

Lawrence BP, Warren TK, Luong H. Fewer T lymphocytes and decreased pulmonary influenza virus burden in mice exposed to 2,3,7,8-tetrachlorodibenzo-p-dioxin (TCDD). J Toxicol Environ Health A 2000; 61: 39-53.

Lee I, Wang L, Wells AD, Dorf ME, Ozkaynak E, Hancock WW. Recruitment of Foxp3+ T regulatory cells mediating allograft tolerance depends on the CCR4 chemokine receptor. J Exp Med 2005; 201: 1037-44.

Lee JA, Hwang JA, Sung HN, Jeon CH, Gill BC, Youn HJ, et al. 2,3,7,8-Tetrachlorodibenzo-p-dioxin modulates functional differentiation of mouse bone marrow-derived dendritic cells Downregulation of RelB by 2,3,7,8-tetrachlorodibenzo-p-dioxin. Toxicol Lett 2007; 173: 31-40.

Luebke RW, Copeland CB, Andrews DL. Host resistance to Trichinella spiralis infection in rats exposed to 2,3,7,8-tetrachlorodibenzo-p-dioxin (TCDD). Fundam Appl Toxicol 1995; 24: 285-9.

Luebke RW, Copeland CB, Daniels M, Lambert AL, Gilmour MI. Suppression of allergic immune responses to house dust mite (HDM) in rats exposed to 2,3,7,8-TCDD. Toxicol Sci 2001; 62: 71-9.

Luebke RW, Copeland CB, Diliberto JJ, Akubue PI, Andrews DL, Riddle MM, et al. Assessment of host resistance to Trichinella spiralis in mice following preinfection exposure to 2,3,7,8-TCDD. Toxicol Appl Pharmacol 1994; 125: 7-16.

Lundberg K, Dencker L, Gronvik KO. 2,3,7,8-Tetrachlorodibenzo-p-dioxin (TCDD) inhibits the activation of antigen-specific T-cells in mice. Int J Immunopharmacol 1992; 14: 699-705.

Luster MI, Germolec DR, Clark G, Wiegand G, Rosenthal GJ. Selective effects of 2,3,7,8-tetrachlorodibenzo-p-dioxin and corticosteroid on in vitro lymphocyte maturation. J Immunol 1988; 140: 928-35.

Lynch KW. Consequences of regulated pre-mRNA splicing in the immune system. Nat Rev Immunol 2004; 4: 931-40.

Lynch KW, Weiss A. A CD45 polymorphism associated with multiple sclerosis disrupts an exonic splicing silencer. J Biol Chem 2001; 276: 24341-7.

Marcus RS, Holsapple MP, Kaminski NE. Lipopolysaccharide activation of murine splenocytes and splenic B cells increased the expression of aryl hydrocarbon receptor and aryl hydrocarbon receptor nuclear translocator. J Pharmacol Exp Ther 1998; 287: 1113-8.

Marlowe JL, Fan Y, Chang X, Peng L, Knudsen ES, Xia Y, et al. The aryl hydrocarbon receptor binds to E2F1 and inhibits E2F1-induced apoptosis. Mol Biol Cell 2008; 19: 3263-71.

Marshall NB, Kerkvliet NI. Dioxin and immune regulation: emerging role of aryl hydrocarbon receptor in the generation of regulatory T cells. Annals of the New York Academy of Sciences 2009; In press.

Marshall NB, Oda SK, London CA, Moulton HM, Iversen PL, Kerkvliet NI, et al. Arginine-rich cell-penetrating peptides facilitate delivery of antisense oligomers into murine leukocytes and alter pre-mRNA splicing. J Immunol Methods 2007; 325: 114-26.

Marshall NB, Vorachek WR, Steppan LB, Mourich DV, Kerkvliet NI. Functional characterization and gene expression analysis of CD4+ CD25+ regulatory T cells generated in mice treated with 2,3,7,8-tetrachlorodibenzo-p-dioxin. J Immunol 2008; 181: 2382-91.

Martins GA, Cimmino L, Shapiro-Shelef M, Szabolcs M, Herron A, Magnusdottir E, et al. Transcriptional repressor Blimp-1 regulates T cell homeostasis and function. Nat Immunol 2006; 7: 457-65.

McClorey G, Moulton HM, Iversen PL, Fletcher S, Wilton SD. Antisense oligonucleotide-induced exon skipping restores dystrophin expression in vitro in a canine model of DMD. Gene Ther 2006; 13: 1373-81.

McHale CM, Zhang L, Hubbard AE, Zhao X, Baccarelli A, Pesatori AC, et al. Microarray analysis of gene expression in peripheral blood mononuclear cells from dioxin-exposed human subjects. Toxicology 2007; 229: 101-13.

McManus MT, Haines BB, Dillon CP, Whitehurst CE, van Parijs L, Chen J, et al. Small Interfering RNA-Mediated Gene Silencing in T Lymphocytes. J Immunol 2002; 169: 5754-5760.

McMillan BJ, Bradfield CA. The aryl hydrocarbon receptor is activated by modified low-density lipoprotein. Proc Natl Acad Sci U S A 2007; 104: 1412-7.

Medicine Io. Veterans and Agent Orange: Update 2006. Washington D.C.: National Academies Press, 2007.

Mellor AL, Chandler P, Baban B, Hansen AM, Marshall B, Pihkala J, et al. Specific subsets of murine dendritic cells acquire potent T cell regulatory functions following CTLA4-mediated induction of indoleamine 2,3 dioxygenase. Int Immunol 2004; 16: 1391-401.

Mendoza L. A network model for the control of the differentiation process in Th cells. Biosystems 2006; 84: 101-14.

Midoux P, Kichler A, Boutin V, Maurizot JC, Monsigny M. Membrane permeabilization and efficient gene transfer by a peptide containing several histidines. Bioconjug Chem 1998; 9: 260-7.

Miniero R, De Felip E, Ferri F, di Domenico A. An overview of TCDD half-life in mammals and its correlation to body weight. Chemosphere 2001; 43: 839-44.

Mitchell KA, Lawrence BP. Exposure to 2,3,7,8-tetrachlorodibenzo-p-dioxin (TCDD) renders influenza virus-specific CD8+ T cells hyporesponsive to antigen. Toxicol Sci 2003a; 74: 74-84.

Mitchell KA, Lawrence BP. T cell receptor transgenic mice provide novel insights into understanding cellular targets of TCDD: suppression of antibody production, but not the response of CD8(+) T cells, during infection with influenza virus. Toxicol Appl Pharmacol 2003b; 192: 275-86.

Miyara M, Sakaguchi S. Natural regulatory T cells: mechanisms of suppression.

Trends Mol Med 2007; 13: 108-16.

Morales JL, Krzeminski J, Amin S, Perdew GH. Characterization of the antiallergic drugs 3-[2-(2-phenylethyl) benzoimidazole-4-yl]-3-hydroxypropanoic acid and ethyl 3-hydroxy-3-[2-(2-phenylethyl)benzoimidazol-4-yl]propanoate as full aryl hydrocarbon receptor agonists. Chem Res Toxicol 2008; 21: 472-82.

Moses M, Prioleau PG. Cutaneous histologic findings in chemical workers with and without chloracne with past exposure to 2,3,7,8-tetrachlorodibenzo-p-dioxin. J Am Acad Dermatol 1985; 12: 497-506.

Moulton HM, Hase MC, Smith KM, Iversen PL. HIV Tat peptide enhances cellular delivery of antisense morpholino oligomers. Antisense Nucleic Acid Drug Dev 2003; 13: 31-43.

Moulton HM, Nelson MH, Hatlevig SA, Reddy MT, Iversen PL. Cellular uptake of antisense morpholino oligomers conjugated to arginine-rich peptides. Bioconjug Chem 2004; 15: 290-9.

Mourich DV, Jendrzejewski JL, Marshall NB, Hinrichs DJ, Iversen PL, Brand RM. Antisense targeting of cFLIP sensitizes activated T cells to undergo apoptosis and desensitizes responses to contact dermatitis. J Invest Dermatol 2009; 129: 1945-53.

Mullen AC, High FA, Hutchins AS, Lee HW, Villarino AV, Livingston DM, et al. Role of T-bet in commitment of TH1 cells before IL-12-dependent selection. Science 2001; 292: 1907-10.

Munn DH, Sharma MD, Mellor AL. Ligation of B7-1/B7-2 by human CD4+ T cells triggers indoleamine 2,3-dioxygenase activity in dendritic cells. J Immunol 2004; 172: 4100-10.

Najafian N, Chitnis T, Salama AD, Zhu B, Benou C, Yuan X, et al. Regulatory functions of CD8+CD28- T cells in an autoimmune disease model. J Clin Invest 2003; 112: 1037-48.

Nakamura K, Kitani A, Strober W. Cell contact-dependent immunosuppression by CD4(+)CD25(+) regulatory T cells is mediated by cell surface-bound transforming growth factor beta. J Exp Med 2001; 194: 629-44.

Nakase I, Niwa M, Takeuchi T, Sonomura K, Kawabata N, Koike Y, et al. Cellular uptake of arginine-rich peptides: roles for macropinocytosis and actin rearrangement. Mol Ther 2004; 10: 1011-22.

Nebert DW, Roe AL, Dieter MZ, Solis WA, Yang Y, Dalton TP. Role of the aromatic hydrocarbon receptor and [Ah] gene battery in the oxidative stress

response, cell cycle control, and apoptosis. Biochem Pharmacol 2000; 59: 65-85.

Neff-LaFord H, Teske S, Bushnell TP, Lawrence BP. Aryl hydrocarbon receptor activation during influenza virus infection unveils a novel pathway of IFN-gamma production by phagocytic cells. J Immunol 2007; 179: 247-55.

Negishi T, Kato Y, Ooneda O, Mimura J, Takada T, Mochizuki H, et al. Effects of aryl hydrocarbon receptor signaling on the modulation of TH1/TH2 balance. J Immunol 2005; 175: 7348-56.

Nohara K, Fujimaki H, Tsukumo S, Inouye K, Sone H, Tohyama C. Effects of 2,3,7,8-tetrachlorodibenzo-p-dioxin (TCDD) on T cell-derived cytokine production in ovalbumin (OVA)-immunized C57Bl/6 mice. Toxicology 2002; 172: 49-58.

Norbury CC, Hewlett LJ, Prescott AR, Shastri N, Watts C. Class I MHC presentation of exogenous soluble antigen via macropinocytosis in bone marrow macrophages. Immunity 1995; 3: 783-91.

Nouri-Aria KT, Durham SR. Regulatory T cells and allergic disease. Inflamm Allergy Drug Targets 2008; 7: 237-52.

Oberg M, Bergander L, Hakansson H, Rannug U, Rannug A. Identification of the tryptophan photoproduct 6-formylindolo[3,2-b]carbazole, in cell culture medium, as a factor that controls the background aryl hydrocarbon receptor activity. Toxicol Sci 2005; 85: 935-43.

Ochoa JB, Strange J, Kearney P, Gellin G, Endean E, Fitzpatrick E. Effects of L-arginine on the proliferation of T lymphocyte subpopulations. JPEN J Parenter Enteral Nutr 2001; 25: 23-9.

Ohtake F, Baba A, Takada I, Okada M, Iwasaki K, Miki H, et al. Dioxin receptor is a ligand-dependent E3 ubiquitin ligase. Nature 2007; 446: 562-6.

Ohtake F, Takeyama K, Matsumoto T, Kitagawa H, Yamamoto Y, Nohara K, et al. Modulation of oestrogen receptor signalling by association with the activated dioxin receptor. Nature 2003; 423: 545-50.

Okey AB, Riddick DS, Harper PA. The Ah receptor: mediator of the toxicity of 2,3,7,8-tetrachlorodibenzo-p-dioxin (TCDD) and related compounds. Toxicol Lett 1994; 70: 1-22.

O'Sullivan A, Chang HC, Yu Q, Kaplan MH. STAT4 is required for interleukin-12-induced chromatin remodeling of the CD25 locus. J Biol Chem 2004; 279: 7339-45.

Oughton JA, Kerkvliet NI. Novel phenotype associated with in vivo activated CTL precursors. Clin Immunol 1999; 90: 323-33.

Phelan D, Winter GM, Rogers WJ, Lam JC, Denison MS. Activation of the Ah receptor signal transduction pathway by bilirubin and biliverdin. Arch Biochem Biophys 1998; 357: 155-63.

Platten M, Ho PP, Youssef S, Fontoura P, Garren H, Hur EM, et al. Treatment of autoimmune neuroinflammation with a synthetic tryptophan metabolite. Science 2005; 310: 850-5.

Poland A, Glover E, Kende AS. Stereospecific, high affinity binding of 2,3,7,8-tetrachlorodibenzo-p-dioxin by hepatic cytosol. Evidence that the binding species is receptor for induction of aryl hydrocarbon hydroxylase. J Biol Chem 1976; 251: 4936-46.

Poland AP, Glover E, Robinson JR, Nebert DW. Genetic expression of aryl hydrocarbon hydroxylase activity. Induction of monooxygenase activities and cytochrome P1-450 formation by 2,3,7,8-tetrachlorodibenzo-p-dioxin in mice genetically "nonresponsive" to other aromatic hydrocarbons. J Biol Chem 1974; 249: 5599-606.

Prell RA, Dearstyne E, Steppan LG, Vella AT, Kerkvliet NI. CTL hyporesponsiveness induced by 2,3,7, 8-tetrachlorodibenzo-p-dioxin: role of cytokines and apoptosis. Toxicol Appl Pharmacol 2000; 166: 214-21.

Prell RA, Oughton JA, Kerkvliet NI. Effect of 2,3,7,8-tetrachlorodibenzo-p-dioxin on anti-CD3-induced changes in T-cell subsets and cytokine production. Int J Immunopharmacol 1995; 17: 951-61.

Proudnikov D, Yuferov V, Zhou Y, LaForge KS, Ho A, Kreek MJ. Optimizing primer--probe design for fluorescent PCR. J Neurosci Methods 2003; 123: 31-45.

Pryputniewicz SJ, Nagarkatti M, Nagarkatti PS. Differential induction of apoptosis in activated and resting T cells by 2,3,7,8-tetrachlorodibenzo-p-dioxin (TCDD) and its repercussion on T cell responsiveness. Toxicology 1998; 129: 211-26.

Puccetti P, Grohmann U. IDO and regulatory T cells: a role for reverse signalling and non-canonical NF-kappaB activation. Nat Rev Immunol 2007; 7: 817-23.

Puga A, Barnes SJ, Dalton TP, Chang C, Knudsen ES, Maier MA. Aromatic hydrocarbon receptor interaction with the retinoblastoma protein potentiates repression of E2F-dependent transcription and cell cycle arrest. J Biol Chem

2000; 275: 2943-50.

Quintana FJ, Basso AS, Iglesias AH, Korn T, Farez MF, Bettelli E, et al. Control of T(reg) and T(H)17 cell differentiation by the aryl hydrocarbon receptor. Nature 2008; 453: 65-71.

Radstake TR, van Bon L, Broen J, Wenink M, Santegoets K, Deng Y, et al. Increased frequency and compromised function of T regulatory cells in systemic sclerosis (SSc) is related to a diminished CD69 and TGFbeta expression. PLoS One 2009; 4: e5981.

Ramadoss P, Perdew GH. Use of 2-azido-3-[125I]iodo-7,8-dibromodibenzo-p-dioxin as a probe to determine the relative ligand affinity of human versus mouse aryl hydrocarbon receptor in cultured cells. Mol Pharmacol 2004; 66: 129-36.

Ranganath S, Ouyang W, Bhattarcharya D, Sha WC, Grupe A, Peltz G, et al. GATA-3-dependent enhancer activity in IL-4 gene regulation. J Immunol 1998; 161: 3822-6.

Registry AfTSaD. Dioxins. ToxFAQs: Chemical Agent Briefing Sheet: Division of Toxicology and Environmental Medicine, 2006.

Rifa'i M, Kawamoto Y, Nakashima I, Suzuki H. Essential roles of CD8+CD122+ regulatory T cells in the maintenance of T cell homeostasis. J Exp Med 2004; 200: 1123-34.

Roncarolo MG, Gregori S, Battaglia M, Bacchetta R, Fleischhauer K, Levings MK. Interleukin-10-secreting type 1 regulatory T cells in rodents and humans. Immunol Rev 2006; 212: 28-50.

Rothbard JB, Kreider E, VanDeusen CL, Wright L, Wylie BL, Wender PA. Arginine-rich molecular transporters for drug delivery: role of backbone spacing in cellular uptake. J Med Chem 2002; 45: 3612-8.

Ruby CE, Funatake CJ, Kerkvliet NI. 2,3,7,8 Tetrachlorodibenzo-p-Dioxin (TCDD) directly enhances the maturation and apoptosis of dendritic cells in vitro. J Immunotoxicol 2005; 1: 159-66.

Ruby CE, Leid M, Kerkvliet NI. 2,3,7,8-Tetrachlorodibenzo-p-dioxin suppresses tumor necrosis factor-alpha and anti-CD40-induced activation of NF-kappaB/Rel in dendritic cells: p50 homodimer activation is not affected. Mol Pharmacol 2002; 62: 722-8.

Sakaguchi S, Sakaguchi N, Asano M, Itoh M, Toda M. Immunologic self-tolerance maintained by activated T cells expressing IL-2 receptor alpha-chains

(CD25). Breakdown of a single mechanism of self-tolerance causes various autoimmune diseases. J Immunol 1995; 155: 1151-64.

Sancho D, Gomez M, Sanchez-Madrid F. CD69 is an immunoregulatory molecule induced following activation. Trends Immunol 2005; 26: 136-40.

Sasaki T, Sasaki-Irie J, Penninger JM. New insights into the transmembrane protein tyrosine phosphatase CD45. Int J Biochem Cell Biol 2001; 33: 1041-6.

Schaldach CM, Riby J, Bjeldanes LF. Lipoxin A4: a new class of ligand for the Ah receptor. Biochemistry 1999; 38: 7594-600.

Schecter A, Gasiewicz TA. Dioxins and Health, 2nd Edition. Hoboken, NJ: John Wiley and Sons, Inc., 2003.

Schmidt JV, Bradfield CA. Ah receptor signaling pathways. Annu Rev Cell Dev Biol 1996; 12: 55-89.

Schneider D, Manzan MA, Yoo BS, Crawford RB, Kaminski N. Involvement of Blimp-1 and AP-1 dysregulation in the 2,3,7,8-tetrachlorodibenzo-p-dioxin-mediated suppression of the IgM response by B cells. Toxicol Sci 2009.

Schulz EG, Mariani L, Radbruch A, Hofer T. Sequential polarization and imprinting of type 1 T helper lymphocytes by interferon-gamma and interleukin-12. Immunity 2009; 30: 673-83.

Seidel SD, Winters GM, Rogers WJ, Ziccardi MH, Li V, Keser B, et al. Activation of the Ah receptor signaling pathway by prostaglandins. J Biochem Mol Toxicol 2001; 15: 187-96.

Shaw AS. Lipid rafts: now you see them, now you don't. Nat Immunol 2006; 7: 1139-42.

Shen ES, Whitlock JP, Jr. Protein-DNA interactions at a dioxin-responsive enhancer. Mutational analysis of the DNA-binding site for the liganded Ah receptor. J Biol Chem 1992; 267: 6815-9.

Shepherd DM, Dearstyne EA, Kerkvliet NI. The effects of TCDD on the activation of ovalbumin (OVA)-specific DO11.10 transgenic CD4(+) T cells in adoptively transferred mice. Toxicol Sci 2000; 56: 340-50.

Shevach EM, Stephens GL. The GITR-GITRL interaction: co-stimulation or contrasuppression of regulatory activity? Nat Rev Immunol 2006; 6: 613-8.

Shi LZ, Faith NG, Nakayama Y, Suresh M, Steinberg H, Czuprynski CJ. The aryl hydrocarbon receptor is required for optimal resistance to Listeria monocytogenes infection in mice. J Immunol 2007; 179: 6952-62.

Shimizu J, Yamazaki S, Takahashi T, Ishida Y, Sakaguchi S. Stimulation of CD25+CD4+ regulatory T cells through GITR breaks immunological self-tolerance. 2002; 3: 135-142.

Shoemaker J, Saraiva M, O'Garra A. GATA-3 directly remodels the IL-10 locus independently of IL-4 in CD4+ T cells. J Immunol 2006; 176: 3470-9.

Sinal CJ, Bend JR. Aryl hydrocarbon receptor-dependent induction of cyp1a1 by bilirubin in mouse hepatoma hepa 1c1c7 cells. Mol Pharmacol 1997; 52: 590-9.

Staples JE, Murante FG, Fiore NC, Gasiewicz TA, Silverstone AE. Thymic alterations induced by 2,3,7,8-tetrachlorodibenzo-p-dioxin are strictly dependent on aryl hydrocarbon receptor activation in hemopoietic cells. J Immunol 1998; 160: 3844-54.

Stein D, Foster E, Huang SB, Weller D, Summerton J. A specificity comparison of four antisense types: morpholino, 2'-O-methyl RNA, DNA, and phosphorothioate DNA. Antisense Nucleic Acid Drug Dev 1997; 7: 151-7.

Stoecklin G, Tenenbaum SA, Mayo T, Chittur SV, George AD, Baroni TE, et al. Genome-wide analysis identifies interleukin-10 mRNA as target of tristetraprolin. J Biol Chem 2008; 283: 11689-99.

Sulentic CE, Holsapple MP, Kaminski NE. Aryl hydrocarbon receptor-dependent suppression by 2,3,7, 8-tetrachlorodibenzo-p-dioxin of IgM secretion in activated B cells. Mol Pharmacol 1998; 53: 623-9.

Summerton J, Weller D. Uncharged morpholino-based polymers having phosphorus containing chiral intersubunit linkages. US Patent 5185444, 1993.

Summerton J, Weller D. Morpholino antisense oligomers: design, preparation, and properties. Antisense Nucleic Acid Drug Dev 1997; 7: 187-95.

Sun YV, Boverhof DR, Burgoon LD, Fielden MR, Zacharewski TR. Comparative analysis of dioxin response elements in human, mouse and rat genomic sequences. Nucleic Acids Res 2004; 32: 4512-23.

Suwanmanee T, Sierakowska H, Lacerra G, Svasti S, Kirby S, Walsh CE, et al. Restoration of human beta-globin gene expression in murine and human IVS2-654 thalassemic erythroid cells by free uptake of antisense oligonucleotides. Mol Pharmacol 2002; 62: 545-53.

Szabo SJ, Dighe AS, Gubler U, Murphy KM. Regulation of the interleukin (IL)-12R beta 2 subunit expression in developing T helper 1 (Th1) and Th2 cells. J Exp Med 1997; 185: 817-24.

Szabo SJ, Kim ST, Costa GL, Zhang X, Fathman CG, Glimcher LH. A novel transcription factor, T-bet, directs Th1 lineage commitment. Cell 2000; 100: 655-69.

Takahashi T, Kuniyasu Y, Toda M, Sakaguchi N, Itoh M, Iwata M, et al. Immunologic self-tolerance maintained by CD25+CD4+ naturally anergic and suppressive T cells: induction of autoimmune disease by breaking their anergic/suppressive state. Int Immunol 1998; 10: 1969-80.

Tao R, de Zoeten EF, Ozkaynak E, Chen C, Wang L, Porrett PM, et al. Deacetylase inhibition promotes the generation and function of regulatory T cells. Nat Med 2007; 13: 1299-307.

Tas SW, Vervoordeldonk MJ, Hajji N, Schuitemaker JH, van der Sluijs KF, May MJ, et al. Noncanonical NF-kappaB signaling in dendritic cells is required for indoleamine 2,3-dioxygenase (IDO) induction and immune regulation. Blood 2007; 110: 1540-9.

Terness P, Bauer TM, Rose L, Dufter C, Watzlik A, Simon H, et al. Inhibition of allogeneic T cell proliferation by indoleamine 2,3-dioxygenase-expressing dendritic cells: mediation of suppression by tryptophan metabolites. J Exp Med 2002; 196: 447-57.

Teske S, Bohn AA, Regal JF, Neumiller JJ, Lawrence BP. Activation of the aryl hydrocarbon receptor increases pulmonary neutrophilia and diminishes host resistance to influenza A virus. Am J Physiol Lung Cell Mol Physiol 2005; 289: L111-24.

Tesmer LA, Lundy SK, Sarkar S, Fox DA. Th17 cells in human disease. Immunol Rev 2008; 223: 87-113.

Thigpen JE, Faith RE, McConnell EE, Moore JA. Increased susceptibility to bacterial infection as a sequela of exposure to 2,3,7,8-tetrachlorodibenzo-p-dioxin. Infect Immun 1975; 12: 1319-24.

Thornton AM, Shevach EM. CD4+CD25+ immunoregulatory T cells suppress polyclonal T cell activation in vitro by inhibiting interleukin 2 production. J Exp Med 1998; 188: 287-96.

Thurmond TS, Gasiewicz TA. A single dose of 2,3,7,8-tetrachlorodibenzo-p-dioxin produces a time- and dose-dependent alteration in the murine bone marrow B-lymphocyte maturation profile. Toxicol Sci 2000; 58: 88-95.

Thurmond TS, Staples JE, Silverstone AE, Gasiewicz TA. The aryl hydrocarbon receptor has a role in the in vivo maturation of murine bone marrow B lymphocytes and their response to 2,3,7,8-tetrachlorodibenzo-p-dioxin.

Toxicol Appl Pharmacol 2000; 165: 227-36.

Tian Y, Ke S, Denison MS, Rabson AB, Gallo MA. Ah receptor and NF-kappaB interactions, a potential mechanism for dioxin toxicity. J Biol Chem 1999; 274: 510-5.

Tilley LD, Hine OS, Kellogg JA, Hassinger JN, Weller DD, Iversen PL, et al. Gene-specific effects of antisense phosphorodiamidate morpholino oligomer-peptide conjugates on Escherichia coli and Salmonella enterica serovar typhimurium in pure culture and in tissue culture. Antimicrob Agents Chemother 2006; 50: 2789-96.

Tilley LD, Mellbye BL, Puckett SE, Iversen PL, Geller BL. Antisense peptide-phosphorodiamidate morpholino oligomer conjugate: dose-response in mice infected with Escherichia coli. J Antimicrob Chemother 2007; 59: 66-73.

Trinchieri G. Interleukin-10 production by effector T cells: Th1 cells show self control. J Exp Med 2007; 204: 239-43.

Tucker AN, Vore SJ, Luster MI. Suppression of B cell differentiation by 2,3,7,8-tetrachlorodibenzo-p-dioxin. Mol Pharmacol 1986; 29: 372-7.

Ueda H, Howson JM, Esposito L, Heward J, Snook H, Chamberlain G, et al. Association of the T-cell regulatory gene CTLA4 with susceptibility to autoimmune disease. Nature 2003; 423: 506-11.

Unutmaz D. RORC2: the master of human Th17 cell programming. Eur J Immunol 2009; 39: 1452-5.

Vaknin-Dembinsky A, Balashov K, Weiner HL. IL-23 is increased in dendritic cells in multiple sclerosis and down-regulation of IL-23 by antisense oligos increases dendritic cell IL-10 production. J Immunol 2006; 176: 7768-74.

Valmori D, Tosello V, Souleimanian NE, Godefroy E, Scotto L, Wang Y, et al. Rapamycin-mediated enrichment of T cells with regulatory activity in stimulated CD4+ T cell cultures is not due to the selective expansion of naturally occurring regulatory T cells but to the induction of regulatory functions in conventional CD4+ T cells. J Immunol 2006; 177: 944-9.

Veldhoen M, Hirota K, Westendorf AM, Buer J, Dumoutier L, Renauld JC, et al. The aryl hydrocarbon receptor links TH17-cell-mediated autoimmunity to environmental toxins. Nature 2008; 453: 106-9.

Vieira PL, Christensen JR, Minaee S, O'Neill EJ, Barrat FJ, Boonstra A, et al. IL-10-secreting regulatory T cells do not express Foxp3 but have comparable regulatory function to naturally occurring CD4+CD25+ regulatory T cells. J

Immunol 2004; 172: 5986-93.

Vives E, Brodin P, Lebleu B. A truncated HIV-1 Tat protein basic domain rapidly translocates through the plasma membrane and accumulates in the cell nucleus. J Biol Chem 1997; 272: 16010-7.

Vives E, Richard JP, Rispal C, Lebleu B. TAT peptide internalization: seeking the mechanism of entry. Curr Protein Pept Sci 2003; 4: 125-32.

Vogel CF, Goth SR, Dong B, Pessah IN, Matsumura F. Aryl hydrocarbon receptor signaling mediates expression of indoleamine 2,3-dioxygenase. Biochem Biophys Res Commun 2008; 375: 331-5.

Vogel CF, Matsumura F. A new cross-talk between the aryl hydrocarbon receptor and RelB, a member of the NF-kappaB family. Biochem Pharmacol 2009; 77: 734-45.

Vorderstrasse BA, Dearstyne EA, Kerkvliet NI. Influence of 2,3,7,8-tetrachlorodibenzo-p-dioxin on the antigen-presenting activity of dendritic cells. Toxicol Sci 2003; 72: 103-12.

Vorderstrasse BA, Kerkvliet NI. 2,3,7,8-Tetrachlorodibenzo-p-dioxin affects the number and function of murine splenic dendritic cells and their expression of accessory molecules. Toxicol Appl Pharmacol 2001; 171: 117-25.

Vorderstrasse BA, Lawrence BP. Protection against lethal challenge with Streptococcus pneumoniae is conferred by aryl hydrocarbon receptor activation but is not associated with an enhanced inflammatory response. Infect Immun 2006; 74: 5679-86.

Vorderstrasse BA, Steppan LB, Silverstone AE, Kerkvliet NI. Aryl hydrocarbon receptor-deficient mice generate normal immune responses to model antigens and are resistant to TCDD-induced immune suppression. Toxicol Appl Pharmacol 2001; 171: 157-64.

Vos JG, Kreeftenberg JG, Engel HW, Minderhoud A, Van Noorle Jansen LM. Studies on 2,3,7,8-tetrachlorodibenzo-p-dioxin induced immune suppression and decreased resistance to infection: endotoxin hypersensitivity, serum zinc concentrations and effect of thymosin treatment. Toxicology 1978; 9: 75-86.

Wadia JS, Stan RV, Dowdy SF. Transducible TAT-HA fusogenic peptide enhances escape of TAT-fusion proteins after lipid raft macropinocytosis. Nat Med 2004; 10: 310-5.

Wagstaff KM, Jans DA. Protein transduction: cell penetrating peptides and their therapeutic applications. Curr Med Chem 2006; 13: 1371-87.

Warren TK, Mitchell KA, Lawrence BP. Exposure to 2,3,7,8-tetrachlorodibenzo-p-dioxin (TCDD) suppresses the humoral and cell-mediated immune responses to influenza A virus without affecting cytolytic activity in the lung. Toxicol Sci 2000; 56: 114-23.

Wei G, Wei L, Zhu J, Zang C, Hu-Li J, Yao Z, et al. Global mapping of H3K4me3 and H3K27me3 reveals specificity and plasticity in lineage fate determination of differentiating CD4+ T cells. Immunity 2009; 30: 155-67.

Wei YD, Helleberg H, Rannug U, Rannug A. Rapid and transient induction of CYP1A1 gene expression in human cells by the tryptophan photoproduct 6-formylindolo[3,2-b]carbazole. Chem Biol Interact 1998; 110: 39-55.

Weiner HL. Induction and mechanism of action of transforming growth factor-beta-secreting Th3 regulatory cells. Immunol Rev 2001; 182: 207-14.

Wilson NJ, Boniface K, Chan JR, McKenzie BS, Blumenschein WM, Mattson JD, et al. Development, cytokine profile and function of human interleukin 17-producing helper T cells. Nat Immunol 2007; 8: 950-7.

Wyman A, Lavin AL, Wilding GE, Gasiewicz TA. 2,3,7,8-tetrachlorodibenzo-p-dioxin does not directly alter the phenotype of maturing B cells in a murine coculture system. Toxicol Appl Pharmacol 2002; 180: 164-77.

Wysocki CA, Jiang Q, Panoskaltsis-Mortari A, Taylor PA, McKinnon KP, Su L, et al. Critical role for CCR5 in the function of donor CD4+CD25+ regulatory T cells during acute graft-versus-host disease. Blood 2005; 106: 3300-7.

Yao EF, Denison MS. DNA sequence determinants for binding of transformed Ah receptor to a dioxin-responsive enhancer. Biochemistry 1992; 31: 5060-7.

Youngblood DS, Hatlevig SA, Hassinger JN, Iversen PL, Moulton HM. Stability of cell-penetrating peptide-morpholino oligomer conjugates in human serum and in cells. Bioconjug Chem 2007; 18: 50-60.

Yuan J, Stein DA, Lim T, Qiu D, Coughlin S, Liu Z, et al. Inhibition of Coxsackievirus B3 in Cell Cultures and in Mice by Peptide-Conjugated Morpholino Oligomers Targeting the Internal Ribosome Entry Site. J. Virol. 2006; 80: 11510-11519.

Zeiser R, Nguyen VH, Hou JZ, Beilhack A, Zambricki E, Buess M, et al. Early CD30 signaling is critical for adoptively transferred CD4+CD25+ regulatory T cells in prevention of acute graft-versus-host disease. Blood 2007; 109: 2225-33.

Zeng WP, Chang C, Lai JJ. Immune suppressive activity and lack of T helper

differentiation are differentially regulated in natural regulatory T cells. J Immunol 2009; 183: 3583-90.

Zhang S, Qin C, Safe SH. Flavonoids as aryl hydrocarbon receptor agonists/antagonists: effects of structure and cell context. Environ Health Perspect 2003; 111: 1877-82.

Zhao Z, Yu S, Fitzgerald DC, Elbehi M, Ciric B, Rostami AM, et al. IL-12R beta 2 promotes the development of CD4+CD25+ regulatory T cells. J Immunol 2008; 181: 3870-6.

Zheng SG, Gray JD, Ohtsuka K, Yamagiwa S, Horwitz DA. Generation ex vivo of TGF-beta-producing regulatory T cells from CD4+CD25- precursors. J Immunol 2002; 169: 4183-9.

Zheng SG, Wang J, Horwitz DA. Cutting edge: Foxp3+CD4+CD25+ regulatory T cells induced by IL-2 and TGF-beta are resistant to Th17 conversion by IL-6. J Immunol 2008; 180: 7112-6.

APPENDIX

A 5-step Screening Process for Selecting an Optimal Antisense Oligomer for Gene-Targeting in Leukocytes

Authors: Nikki B. Marshall

Nancy I. Kerkvliet

Dan V. Mourich

Abstract

Antisense technologies are used widely for inhibition of gene expression. Though traditionally the AUG start codon of the open reading frame is targeted to disrupt ribosome assembly and initiation, an emerging approach is targeting sequences to disrupt pre-mRNA splicing. The primary advantage to this approach is a positive read-out for an antisense effect through detection of a novel splice product. The antisense compounds used here are phosphorodiamidate morpholino oligomers conjugated to an Arginine-rich cell penetrating peptide (P-PMO). We describe a 5-step process for selecting the best candidate antisense compound for altering IL-12Rb2 expression including (1) detecting mRNA splice products by RT-PCR, (2) measuring protein expression, (3) evaluating protein function, (4) checking cellular viability, and (5) validating efficacy of the final candidate compound. The significance of targeting exons consisting of a number of bp divisible by 3, and the recognition of cryptic splice sites are also discussed. The screening steps used to evaluate P-PMO targeting IL-12Rb2 expression here should be applied for designing and screening antisense compounds for other gene targets.

Introduction

Antisense technologies are widely used for altering gene expression to examine the role of specific genes in biological processes. Treating with antisense compounds conditionally affects gene expression in contrast to the use gene-

deficient animals which are challenged by confounded developmental questions. The classic approach to antisense design is targeting the AUG start codon to interfere with ribosome initiation and assembly. However, a drawback to this approach is that the assay read-out for effectiveness is the lack of detection of mRNA and protein. This introduces the potential for false positives due to factors related to the assay technique or the treatment and viability of targeted cells. A preferred approach for measuring antisense efficacy is an assay that provides a positive read-out achieved by altering the normal splice pattern of pre-mRNA. The splicesome recognizes conserved sequences within the pre-mRNA sequence which determine the splice-acceptor (5') and splice donor (3') ends of an exon. The splicesome, in turn, excises intronic sequences as a lariat, and ligates the exons to produce a mature mRNA transcript. If the splice-recognition sequences are blocked due to the binding of a sequence-specific antisense molecule, the unrecognized splice site is excised out with the surrounding intronic sequence as the splicesome then proceeds along the transcript to find subsequent splice recognition sites. Disrupting the open reading frame using this antisense approach can produce the expression of a unique mRNA transcript. The unique mRNA is then quantifiable by RT-PCR and translates to a measurable reduction in protein levels and/or protein function.

Here we used phosphorodiamidate morpholino oligomers conjugated to an Arginine-rich delivery peptide (P-PMO); an antisense platform repeatedly proven to be efficacious for altering gene expression (Mitev et al., 2009; Mourich et al., 2009; Stein, 2008; Wu et al., 2008), including splice-altering in leukocytes (Marshall et al.,

2007). Six P-PMO compounds were synthesized to target a subunit of a heterodimeric receptor found on activated T cells, IL-12Rb2. The goal was to sufficiently disrupt IL-12Rb2 expression to inhibit IL-12R signaling through phosphorylation of STAT4. After screening for altered mRNA splice products, protein expression, protein function, and cellular viability, we chose a sequence targeting the splice-acceptor site of exon 3 (SA3). SA3 was shown to sufficiently disrupt IL-12Rb2 mRNA expression in a dose-dependent manner by inducing excision of exon 3, which effectively inhibited expression of phosphorylated STAT4. These same steps were then used to screen P-PMO targeting the ligand of IL-12Rb2, IL-12A. The best candidate compound targeting the splice acceptor site of exon 6 induced recognition of an apparent cryptic splice site, resulting in inclusion of intron sequence in the mature mRNA to effectively disrupt normal IL-12 expression.

Materials and Methods

Mice

C57Bl/6 mice (Jackson Laboratories) were housed in microisolator cages under pathogen-free conditions and treated according to animal use protocols approved by the Institutional Animal Care and Use Committee of Oregon State University.

Cell isolation and culture

Splenocyte suspensions were prepared by dissociation of spleens between frosted microscope slides in HBSS containing 2.5% FBS, 50 µg/ml gentamicin, and 20 mM HEPES followed by a 10-s hypotonic water lysis of red blood cells. Splenocytes were cultured in RPMI 1640 medium containing L-glutamine and supplemented with 10% FBS, 50 µg/ml gentamicin, and 50 µM 2-ME. Cells were stimulated for 48 hrs with either 5 µg/ml platebound anti-CD3, soluble anti-CD3 (0.5 µg/ml) and anti-CD28 (1 µg/ml) (eBioscience), or 5 µg/ml concanvalin-A (Sigma) as indicated. RAW 264.7 cells were cultured in DMEM supplemented with 10% FBS and 50 µg/ml gentamicin, and stimulated for 48 hrs with 100 ng/ml LPS (*E. coli* 0111:B4, Sigma).

P-PMO antisense compounds

Phosphorodiamidate morpholino oligomers conjugated to Arginine-rich peptide NH_2-RXRRXRRXRRXRXB-COOH (where X represents 6-aminohexanoic acid, and B represents β-alanine) (P-PMO) were designed and synthesized at AVI BioPharma Inc. (Corvallis, OR. USA) to greater than 90% purity. Lyophilized P-PMO were dissolved in DI water at 1-2 mM and added to culture media at a final concentration (µM) as indicated.

Flow cytometry

Cultured splenocytes were washed and stained on ice in PBS supplemented with 1% BSA and 0.1% sodium azide. Cells were first incubated with Rat IgG (200 µg/ml; Jackson ImmunoResearch) for FC receptor blocking, and stained with

optimal concentrations of anti-mouse monoclonal antibodies including: APC-Alexa Fluor 750-CD4 (clone RM4-5, eBioscience); purified-IL-12 R β2 (clone HAM10B9; BD Pharmingen), and FITC-anti-armenian hamster IgG (eBioscience). STAT4 was measured using BD Phosflow reagents including mouse PE-STAT4 (clone 38/p-Stat4) as per the manufacturer's instructions. Samples lacking one of the individual stains (fluorescence minus one (FMO)) were used as staining controls. Viability of unfixed cells was measured with 7-aminoactinomycin D (7-AAD, Calbiochem). A minimum of 10,000 CD4+ T cell events were collected per sample on a Beckman Coulter FC-500 flow cytometer. Data analysis and software compensation were performed using WinList (Verity Software).

RT-PCR and sequencing

Total RNA was extracted from cultured cells (Qiagen RNeasy mini kit) and used as template material for RT-PCR (Invitrogen SuperScript III One-Step RT-PCR System with Platinum Taq DNA Polymerase) using sequence specific primers. Primer pair #1: FWD 5'-TCTGGAGAACCAGAGGTTGC-3'; REV 5'-CTCCAATTACTCCAACTTCCTC-3'; Primer pair #2: FWD 5'-GTCTGAATCCATCAGAGG-3'; REV 5'-TCTGCTGTCGAGTCTCGTTC-3' (annealed at 55°). IL-12 primers: FWD 5'TGTACCAGACAGAGTTCCAG-3'; REV 5'-GGGGTGACTGAGTGTTTTC-3'. Primers were designed using Vector NTI software (Invitrogen) and synthesized by IDT. PCR reactions were performed on a DNA engine (MJ Research), and the products were visualized by agarose gel electrophoresis. A 100 bp DNA ladder served as a molecular weight marker

(Invitrogen). Selected PCR products were excised and purified (Qiagen QIAquick Gel Extraction Kit). The fragments were cloned into pCR4-TOPO vector (Invitrogen TOPO TA Cloning Kit) and plasmid DNA was purified (Qiagen QIAprep Spin Miniprep Kit). DNA was sequenced using an ABI Prism 3730 Genetic Analyzer at the CGRB Core Laboratory at Oregon State University.

Results

Step 1: Detecting altered splice products by end-point RT-PCR

We chose to target the mouse IL-12Rb2 gene (Gene ID: NM_008354), part of the heterodimer which makes up the interleukin-12 (IL-12) receptor found on activated T cells. P-PMO sequences (Table A.1) were selected to target 6 areas within the gene's open reading frame including the AUG start codon and 5' splice acceptor (SA) ends of exons 3, 5, 7, 9, and 11 (Figure 1A). The initial step for screening efficacy of the compounds was visual detection of splice-altered mRNA products through amplification of the target region by RT-PCR. Designing primer pairs that amplify smaller regions of the target gene allow smaller RT-PCR products to be easily visualized on an agarose gel. Thus, for IL-12Rb2, we designed two primer sets which spanned exons 2-7 and 9-12, amplifying PCR products around 1000 and 500 base pairs (bp), respectively.

Whole RNA was isolated from splenocytes stimulated with concanvalin-A and treated with 5 μM P-PMO for 48 hrs. The RNA was reverse transcribed into cDNA and added to PCR reactions containing the appropriate primer pairs. As

shown in Figure 1B, smaller RT-PCR products were clearly identified by agarose gel electrophoresis for samples treated with SA3, SA5, SA9, and SA11 P-PMO compared to the full size product seen in the control. No full-size PCR product was detected in the AUG-treated sample, or the SA7 sample (due to placement of the reverse primer in exon 7). This confirmed that all of the antisense compounds targeting IL-12Rb2 effectively altered pre-mRNA splicing.

Step 2: Measuring antisense effects on protein expression

Typically, the goal of antisense treatment is to disrupt the normal translation of the target gene into functional protein. Thus, we measured surface expression of IL-12Rb2 protein on P-PMO-treated cells by flow cytometry. Splenocytes were stimulated for 48 hrs with plate-bound anti-CD3 and treated with 5 μM P-PMO. As shown in Figure 2, decreased IL-12Rb2 expression was measured on CD4+ T cells for AUG-, SA7-, SA9- and SA11-treated samples both in the percent of cells (Figure 2A), and the mean fluorescence intensity (Figure 2B). This suggested AUG, SA7, SA9 and SA11 were effectively disrupting translation of IL-12Rb2 mRNA. However we did not yet exclude the other compounds, as it was possible that the epitope the anti-IL-12Rb2 antibody bound to was preserved on protein that was non-functional.

Step 3: Measuring antisense effects on protein function

It is important to consider the role of the target gene within a signaling pathway or other cellular process as a lack of an effect on protein expression does

not indicate the compound is not effective. For IL-12Rb2, the binding of IL-12 to the IL-12Rb1 and IL-12Rb2 heterodimer causes the dimerization and phosphorylation of STAT4. Thus if IL-12Rb2 protein expression was disrupted, we expected to see a decrease in STAT4 phosphorylation. Splenocytes were stimulated with soluble anti-CD3 and anti-CD28 for 72 hrs with 5 μM P-PMO and pulsed with 5 ng/ml IL-12 for 2 hrs. Intracellular phosphorylated STAT4 protein was analyzed by flow cytometry (Figure 3A). As shown in Figure 3B, the mean fluorescence intensity of phosphorylated STAT4 staining was decreased in cells treated with AUG, SA3, SA7, and SA9. Of these, SA3 was the only compound that did not also cause decreased IL-12Rb2 protein expression on treated cells (Figure 2). Thus, after examining mRNA splicing, protein expression, and protein function, AUG, SA3, SA7 and SA9 were the four leading candidate compounds.

Step 4: Determining antisense effects on cellular viability

An alternate explanation for reduced protein expression in cells is a decrease in viability. To determine if any of the P-PMO compounds affected cellular viability, splenocytes were stimulated with plate-bound anti-CD3 for 48 hrs with P-PMO treatment and then stained with 7-Amino-actinomycin D (7-AAD) which is excluded from intact viable cells, and then analyzed by flow cytometry (Figure 4A). As shown in Figure 4B, there was a decrease in the percentage of cells that excluded 7-AAD in the AUG-, SA5- and SA7-treated samples suggesting a loss of cellular integrity, likely due to cell death. A loss in viability likely explains why a decrease in IL-12Rb2 protein expression was measured for cells treated with these three

compounds. Thus, due to their effects on cellular viability, AUG, SA5 and SA7 were omitted as candidate compounds. In some cases however, inhibiting expression of a target gene could cause a cell to die, as the gene may play a role in preserving cell survival. Thus the decision to exclude compounds that impact cellular viability must be carefully considered depending on the gene target.

An interesting observation we have made when treating T cells with various AUG-specific P-PMO is a reduction in cellular viability. We have observed this in cells treated with P-PMO targeting the AUG of CTLA-4, a negative costimulatory molecule expressed by T cells, and the AUG of Foxp3, a transcription factor that confers suppressive regulatory function to T cells (data not shown). We again saw this effect when targeting the AUG of IL-12Rb2. The significance of this is not know, however it presents another advantage to using a splice-altering approach to antisense design over targeting the AUG start codon, particularly in T cells.

Step 5: Final selection and validation of the optimal antisense compound

We had excluded AUG, SA5, SA7 and SA11 because treatment either reduced the viability of the T cells and/or had no effect on phosphorylated STAT4 protein expression. This left SA3 and SA9 as the two remaining candidate compounds. The altered RT-PCR product from the SA3-treated sample was cloned and sequenced to determine why a change in expression of IL-12Rb2 protein was not detected, despite altered mRNA expression and decreased expression of phosphorylated STAT4. The sequence lacked exon 3, instead replaced by the joining of exons 2 and 4 (Figure 5A). This indicated that the splicesome had continued onto

the exon 4 SA site when the exon 3 SA site was blocked by the P-PMO. Interestingly, exon 3 is made up of 327 bp which is divisible by 3, the number of nucleotides in a codon which encodes for an amino acid. Thus, after excision of exon 3, the remaining transcript was left in frame for further translation, explaining why we were unable to measure a change in IL-12Rb2 protein expression. To further validate the efficacy of SA3, a dose-dependent induction of altered splicing of IL-12Rb2 mRNA in SA3-treated cells was measured (Figure 5B). After 48 hours, a full conversion to the splice-altered product was visible at the 2- and 4-μM treatments.

We then followed these same screening steps used for P-PMO targeting IL-12Rb2 for screening P-PMO targeting the ligand of IL-12Rb2, IL-12A. Interestingly, we found that the altered splice product produced in RAW 264.7 cells treated with P-PMO targeting the SA site of exon 6 (IL-12SA6) (Table 1) was larger than the control RT-PCR product (Figure 6A). Upon cloning and sequencing, we discovered that this altered RT-PCR band included 153 bp of intronic sequence directly 5' of exon 6 (Figure 6B). This suggests a cryptic splice site was recognized by the splicesome when the SA site of exon 6 was blocked by the P-PMO. This resulted in out-of-frame translation, introduction of a premature stop codon, and loss of detectable IL-12 protein (data not shown). Thus preservation of in-frame translation and/or recognition of cryptic splice sites are a potential consequence of this antisense approach; thus it is important to recognize when it occurs when validating an antisense compound and elucidating its mechanism of action.

Discussion

Five screening steps were utilized to select the best candidate P-PMO targeting IL-12Rb2; (1) detecting mRNA splice products by RT-PCR, (2) measuring protein expression, (3) evaluating protein function, (4) checking cellular viability, and (5) validating efficacy of the final candidate compound. The initial screen for splice-altered mRNA products by RT-PCR showed that all P-PMO tested disrupted normal IL-12Rb2 mRNA expression. Next, AUG, SA7 and SA9 were found to inhibit IL-12Rb2 protein expression, and along with SA3, inhibited expression of phosphorylated-STAT4. Of these four remaining candidates, AUG and SA7 were eliminated due to decreased cellular viability in treated cells. With SA3 and SA9 remaining, we ultimately chose SA3 because it potently induced splice-altering of the mRNA transcript to produce a single alternate PCR product. We learned its mechanism of action was removal of exon 3 from the mature IL-12Rb2 mRNA transcript which preserved in-frame translation of the protein, but sufficiently disrupted IL-12Rb2 protein function.

And yet, the skipping of exons made up of a number of bp divisible by 3 by the splicesome does not guarantee a frame-shift will not occur. Rather than find the next splice acceptor/donor site on the subsequent exon, the splicesome may identify a cryptic splice site within exonic or intronic sequence as observed in cells treated with IL-12SA6. There are natural protective mechanisms in place for when this occurs as aberrant mRNA and protein expression could be detrimental to the organism. Exon-junction complexes and the ribosome can recognize where aberrant

splicing occurs according to the position of other landmarks on the transcript. This results in nonsense-mediated decay of the transcript by the proteosome (Chang et al., 2007) resulting in degradation of the nonsense mRNA. For antisense targeting of splice recognition sites, this is likely a common mechanism for inhibition of normal gene expression.

The greatest advantage to targeting 5' and 3' splice recognition ends of exons to disrupt mRNA splicing is a positive read-out for an antisense effect. Though often the goal of antisense treatment is to inhibit normal gene expression, it is estimated that at least 50% of genes are alternatively spliced, producing spliceforms that play a specific role in biological processes. This then allows antisense to be used to redirect splicing to induce naturally-occurring splice forms as an approach to altering the function of a gene product. For example, targeting the SA site on exon 2 of the mouse CTLA-4 gene with P-PMO resulted in removal of exon 2 which encodes for the domain which interacts with B7 molecules on dendritic cells (Mourich, D.V. et al., manuscript in preparation). This form can occur naturally in mice, although at disproportionally low levels in the non-obese diabetic (NOD) mouse which is linked to their spontaneous development of Type 1 diabetes (Vijayakrishnan et al., 2004). Treating NOD mice with SA2 P-PMO resulted in the protection from development of diabetes through the increased production of a CTLA-4 spliceform that was ligand-independent. Thus, there are numerous possibilities for the use of gene-specific splice-altering antisense compounds to alter biological processes. The critical step remains careful screening for efficacious compounds as it is otherwise easy to overlook the best candidate.

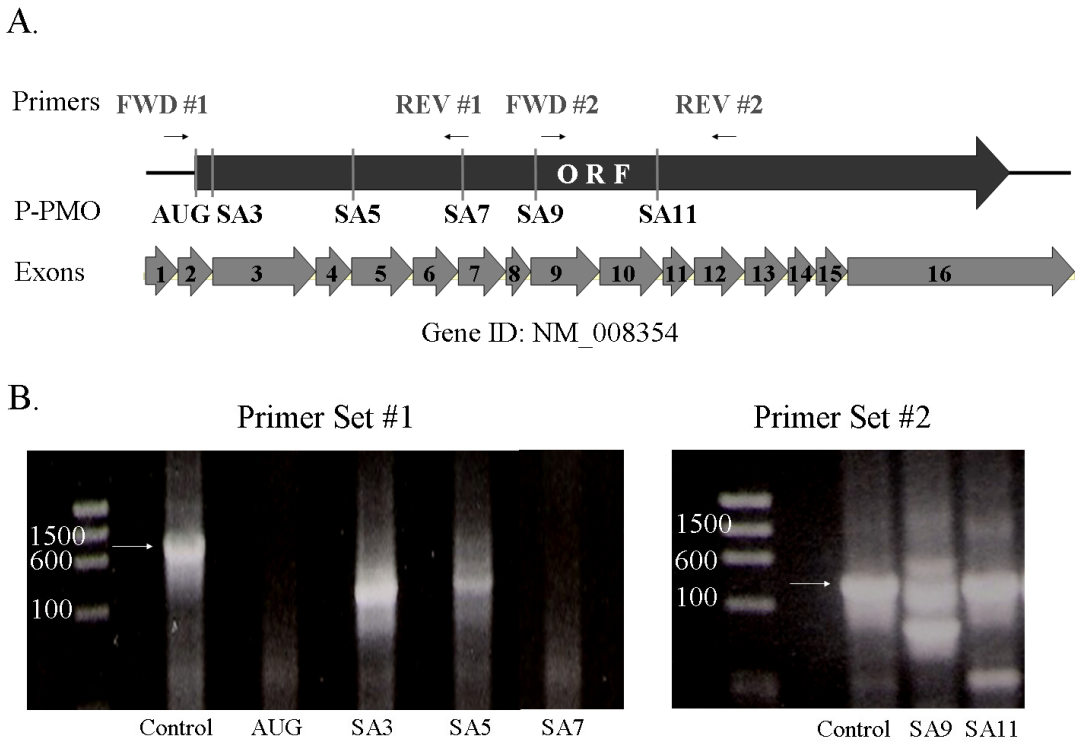

Figure A.1. P-PMO targeting IL-12Rb2 alter pre-mRNA expression. P-PMO were designed to target the AUG start codon and 5' splice acceptor sites (SA) of exons 3, 5, 7, 9, and 11 of the IL-12Rb2 gene (A). C57/Bl6 splenocytes were stimulated with 5 µg/ml concanvalin-A and treated with 5 µM P-PMO for 48 hrs. Whole RNA was isolated and reverse transcribed into cDNA then added to PCR reactions containing primer pairs (FWD, REV) #1 or #2 (A) to amplify the target region. The RT-PCR products were visually examined by agarose gel electrophoresis (B). The white arrows indicate expected RT-PCR products.

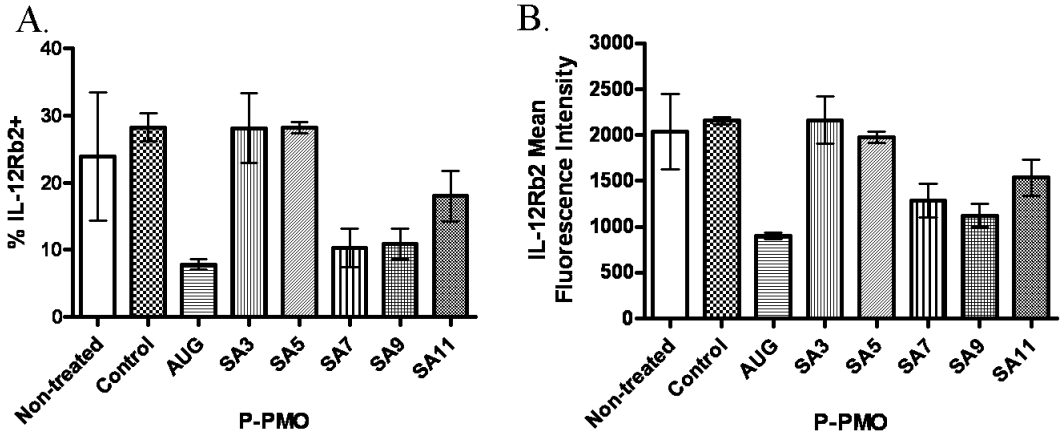

Figure A.2. The effects of P-PMO on IL-12Rb2 protein expression on CD4+ T cells.
Splenocytes were stimulated for 48 hrs with plate-bound anti-CD3 (5 µg/ml) with 5 µM P-PMO. Cells were stained with anti-mouse APC-Alexa Fluor 750-CD4 and IL-12Rb2 followed by FITC-anti-hamster IgG secondary and analyzed on a flow cytometer. The percent of cells that were IL-12Rb2-FITC+ (A) and the mean FITC fluorescence intensity (B) was measured on CD4+ T cells (mean ± SEM).

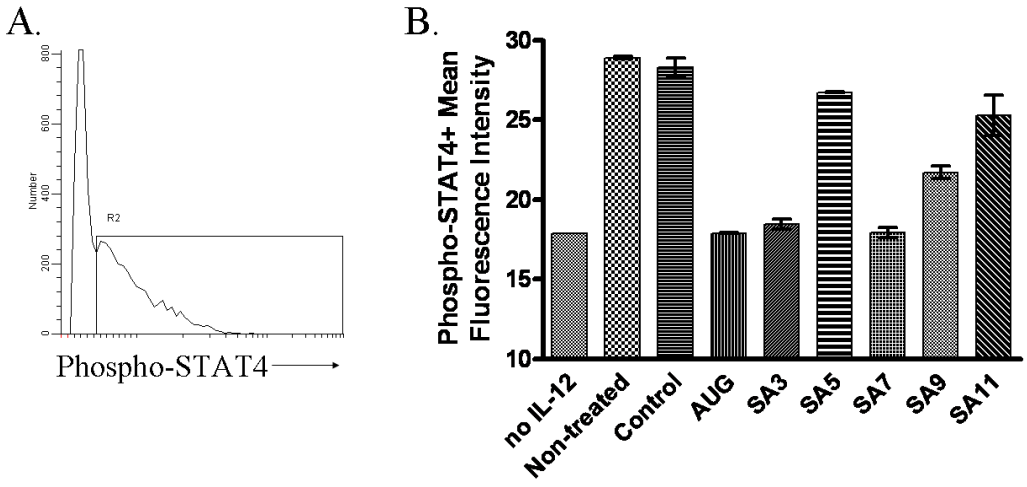

Figure A.3. The effects of P-PMO on phosphorylated-STAT4 protein expression in CD4+ T cells.
Splenocytes were stimulated with soluble anti-CD3 and anti-CD28 for 72 hrs with 5 μM P-PMO and pulsed with 5 ng/ml IL-12 for 2 hrs. Phosphorylated STAT4 protein was measured intracellularly using BD PhosFlow reagents and analyzed by flow cytometry (A). The mean fluorescence intensity of phospho-STAT4 staining was measured in CD4+ T cells (mean ± SEM) (B).

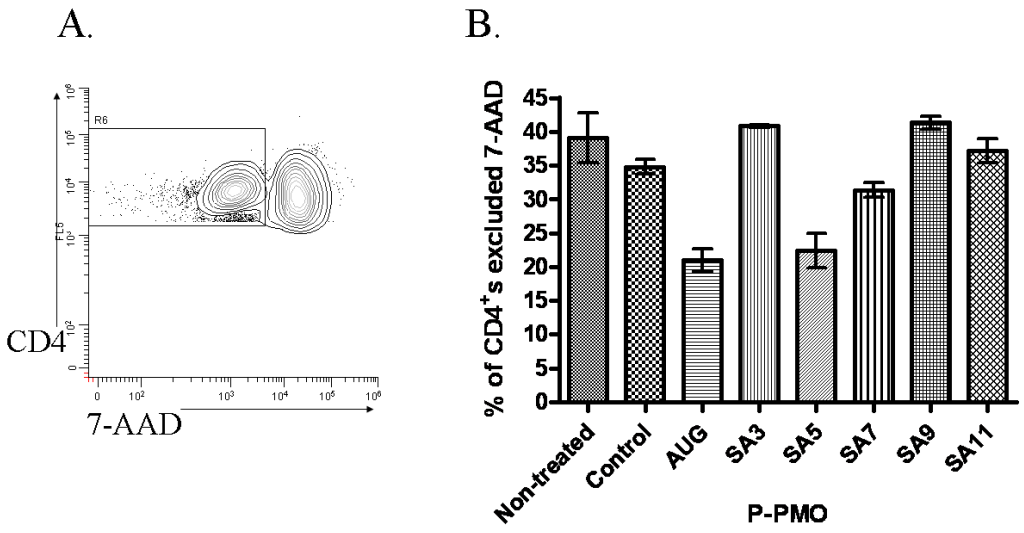

Figure A.4. The effects of P-PMO on CD4+ T cell viability (7-AAD exclusion). Splenocytes were stimulated for 48 hrs with plate-bound anti-CD3 (5 µg/ml) and treated with 5 µM P-PMO. Cells were harvested and stained with anti-mouse APC-Alexa Fluor 750-CD4, washed, and stained with 2 µg/ml 7-AAD for 15 minutes, and analyzed by flow cytometry (A). The percent of CD4+ cells that excluded 7-AAD was measured (mean ± SEM) (B).

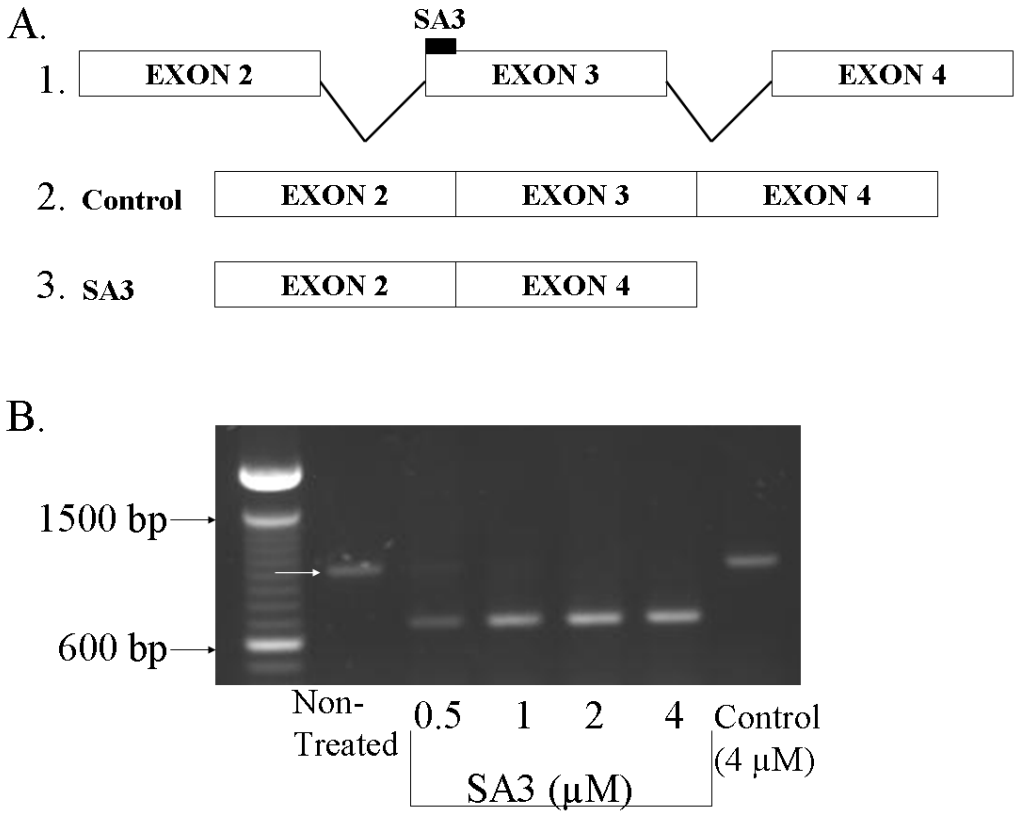

Figure A.5. SA3 induces dose-dependent excision of exon 3 from the IL-2Rb2 mRNA transcript.
The splice-altered PCR product produced from SA3-treated cells was excised from the agarose gel, cloned, and sequenced. The sequence showed the absence of exon 3 and the joining of exons 2 and 4 (A). Splenocytes were stimulated with 0.5 µg/ml soluble anti-CD3 and 1 µg/ml anti-CD28 and treated with 0, 0.5, 1, 2, or 4 µM SA3 or 4 µM control P-PMO for 48 hrs. IL-12Rb2-specific RT-PCR products were identified by agarose gel electrophoresis (B).

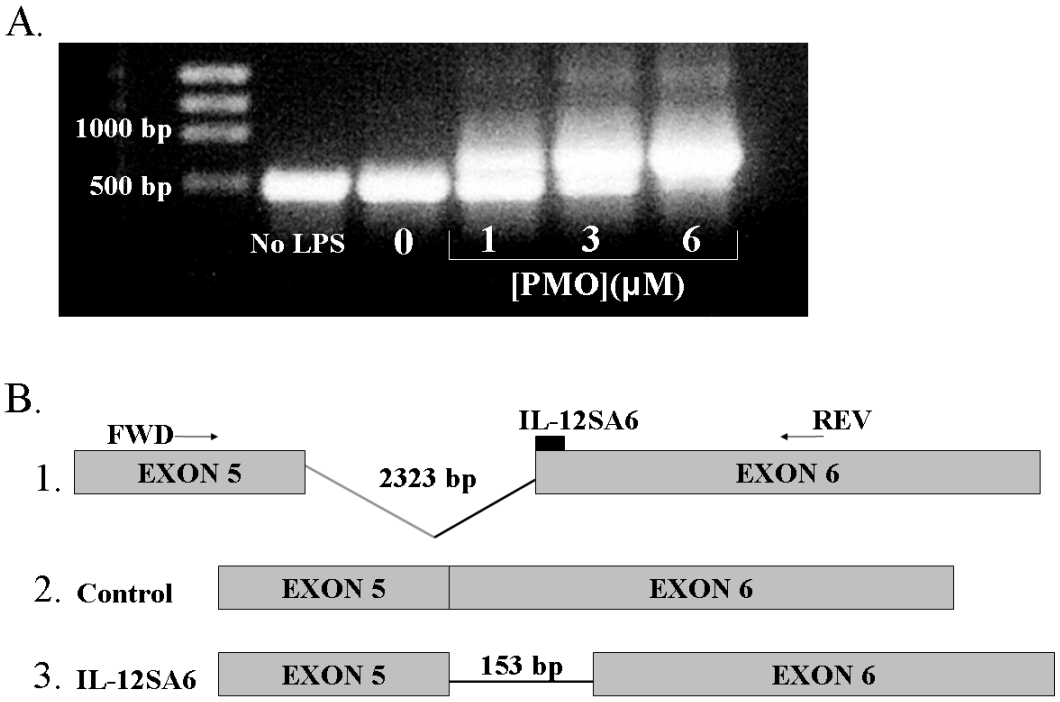

Figure A.6. IL-12SA6 treatment induces dose-dependent inclusion of intronic sequence 5' to exon 6 in IL-12 pre-mRNA transcript.
RAW 264.7 cells were stimulated with 100 ng/ml LPS and treated with 0, 1, 3, or 6 μM IL-12SA6 for 48 hrs. IL-12-specific RT-PCR products were identified by agarose gel electrophoresis (A). The splice-altered RT-PCR product produced from IL-12SA6-treated cells was excised from the agarose gel, cloned, and sequenced. The sequence showed inclusion of 153 bp of intronic sequence 5' of exon 6 (B).

Table A.1. P-PMO Sequences

Name	Sequence (5´→ 3´)
Control*	CCTCTTACCTCAGTTACA
AUG	CAGTCTGTGCCATGAGTCTTC
SA3	CAGTGCCAAGCTTGCACACAT
SA5	AGATTGTTTGGTCCACTTAAC
SA7	TTTGGCATTTGTAGCATTGAC
SA9	TGCCTCTGATGGATTCAGACT
SA11	AGATATAGGGCTTTATGTTCT
IL-12SA6	CTCGCCATTATGATTCAGAGA

* Control sequence is non-specific for mouse.

References

Mitev GM, Mellbye BL, Iversen PL, and Geller BL. Inhibition of intracellular growth of Salmonella enterica serovar typhimurium in tissue culture by antisense peptide-phosphorodiamidate morpholino oligomer. Antimicrob Agents Chemother 2009 epub.

Mourich DV, Jendrzejewski JL, Marshall NB, Hinrichs DJ, Iversen PL, Brand RM. Antisense targeting of cFLIP sensitizes activated T cells to undergo apoptosis and desensitizes responses to contact dermatitis. J Invest Dermatol 2009; 129: 1945-1953.

Stein DA. Inhibition of RNA virus infections with peptide-conjugated morpholino oligomers. Curr Pharm Des 2008; 14: 2619-2634.

Wu B, Moulton HM, Iversen PL, Jiang J, Li J, Spurney CF, Sali A, Guerron AD, Nagaraju K, Doran T, Lu P, Xiao X, and Lu, QL. Effective rescue of dystrophin improves cardiac function in dystrophin-deficient mice by a modified morpholino oligomer. Proc Natl Acad Sci 2008; 105: 14814-14819.

Marshall NB, Oda SK, London CA, Moulton HM, Iversen PL, Kerkvliet NI, Mourich DV. Arginine-rich cell-penetrating peptides facilitate delivery of antisense oligomers into murine leukocytes and later pre-mRNA splicing. J Immunol Methods 2007; 325: 114-126.

Chang YF, Imam JS, and Wilkinson MF. The nonsense-mediated decay RNA surveillance pathway. Annu Rev Biochem 2007; 76: 51-74.

Vijayakrishnan L, Slavik JM, Illes N, Greenwald RJ, Rainbow D, Greve B, Peterson LB, Hafler DA, Freeman GJ, Sharpe AH, Wicker LS, Kuchroo, VK. An autoimmune disease-associated CTLA-4 splice variant lacking the B7 binding domain signals negatively in T cells. Immunity 2004; 20: 563-575.